Role of PRC2-mediated chromatin regulation in fine tuning Arabidopsis root development

Chean Sern Jacobs

Numéro National de Thèse : 2020LYSEN085

THESE de DOCTORAT DE L'UNIVERSITE DE LYON
opérée par
l'Ecole Normale Supérieure de Lyon

Ecole Doctorale N° 340
Biologie Moléculaire, Intégrative et Cellulaire

Discipline : Sciences de la vie et de la santé
Spécialité du doctorat : Epigénétique du Développement

Soutenue publiquement le 18/12/2020, par :
Chean Sern JACOBS

Role of PRC2-mediated chromatin regulation in fine tuning *Arabidopsis* root development

Rôle de la régulation chromatinienne par PRC2 dans le contrôle du développement racinaire chez *Arabidopsis thaliana*

Devant le jury composé de :

RAYNAUD, Cécile	Dir. de recherche, Univ. Paris-Saclay	Rapporteure
GOODRICH, Justin	Professeur, University of Edinburgh	Rapporteur
PROBST, Aline	Dir. de recherche, Univ. Clermont Auvergne	Examinatrice
BESNARD, Fabrice	Chargé de recherche, ENS de Lyon	Examinateur
ROUDIER, François	Professeur, ENS de Lyon	Directeur de thèse

Acknowledgements

Firstly, I have to thank the person who gave me the opportunity to work on this fascinating subject: my PhD supervisor François Roudier. In spite of our different temperament, we got along very well over the nearly four years we worked together, I must say thanks to his boundless patience and empathy towards his students. Furthermore, his insightful feedback pushed me to challenge my ideas, essential to my development as a young scientist. I will definitely miss working with you!

I also would like to thank all the members of the EpiCDev team, for their moral, and scientific support during our numerous discussions. From help on big experiments, advice and scientific discussions, to ponderings of existential questions, fresh figs and homemade jams, the members of our small team have always been there for me. This even after my team presentations were about 3 times longer than planned on multiple occasions.

All these great conditions, in the amazing RDP lab environment. The lively discussions that occur during lunch, in hallways or after work have been fascinating with points of view from different fields. The inclusive, community-based running of the lab is definitely a positive influence and makes you feel like you are working together, with neighbours always ready to lend a hand. Not to mention on the social side, with large lab outings and smaller discovery trips of Lyon, the gastronomy capital of France, if not the world (citation needed). A special mention goes to my amazing office-mates.

I thank all the people who helped guide me during my PhD committees, that is Christel Carles, Gael Yvert and Daniel Bouyer, and also the jury members of my defence for their comments and discussion.

Lastly, I would like to thank my Malaysian family and Marseillaise fiancée for their inexhaustible kind words and support through these past years. I would never have made it without you!

Rôle de la régulation chromatinienne par PRC2 dans le contrôle du développement racinaire chez *Arabidopsis thaliana*

Mots-clés :
Chromatine, PRC2, différentiation cellulaire, Arabidopsis

Résumé

La régulation de l'expression des gènes par la voie des mécanismes chromatiniennes sont critiques dans la modulation et la stabilisation de l'expression des programmes génétiques, essentielles pour l'organogenèse et le développement. Le complexe répresseur Polycomb 2 (PRC2) catalyse le triple méthylation du lysine 27 de l'histone H3 auprès des gènes cibles. Ceci est un régulateur des programmes du développement, globalement conservé chez les eucaryotes multicellulaires.

Afin de déterminer l'implication de PRC2 au cours des transitions de l'identité cellulaire, j'ai caractérisé le paysage chromatinien d'un type cellulaire unique de la niche des cellules souches racinaire. L'intégration quantitative des données épigénomique a révélé trois types chromatiniens qui corrèle avec des niveaux d'activité transcriptionnelle, ainsi que des profils d'expression bien distincts, au cours de la différentiation cellulaire. Ces données suggèrent que la régulation par PRC2 est importante pour maintenir le contrôle temporel des gènes pendant l'avancé de la différentiation cellulaire.

De plus, j'ai effectué des études fonctionnelles sur deux homologues de la sous unité catalytique de PRC2 qui indique que au moins deux complexes PRC2 de composition diffèrent peuvent coopérer afin de moduler finement la régulation des gènes clés du développement.

En conclusion, le travail mené souligne l'importance de PRC2 dans le contrôle précis des profils d'expression des gènes, et aussi la capacité des données épigénétique d'un état précoce de différentiation de prédire l'activité transcriptionnelle dans les étapes plus tardives.

Role of PRC2-mediated chromatin regulation in fine-tuning *Arabidopsis* root development

Keywords

Chromatin, PRC2, cell differentiation, Arabidopsis

Summary

Chromatin-based mechanisms are pivotal regulators of transcriptional patterns that are central to cell fate determination, organogenesis and development in multicellular organisms. The activity of Polycomb Repressive Complex 2 (PRC2) is involved in the maintenance of transcriptional gene repression by catalysing the trimethylation of histone H3 on lysine 27 at specific loci, and is a conserved modulator of developmental programs.

To reveal the extent to which PRC2 shapes transcriptional decisions during cell fate specification, I have characterized the epigenome organization of a single cell type from the root stem cell niche (SCN). Quantitative integration of (epi)-genomic data revealed three main chromatin states that correlate with distinct gene expression levels as well as patterns along the differentiation gradient. These results indicate that PRC2 activity over specific genes within the SCN regulates their timing of expression in daughter cells, at successive differentiation stages.

In addition, functional studies of PRC2 catalytic subunit homologues support the notion that distinct PRC2 complexes with different compositions cooperate to fine-tune the transcriptional regulation of key regulatory genes during root development.

Taken together, this work highlights the importance of PRC2-regulated chromatin states in shaping expression patterns along a differentiation gradient. They also pinpoint the potential of such epigenetic studies in predicting, from an initial chromatin state, the timing of gene transcriptional activation in subsequent differentiation stages.

Contents

1. General Introduction

A central aim in developmental biology is to understand how one set of identical genetic information is able to produce the wide array of phenotypic diversity required to build multicellular organisms. The nearly 60 years of research since Jacques Monod and François Jacob first demonstrated that genes are tightly regulated has broadly expanded our understanding that the multitude of cellular phenotypes are linked to the selective readout of the genetic information within each cell.

DNA is stored as chromatin in the nuclei of eukaryotes. The basic subunit of chromatin is the nucleosome which consists of 147 bases of DNA wrapped around a histone octamer of four canonical histones (H2A, H3B, H3 and H4). Regulation of chromatin activity is the sum of effects from a plethora of elements including, but not limited to transcription factors, histone variants, chromatin and DNA modifiers, non-coding RNA, and higher-order chromatin conformation.

One category of chromatin modifications that has been extensively studied is the covalent modification of histones, widely called histone marks. These refer to the array of chemical groups such as methyl, acetyl, or phosphate groups found at specific amino acid positions on histones (Bannister et al., 2011). Combinations of different histone marks results distinct chromatin states with different degrees of accessibility that are permissive or unfavourable for transcription. The main chromatin mechanism underlying gene expression is likely the alteration of the nucleosome physical properties. This may not only directly modify the stability of the nucleosome by weakening or strengthening electrostatic and polar interactions, but also affect the affinity of proteins, coined as “readers” which recognise and bind the marks essentially providing the functionality of chromatin (Bannister et al., 2011).

Efforts to integrate combinations of histone marks and other chromatin signatures along the genome in cell cultures (Ernst and Kellis, 2010), Drosophila (Filion et al., 2010) or *Arabidopsis thaliana* (Roudier et al., 2011; Sequeira-Mendes et al., 2014) have led to an understanding of which marks are associated to what genomic elements and genomic activity, with a limited number of functional chromatin states. A recurrent finding across these studies

is that expressed and repressed genes are mostly in chromatin groups primarily defined by the trimethylation of lysine 4 of histone H3 (H3K4me3) and H3K27me3, respectively. Bivalent genes, which present both of these antagonist histone marks over the same group of nucleosomes have been demonstrated in plants and animals (Bernstein et al., 2006; Roh et al., 2006; Sequeira-Mendes et al., 2014), and usually to correspond to intermediate transcriptional situations, awaiting additional signalling to proceed.

An important point to note is that chromatin states are highly dynamic during development, and these changes over the course of an organism's life are mainly the result of "writers" and "erasers" which are able to add or remove histone marks, usually in a specific manner.

1.1 Polycomb Repressive Complex 2 structure and function

H3K27me3 is catalysed by the conserved Polycomb Repressive Complex 2 (PRC2) which is constituted of four core subunits, Enhancer of Zeste (E(z)), containing the SET domain conferring the methyltransferase activity, and three regulatory or binding subunits, Suppressor of Zeste (Su(z)), Extra Sex Combs (ESC) and NURF55 that are all necessary for optimal PRC2 activity (Fig. 1).

In addition to contributing to PRC2 "writing" activity, the human ESC homologue, Eed, has been shown to confer a reading capacity to the PRC2 complex, via its WD40 domain (Margueron et al., 2009). In addition to facilitating the propagation of H3K27me3 from mother to daughter cells, the interaction of H3K27me3 with Eed has been shown to induce a conformational change in the PRC2 complex, increasing its catalytic activity (Lee et al., 2018). The conservation of the key aromatic tyrosine cage and WD-40 domain in ESC homologues from yeast, fungi, humans and plants leads to consider that this mechanism is central to PRC2 regulation across eucaryotes (Mozgova and Hennig, 2015; Moritz et al., 2018). The importance of this dual, writing-and-reading potential of PRC2 in the ability to maintain transcriptional states over divisions is developed in the review in Frontiers in Plant Sciences (Hugues et al., 2020) that is presented later in this introduction.

PRC2 recruitment to chromatin however, differs greatly from species to species. Drosophila PRC2 is recruited to chromatin via Polycomb Response Elements (PREs), which are

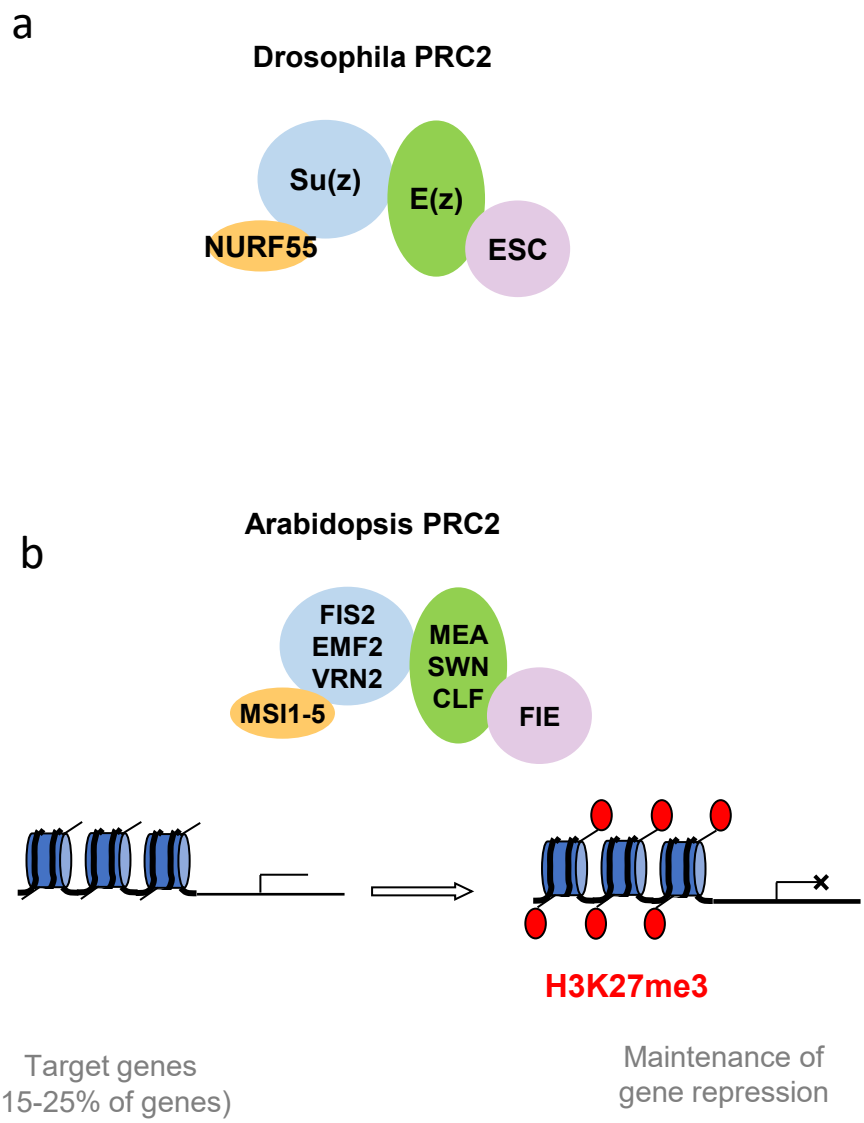

Figure 1 PRC2 composition in Drosophila and Arabidopsis. **(a)** Schematic representation of the PRC2 complex with each homologue of the core subunits indicated. **(b)** Plant homologues of the Drosophila PRC2 complex. The number of genes regulated by PRC2 in Arabidopsis whole seedlings varies between 15 and 25% from study to study.

cis-regulatory motifs present in most PRC2 targets of the species (Schuettengruber et al., 2017). The existence or functionality of PREs are not as clear in mammalian or plant genomes, in which PRC2 recruitment is distributed over a number of different DNA sequence motifs and targeting is dependent on many factors including long non-coding RNA and CpG island methylation status (Yu et al., 2019; Xiao et al., 2017).

One reason for this could be the differences in PRC2 accessory proteins between species. Mammalian PRC2 associates with Jarid2 and Aebp2 that stimulate its catalytic activity and modify its recruitment via their own chromatin or DNA interaction domains (Margueron and Reinberg, 2011; Chen et al., 2018). Direct homologues of Jarid2 or Aebp2 have not been reported in plants, though accessory PRC2 subunits do exist. For instance VIN3, VRN5 and VAL1 or ALP1/2 have been revealed to fine-tune PRC2 activity at a subset of targets (Yang et al., 2017; Velanis et al., 2020). Therefore, while the core function and effects of PRC2 activity appear similar between species, the precise mechanisms modulating its activity during development appear quite independent.

1.2 The role of PRC2 regulation in plant development

PRC2 plays an important role in maintaining repressive chromatin state over genes that are not needed at a particular developmental stage. A range of PRC2-related dysfunctions have been catalogued in mammals leading to cancer, or if absent at an early stage, embryonic lethality (reviewed in Yu et al., 2019). Plants lacking PRC2 activity show severe alterations in organogenesis and are not viable outside of *in vitro* conditions (Fig. 2) (Bouyer et al., 2011).

In most organisms, PRC2 core subunits are encoded by multigene families (reviewed in Mozgova and Hennig, 2015). In *Arabidopsis thaliana*, there are three *AtE(z)* and *AtSu(z)* homologues, as well as five NURF55 (*MSI1-5*) homologues (Fig. 1). The ESC homologue *FERTILISATION INDEPENDENT ENDOSPERM (FIE)* is present in a single copy in the genome. Roles for the *AtSu(z)* homologues have been described in specific developmental processes or stages such as vernalization response or seed development (Gendall et al., 2001; Qiu et al., 2016), and among the *MSI* genes, only *MSI1* has been shown to play a role in PRC2 function (Hennig et al., 2003; Kohler et al., 2003). As for the *AtE(z)* homologues, *MEDEA (MEA)* is associated with seed development in the stage-specific FIS2-PRC2 complex (Spillane et al.,

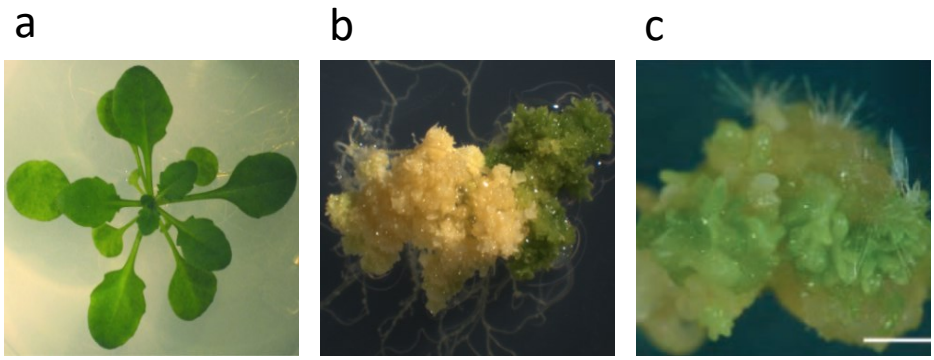

Figure 2 PRC2 in Arabidopsis. 30 day-old (a) WT plant (b) *fie* mutant (images from Bouyer et al., 2011) and a (c) *swn clf* double mutant (image from Chanvivattana et al., 2004).

2007), while *CURLY LEAF (CLF)* and *SWINGER (SWN)* are both active after seed germination and throughout the life cycle (Chanvivattana et al., 2004; de Lucas et al., 2016).

While defects in *CLF* were very early on associated with a loss of H3K27me3 (Schubert et al., 2006), alteration of SWN function has not been consistently reported to affect H3K27me3, leading to the deduction that *CLF* is the main vegetative *AtE(z)* that sustains the large part of PRC2 regulation. *CLF* was initially discovered via its importance in controlling flowering time and leaf shape, primarily by the regulation of *AGAMOUS* (*AG*) and *SEPALLATA3* (*SEP3*) (Goodrich et al., 1997; Lopez-Vernaza et al., 2012). More recently, *swn* mutants were shown to have a subtle antagonistic role in regulating phase transitions (Xu et al., 2016; Shu et al., 2019).

While *AtE(z)* single mutants exhibit relatively weak phenotypes, the *swn clf* double mutant fails to produce aerial organs and derives into a mass of disorganised cells, actually phenocopying *fie* mutants (Fig. 2) (Chanvivattana et al., 2004; Lafos et al., 2011; Bouyer et al., 2011). This reveals a redundancy between the two AtE(Z) proteins in assuring PRC2 activity. Consistent with this, *SWN* and *CLF* have largely overlapping expression domains in roots (de Lucas et al., 2016) and in shoots (Goodrich et al., 1997; Chanvivattana et al., 2004). Nevertheless, the respective role of these two *AtE(z)* that would explain their evolutionary maintenance throughout the Brassicaceae family, as well as in other angiosperms and gymnosperms (Spillane et al., 2007) remains unclear.

1.3 The inheritance of H3K27me3 and its impact on development

Review article follows:

frontiers in Plant Science

REVIEW
published: 09 March 2020
doi: 10.3389/fpls.2020.00262

Mitotic Inheritance of PRC2-Mediated Silencing: Mechanistic Insights and Developmental Perspectives

Alice Hugues[1,2], *Chean Sern Jacobs*[1] *and François Roudier*[1]*

[1] *Laboratoire Reproduction et Développement des Plantes, ENS de Lyon, UCB Lyon 1, CNRS, INRAE, INRIA, Université de Lyon, Lyon, France,* [2] *Master de Biologie, École Normale Supérieure de Lyon, Université Claude Bernard Lyon I, Université de Lyon, Lyon, France*

Maintenance of gene repression by Polycomb Repressive Complex 2 (PRC2) that catalyzes the trimethylation of histone H3 at lysine 27 (H3K27me3) is integral to the orchestration of developmental programs in most multicellular eukaryotes. Faithful inheritance of H3K27me3 patterns across replication ensures the stability of PRC2-mediated transcriptional silencing over cell generations, thereby safeguarding cellular identities. In this review, we discuss the molecular and mechanistic principles that underlie H3K27me3 restoration after the passage of the replication fork, considering recent advances in different model systems. In particular, we aim at emphasizing parallels and differences between plants and other organisms, focusing on the recycling of parental histones and the replenishment of H3K27me3 patterns post-replication thanks to the remarkable properties of the PRC2 complex. We then discuss the necessity for fine-tuning this genuine epigenetic memory system so as to allow for cell fate and developmental transitions. We highlight recent insights showing that genome-wide destabilization of the H3K27me3 landscape during chromatin replication participates in achieving this flexible stability and provides a window of opportunity for subtle transcriptional reprogramming.

Keywords: polycomb repressive complex 2, H3K27me3 inheritance, epigenetic memory, chromatin, replication

OPEN ACCESS

Edited by:
Marc Libault,
University of Nebraska–Lincoln,
United States

Reviewed by:
Martin Howard,
John Innes Centre, United Kingdom
Lin Xu,
Institute of Plant Physiology and Ecology, Shanghai Institutes for Biological Sciences (CAS), China

****Correspondence:***
François Roudier
francois.roudier@ens-lyon.fr

Specialty section:
This article was submitted to Plant Cell Biology, a section of the journal Frontiers in Plant Science

Received: *08 December 2019*
Accepted: *19 February 2020*
Published: *09 March 2020*

Citation:
Hugues A, Jacobs CS and Roudier F (2020) Mitotic Inheritance of PRC2-Mediated Silencing: Mechanistic Insights and Developmental Perspectives. Front. Plant Sci. 11:262. doi: 10.3389/fpls.2020.00262

INTRODUCTION

Polycomb repressive complex 2 (PRC2) is a conserved chromatin-modifying complex that catalyzes the trimethylation of lysine 27 of histone H3 (H3K27me3) (Margueron and Reinberg, 2011; Schuettengruber et al., 2017). PRC2 is composed of four core subunits that are necessary for its histone methyltransferase activity: Nurf55, suppressor of zeste 12 [Su(z)12], extra sex combs (ESC), and enhancer of zeste [E(z)], as originally identified in Drosophila. In multicellular organisms, members of these core subunits are often present in multigene families. For instance in the flowering plant *Arabidopsis thaliana*, the Su(z)12 and E(z) subunits are encoded by three homologous genes, leading to several PRC2 complexes with potentially distinct biochemical properties and developmental roles (Mozgova and Hennig, 2015). Further functional diversity is brought about by an array of additional factors that direct PRC2 recruitment to specific loci or affect the activity of the complex (Yu et al., 2019).

Polycomb repressive complex 2 activity orchestrates developmental and cellular programs by preserving the integrity of the gene expression patterns that underpin cell identity and function. Genetic and molecular evidence obtained from many organisms indicate that PRC2 activity is not required to initiate transcriptional repression but is necessary to maintain target gene repression, thereby providing a cellular memory system during development (Schuettengruber et al., 2017; Reinberg and Vales, 2018). Two remarkable properties lie at the heart of this genuine epigenetic process. First, the coupling between PRC2 *writing* and *reading* activities enables H3K27me3 self-propagation over large chromatin domains from an initially small number of nucleating nucleosomes marked by H3K27me3 (Oksuz et al., 2018; Yu et al., 2019). Second, H3K27me3 patterns are faithfully inherited from mother to daughter cells despite chromatin disassembly ahead of the replication fork that directly conflicts with the transmission of histone post-translational modifications (PTMs) to daughter cells (Annunziato, 2015; Masai and Foiani, 2018). The discoveries that parental histones are recycled and reincorporated into nascent chromatin and that H3K27me3 levels are restored downstream of the replication fork in both animal and plant cell cultures (Xu et al., 2012; Alabert et al., 2015; Jiang and Berger, 2017) highlight the fact that the S-phase is not only about replicating DNA, but also chromatin together with its epigenetic potential (Ramachandran et al., 2017; Escobar et al., 2018; Reverón-Gómez et al., 2018; Serra-Cardona and Zhang, 2018).

The molecular mechanisms responsible for the faithful perpetuation of H3K27me3-marked chromatin through cell division are under active investigation. Whereas strong evidence indicates that H3K27me3 itself is the physical support of the PRC2-based memory system (Xu et al., 2012; Coleman and Struhl, 2017; Laprell et al., 2017), it might not be the only carrier of this epigenetic process *in vivo* (Højfeldt et al., 2018; Sharif and Koseki, 2018). The first part of this review aims at presenting current understanding of the histone recycling machinery and of the self-perpetuation properties that underlie the inheritance of H3K27me3 in nascent chromatin. We then discuss the fact that, in addition to its remarkable stability, this memory system also needs to be flexible and that chromatin replication likely provides a window of opportunity enabling the transcriptional changes that drive cell fate decisions and developmental transitions.

MOLECULAR MECHANISMS UNDERLYING THE MITOTIC INHERITANCE OF PRC2-MEDIATED REPRESSION

Recycling of H3K27me3-Marked Nucleosomes and Incorporation of Neo-Synthesized Histones Into Nascent Chromatin

Parental nucleosomes disassembly at the replication fork (Teves and Henikoff, 2014; Annunziato, 2015; Masai and Foiani, 2018) is at odds with the perpetuation of parental H3K27me3 patterns (**Figure 1A**). In order to ensure that both daughter cells inherit the same parental epigenetic information, parental H3–H4 histones should be equiprobably distributed between the leading and the lagging strands downstream of the replication fork. However, the structural asymmetry of the replication fork is likely to induce a bias during the re-deposition of parental histones into nascent chromatin (Snedeker et al., 2017). Numerous studies in yeast and mammalian cells showed that cells manage to compensate for this intrinsic asymmetry via the intricate cooperation between histone chaperones and the DNA replication machinery that enables accurate recycling of parental histones together with their epigenetic marks (Hammond et al., 2017).

Recent studies uncovered strand-specific pathways of parental histone recycling in nascent chromatin (He et al., 2017; Gan et al., 2018; Petryk et al., 2018; Yu et al., 2018). The transfer of parental histones H3–H4 to the lagging strand relies on the synergistic action of the histone chaperone Mini-Chromosome Maintenance Protein 2 (MCM2), a subunit of the MCM helicase, chromosome transmission fidelity 4 (CTF4), and the lagging strand-specific primase DNA polymerase α (Pol-α) (Huang et al., 2015; Gan et al., 2018; Petryk et al., 2018; **Figure 1B**). CTF4 anchors Pol-α in the vicinity of the MCM helicase, thus enabling the transfer of parental histones H3–H4 from MCM2 to the lagging stand via Pol-α. The transfer of parental histones H3–H4 to the leading strand depends on Dpb3-4, a heterodimer associated with the leading strand-specific DNA polymerase ϵ (Pol-ϵ) (He et al., 2017; Yu et al., 2018; **Figure 1B′**). Interestingly, asymmetric inheritance of parental histones H3–H4 in fission yeast lacking either Dpb3 or Dpb4 results in loss of heterochromatin integrity and transcriptional activation, which emphasizes the functional role of epigenetic inheritance in the maintenance of genome stability and transcriptional programs (He et al., 2017; Yu et al., 2018).

Incorporation of newly synthesized H3–H4 dimers into nascent chromatin involves the two histone chaperones anti-silencing function protein 1 (ASF-1) and chromatin assembly factor 1 (CAF-1) (Hammond et al., 2017; **Figure 1C**). Since ASF-1 co-binds parental H3–H4 histones together with MCM2, nucleosome assembly of neo-synthesized histones driven by ASF-1 and CAF-1 might be also involved in the re-deposition of parental histones H3–H4 into nascent chromatin (Huang et al., 2015). Whereas the role of the Arabidopsis ASF-1 homologs AtASF1a/b remains unclear, CAF-1-dependent incorporation of newly synthesized histones is important for the efficient maintenance of histone PTM levels during replication (Jiang and Berger, 2017; Benoit et al., 2019).

Despite its efficiency, the recycling of parental H3 into nascent chromatin is not sufficient on its own to enable the full restoration of H3K27me3 in daughter cells. Indeed, parental H3K27me3 level is diluted twofold after chromatin replication due to the incorporation of newly synthesized, unmethylated histones H3–H4 into nascent chromatin that is required to re-establish the initial density of nucleosomes (**Figure 1**). Therefore, faithful transmission of PRC2-mediated gene repression downstream of the

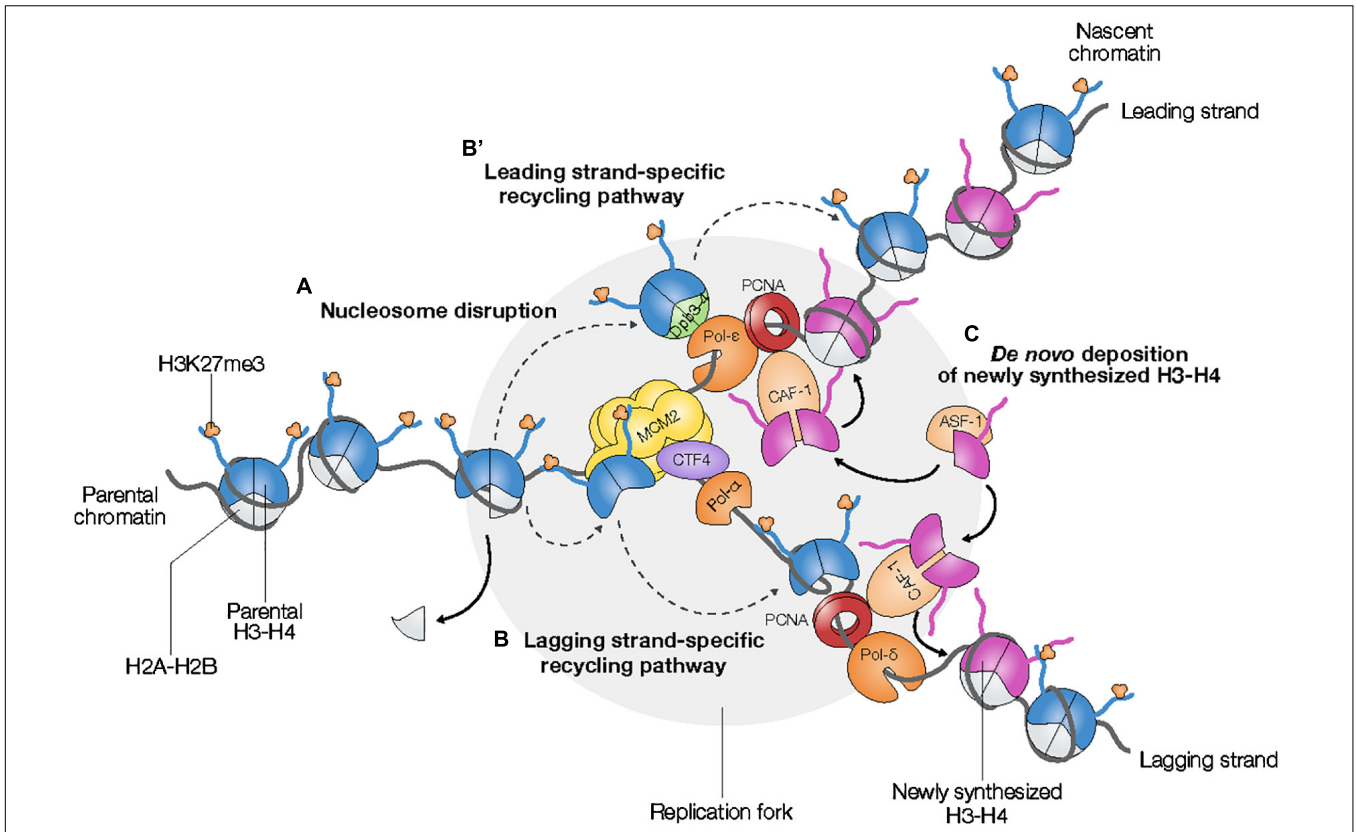

FIGURE 1 | Parental K27-trimethylated histone H3 are transmitted to nascent chromatin via the recycling of histones H3 at the replication fork. **(A)** Parental nucleosomes are disrupted ahead of the replication fork. The putative mechanisms underlying the recycling of parental H3s into nascent chromatin are strand-dependent (**B,B'** dashed gray arrows). Parental H3s are guided either to the leading strand **(B')** or to the lagging strand **(B)** *via* stand-specific pathways involving the heterodimer Dpb3-4 associated to Pol-ϵ and the MCM2-CTF4-Pol-α axis, respectively. **(C)** *De novo* incorporation of newly synthesized H3–H4 dimers *via* histone chaperones ASF-1 and CAF-1 leads to the twofold dilution of parental H3K27me3 levels in nascent chromatin.

replication fork requires specific mechanisms to spread H3K27me3 from parentally modified to newly synthesized, unmodified H3 (Xu et al., 2012; Alabert et al., 2015; Jiang and Berger, 2017).

Filling the Gaps? H3K27me3 Spreading Downstream of the Replication Fork

What Happens to PRC2 at the Passage of the Replication Fork?

The passage of the replication fork does not only destabilize nucleosomes but also results in the eviction of most chromatin- and DNA-binding proteins, including PRC2. Nevertheless, pioneer studies based on cytological and *in vitro* approaches indicated that PRC2 remains localized around DNA replication sites (Hansen et al., 2008). In agreement with these observations, higher-resolution proteomic analyses showed that PRC2 is already associated to nascent chromatin immediately after the passage of the replication fork, suggesting that PRC2 is actively re-established over nascent chromatin thereby ensuring the spreading of H3K27me3 from parental to newly synthesized, unmethylated H3 (Alabert et al., 2014; **Figure 2A**).

The 3D organization of chromatin might facilitate local retention of PRC2 at the replication fork

H3K27me3-marked chromatin domains have been shown to form foci in the nucleus of mammalian cells (Oksuz et al., 2018). Similarly, in plant interphasic nuclei, PRC2 is enriched in nuclear speckles containing PWWP-DOMAIN INTERACTOR OF POLYCOMBS1 (PWO1), a factor that interacts with lamin-like proteins (Mikulski et al., 2019). Although their presence in replicating cells remains to be formally established, such PRC2-enriched micro-environments could participate in maintaining PRC2 close to its targets during the passage of the fork. At a larger scale, loss of nuclear compartmentalization in the Arabidopsis *3h1* mutant lacking histone H1 correlates with a global diminution in H3K27me3 occupancy. This indicates that the 3D organization of chromatin into subnuclear domains probably contributes to the maintenance of H3K27me3 (Rutowicz et al., 2019), although its direct impact during replication needs to be clarified.

PRC2 binds several components of the replication machinery

Interaction of PRC2 with components of the replication machinery likely contributes to its retention at the replication

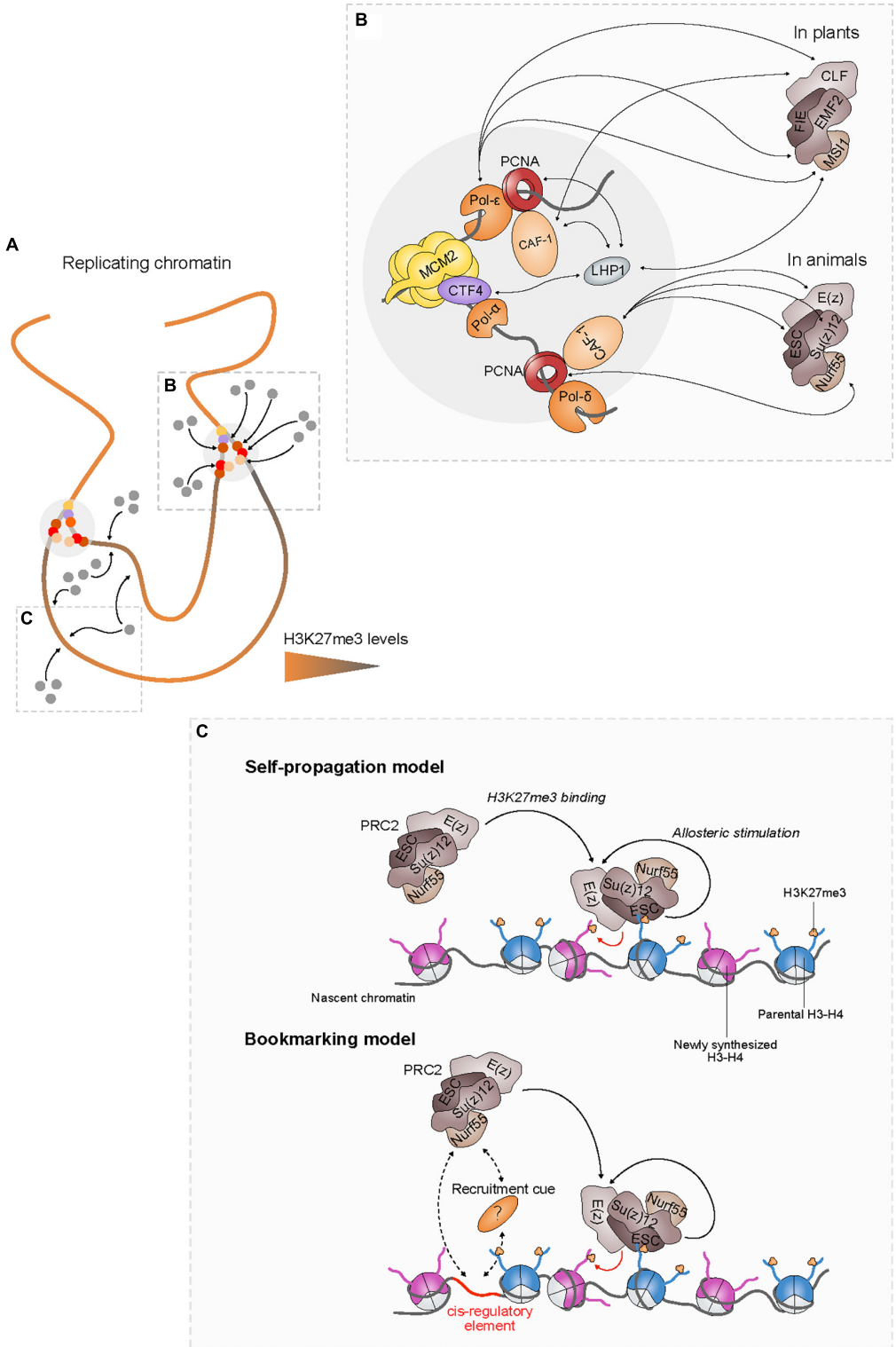

FIGURE 2 | PRC2 recruitment at the replication fork and in nascent chromatin enables faithful restoration of the H3K27me3 landscape. **(A)** In replicating chromatin, H3K27me3 levels (represented by a colored gradient) are diluted twofold during replication. PRC2 (gray dots) recruitment at the fork via components of the replication machinery (colored dots) **(B)** and in nascent chromatin **(C)** facilitates the restoration of parental H3K27me3 levels. **(C, Top)** According to the self-propagation model, the positive feedback loop between PRC2 and H3K27me3 is sufficient to propagate H3K27me3 from inherited to newly synthesized H3, thereby ensuring the maintenance of PRC2-mediated transcriptional silencing through cell division. **(C, Bottom)** *Cis*-regulatory elements might also play a critical role for the restoration of H3K27me3 patterns by enhancing directly or indirectly the recruitment of PRC2 to nascent chromatin.

fork (**Figure 2B**). PRC2 interacts with the proliferating cell nuclear antigen (PCNA) protein through CAF-1 in both plants and animals (Jiang and Berger, 2017; Cheng et al., 2019). Loss of CAF-1 induces strong developmental abnormalities including homeotic transformations in Drosophila that are reminiscent of the phenotypic defects observed in mutants lacking PRC2 activity (Anderson et al., 2011), defects in cell identity maintenance in both mouse embryonic stem cells (ESCs) and Arabidopsis meristems (Kaya et al., 2001; Clémot et al., 2018) as well as increased reprogramming abilities in mouse cells (Cheloufi et al., 2015; Cheloufi and Hochedlinger, 2017). In addition, lack of CAF-1 in Drosophila imaginal discs is associated with a massive decrease of H3K27me3 levels (Anderson et al., 2011; Yee et al., 2019), suggesting that CAF-1 activity is required for the inheritance of H3K27me3 *in vivo*.

Moreover, plant-specific interactions between PRC2 subunits and distinct DNA polymerases have been recently reported in Arabidopsis. Thus, loss of interaction between PRC2 and EARLY IN SHORT DAYS (ESD7), the catalytic subunit of DNA polymerase epsilon (Pol-ε), results in the misexpression of major flowering time regulators such as *AGAMOUS* (*AG*), *SUPPRESSOR OF OVEREXPRESSION OF CO 1* (*SOC1*), and *FLOWERING LOCUS T* (*FT*) (del Olmo et al., 2010, 2016), whose expression is controlled by PRC2. Loss of other DNA polymerases including Pol-α INCURVATA2 (ICU2) and Pol-δ POLD2 also impacts on H3K27me3 distribution, though a direct link with PRC2 subunits remains to be demonstrated (Pedroza-Garcia et al., 2019). These results provide evidence that interactions of PRC2 with multiple DNA polymerases acting at the replication fork likely play a significant role in the maintenance of H3K27me3 landscapes in plants.

The plant-specific protein LIKE HETEROCHROMATIN PROTEIN1 (LHP1) is required for the maintenance of H3K27me3 levels in dividing cells via its interaction with the PRC2 subunit MULTICOPY SUPPRESSOR OF IRA 1 (MSI1), a plant homolog of Nurf55 (Derkacheva et al., 2013; Veluchamy et al., 2016; Feng and Lu, 2017) and is involved in H3K27me3 spreading (Yang et al., 2017). LHP1 also binds several components of the replication fork such as CAF-1 (Li and Luan, 2011; Jiang and Berger, 2017), the CTF4 homolog ENHANCER OF LHP1 (EOL1) (Zhou et al., 2017b), and possibly ICU2 (Barrero et al., 2007; Hyun et al., 2013). Hence, by providing an interaction platform for PRC2 at the replication fork, LHP1 might strengthen the coupling between parental histones recycling and H3K27me3 spreading into nascent chromatin.

Furthermore, LHP1 interacts with components of the plant PRC1 that catalyzes H2A monoubiquitylation (Mozgova and Hennig, 2015). Given its conserved interplay with PRC2 (Yu et al., 2019), PRC1 could be involved in the maintenance of H3K27me3 patterns during replication. Indeed, *in vitro* studies showed that Drosophila PRC1 components remain bound to chromatin during replication (Francis et al., 2009) and that H2A monoubiquitinylation stimulates human PRC2 activity through AEBP2, a mammalian accessory PRC2 subunit (Kalb et al., 2014). In plants, absence of the PRC1 components RING1A/B causes a reduction in H3K27me3 levels over some PRC2 targets (Zhou et al., 2017a). These data indicate therefore that PRC1 could participate, via LHP1, in the recruitment of PRC2 and stimulate its activity at the replication fork.

Taken together, the aforementioned observations suggest that PRC2 is locally retained at the replication fork through multiple and dynamic interactions with components of the replication fork. These synergistic actions likely facilitate the immediate spreading of H3K27me3 over nascent chromatin, thereby participating in the inheritance of transcriptional repression, possibly in a locus-dependent manner (**Figure 2B**).

The Self-Propagation Model: Inherited Parental H3K27me3 Instructs Its Own Spreading Onto Nascent Chromatin

The multimeric structure of PRC2 confers two complementary activities to the complex that are essential for the self-perpetuation of H3K27me3 patterns. Indeed, in addition to the H3K27 trimethylation (*write*) function, PRC2 is also able to *read* H3K27me3 via the specific binding of the ESC subunit (Hansen et al., 2008; Margueron et al., 2009). Moreover, Su(z)12 that is not directly required for H3K27me3 binding, significantly enhances PRC2 affinity for H3K27me3 (Hansen et al., 2008). These built-in *writing* and *reading* properties of PRC2 are not independent from each other since the latter enhances the catalytic activity of the former. Indeed, H3K27me3 binding induces a conformational change of ESC that allosterically stimulates the catalytic activity of E(z) (Margueron et al., 2009). This type of positive feedback loop between chromatin *readers* and *writers* is proposed to be the hallmark property of self-sustained epigenetic memory systems (Reinberg and Vales, 2018). The ability to propagate H3K27me3 over large chromatin domains could provide robustness to PRC2-mediated silencing by limiting the effect of the dilution of H3K27me3 and preventing transcriptional reactivation after replication (Xu et al., 2012). It might also compensate for the stochasticity of parental histone distribution to nascent chromatin, thereby resulting in equal spreading of the mark over daughter strands (Ramachandran and Henikoff, 2015). Thus, faithful restoration of H3K27me3 domains after replication would largely rely on the recycling of parental H3K27me3-containing nucleosomes to nascent chromatin that, in turn, instruct the recruitment of PRC2 and stimulate its *write-and-read* property, leading to the propagation of the mark (**Figure 2C**, top).

The mechanisms that spatially limit H3K27me3 spreading to preserve the boundaries of H3K27me3 regions through DNA replication are still poorly understood (Yu et al., 2019). H3K27me3 demethylases could be involved in this process, such as the Arabidopsis Jumonji-type EARLY FLOWERING 6 (ELF6), RELATIVE OF EARLY FLOWERING 6 (REF6), and JM13 that restricts H3K27me3 domains in a tissue-specific manner (Yan et al., 2018) or the mammalian KDM6A/UTX that clears up H3K27me3 from tissue-specific enhancers (Saxena et al., 2017). Whether these

activities directly contribute to the faithful restoration of PRC2-mediated regulation upon replication remains to be directly investigated.

A Change of Paradigm? the Genomic Bookmarking Hypothesis

The prevalence of the self-propagation model described above has been recently challenged by *in vivo* studies suggesting that the inheritance of parental H3K27me3 is not always sufficient to perpetuate long-term transcriptional repression.

In Drosophila, polycomb response elements (PRE) are *cis*-regulatory sequences that locally recruit PRC2 and are necessary and sufficient to mediate long-term silencing (Schuettengruber et al., 2017). Whereas the function of PREs was initially associated with the nucleation of PRC2 to its targets, recent results suggest that these *cis*-elements might also be required for the spreading of H3K27me3 in nascent chromatin and the maintenance of transcriptional silencing through multiple generations of cells. Indeed, excision of a PRE responsible for the repression of the nearby gene resulted in the dilution of H3K27me3 around the excision site and in its transcriptional reactivation within few cells divisions (Coleman and Struhl, 2017; Laprell et al., 2017). However, this decrease in H3K27me3 levels was less important than expected by passive dilution, indicating that PRC2 still maintains a roaming, PRE-independent activity (Coleman and Struhl, 2017). These results argue in favor of a model in which long-term transcriptional silencing also relies on *cis*-regulatory elements that act as bookmarks to anchor PRC2 at silent loci (**Figure 2C**, bottom). Interestingly, modeling and simulations of H3K27me3 genomic distribution in Drosophila embryos based on this bookmarking model showed that PRE excision, rather than DNA replication, can destabilize H3K27me3 domains (Michieletto et al., 2018). Understanding how many genes rely on this recruiting mechanism and at which step of the replication process such *cis*-regulatory elements come into play to maintain the silenced status across cell division will require further investigations.

In contrast to Drosophila, few PRE-like *cis*-regulatory elements have been characterized in plants (Berger et al., 2011; Förderer et al., 2016; Xiao et al., 2017; Zhou et al., 2018) and mammals (Woo et al., 2010; Schorderet et al., 2013). Furthermore, nucleosome-free and hypomethylated CpG islands in gene regulatory regions were found to act as PRC2 recruitment sites in mammals (Mendenhall et al., 2010; Lynch et al., 2012; Klose et al., 2013; Riising et al., 2014; Højfeldt et al., 2018; Oksuz et al., 2018). *In vivo* and *in vitro* deletion of such PRC2 recruitment sites within the *HoxD* cluster and other loci did not lead to a reduction of H3K27me3 levels around the deletion sites (Schorderet et al., 2013; Oksuz et al., 2018), suggesting that neighboring H3K27me3 levels may be sufficient to recruit PRC2 and maintain the mark across the cluster. However, the kinetics of H3K27me3 deposition in mouse ESCs (mESCs) lacking a PRC2 recruitment site was slowed down compared to the wild-type situation (Oksuz et al., 2018). Similar excision experiments at endogenous loci in Arabidopsis would help determining whether such *cis*-elements also impact on the maintenance of gene repression via PRC2 in plants.

As in Drosophila studies, recent observations in mESCs mitigate the prevalent role of H3K27me3 in recruiting PRC2 at its genomics targets. Indeed, H3K27me3 patterns were accurately re-established via *de novo* methylation by PRC2 in mESCs in which H3K27me3 was totally erased from the whole genome, suggesting that additional cues are sufficient to recruit PRC2 to chromatin independently from H3K27me3 (Højfeldt et al., 2018; **Figure 2C**, bottom). Whether such cues are *cis*-encoded or result from unidentified factors associated with initial H3K27me3 deposition remains to be determined. For instance, short non-coding RNA transcribed from CpG islands at genes repressed independently of PRC2 have been demonstrated to dynamically recruit PRC2 via Su(z)12, thus participating to silencing maintenance (Kanhere et al., 2010).

The involvement of *cis*-encoded elements in conveying epigenetic memory is also suggested by observations in plant and yeast. During the vernalization process, the *FLOWERING LOCUS C* (*FLC*) gene gradually acquires H3K27me3 in a small domain of approximately three nucleosomes via *de novo* PRC2 recruitment. In a second phase, H3K27me3 then spreads across the whole locus in an *LHP1*-dependent manner to ensure long-term repression. In the *lhp1* mutant, although spreading is affected, H3K27me3 deposition at the nucleation site is maintained across mitoses much longer than predicted if inheritance was ensured exclusively by the stochastic redistribution of parental histones (Yang et al., 2017). Epigenetic memory independent of histone inheritance has also been reported for small heterochromatin domains in yeast, the silenced state of which is inherited at a higher rate than predicted (Saxton and Rine, 2019).

Taken together, these recent advances indicate that the recruitment of PRC2 to nascent chromatin is likely to be even more multifactorial than initially proposed (Margueron and Reinberg, 2011), involving not only self-propagation mechanisms but also H3K27me3-independent cues such as *cis*-regulatory elements and DNA-binding factors (**Figure 2**). As suggested by the differences observed between drosophila, mammals, and plants, these cues are likely to be both locus- and organism-dependent. These differences may reflect evolutionary changes in fine-tuning the mitotic inheritance of H3K27me3-mediated transcriptional silencing in order to meet distinct developmental strategies.

ROLE OF H3K27me3 INHERITANCE IN CELL FATE DECISIONS AND DEVELOPMENTAL TRANSITIONS

Faithful maintenance of H3K27me3 landscape provides a robust memory system that contributes to safeguard the stability of gene expression patterns, hence cell identity,

through multiple generations. However, the coordinated and specific changes of transcriptional programs that drive cell fate acquisition entail some flexibility in this PRC2-based memory. Alterations of H3K27me3 deposition at few critical genomic loci, such as those encoding developmental regulators, can be sufficient to trigger major transcriptional changes, as recently exemplified for stomata differentiation in Arabidopsis (Lee et al., 2019). Whereas the release from PRC2 silencing can be achieved by multiple means in interphasic cells including the antagonist action of Trithorax group proteins as well as DNA-binding factors (Brand et al., 2019), recent evidence suggests that local interruption or interference with the mechanisms underlying H3K27me3 restoration during replication could be part of the differentiation process.

Time to Forget: How Chromatin Replication Might Enable Genes to Escape From PRC2-Mediated Silencing?

Mathematical modeling suggests that transient dilution of H3K27me3 during chromatin replication weakens the stability of silent chromatin by enhancing fast-switching bistability between the silent and active states (Sneppen and Ringrose, 2019). Whereas dilution of H3K27me3 during chromatin replication is likely to promote this instability, additional mechanisms are necessary to counteract the maintenance activities described in the previous section and potentiate the escape from PRC2 repression. Conceptually, release of PRC2 repression during replication could be achieved at a given locus through distinct, non-mutually exclusive mechanisms that would locally prevent the transfer of H3 parental histones into nascent chromatin, bias the distribution of parental H3K27me3 into daughter strands or hinder PRC2 recruitment or activity over nascent chromatin.

Biasing H3K27me3 Inheritance to Break the Symmetry Between Daughter Chromatins?

Recent work in *Drosophila* male germline stem cells showed that parental H3 can be locally re-deposited in a preferential manner to the leading strand during DNA replication, suggesting that asymmetric division can arise from asymmetric inheritance of parental histones (Wooten et al., 2019). Although the factors responsible for this asymmetric deposition of parental H3 remain to be identified, regulation of asymmetric division could rely on factors disrupting specifically one of the strand-specific recycling pathways of parental H3 (Gan et al., 2018; Petryk et al., 2018; Yu et al., 2018; **Figures 1B,B′**). How such a mechanism affects the inheritance of H3K27me3-marked parental histones and whether it directly participates in asymmetric cell fate decisions requires further investigations in animals and plants.

Modulation of Replication-Dependent H3K27me3 Inheritance Enables Identity Switches

Restoration kinetics of pre-replication H3K27me3 levels may be critical to set out a window of opportunity during which a locus can escape from PRC2-mediated silencing. Interestingly, the kinetics of H3K27me3 restoration seem to differ between plant and animal cells. In mammalian cells, H3K27me3 levels are not fully restored before the late post-mitotic G1 phase (Xu et al., 2012; Alabert et al., 2015). Such a slow methylation rate has been proposed to filter out fluctuations of transcription factors, thus ensuring the stability of silent states through cell divisions (Berry et al., 2017). In tobacco BY-2 cells though, H3K27me3 levels are restored as soon as early pre-mitotic G2 phase. This suggests that plant cells have evolved specific mechanisms allowing for rapid restoration of H3K27me3 after DNA replication (Jiang and Berger, 2017). In contrast to animal cells in which PRC2 is the only complex catalyzing mono-, di-, and tri-methylation of H3K27, in plant cells a pathway involving the plant-specific H3K27 mono-methylases ATXR5/6 exist, independently from PRC2 (Jacob et al., 2014). Anchoring of both ATXR5/6 and PRC2 at the replication fork might favor a rapid restoration of H3K27me3 after replication via the deposition of H3K27me1 on newly synthesized nucleosome, which could serve as a template for PRC2 (Jiang and Berger, 2017). However, understanding the extent to which the kinetics of H3K27me3 restoration impacts on the ability of cells to perpetuate PRC2-driven transcriptional memory requires further studies.

Modulation of H3K27me3 restoration kinetics has been associated with cell fate decisions in mammalian cells. For instance, induction of mESC differentiation slows down the restoration of H3K27me3 due to the recruitment of the H3K27me3 demethylase, ubiquitously transcribed tetratricopeptide repeat X chromosome (UTX) downstream of the replication fork, thereby preventing the spreading of H3K27me3 (Petruk et al., 2017). Slowing down the restoration of H3K27me3 might enlarge the window of opportunity during which chromatin is in a state permissive for transcriptional reprogramming, allowing for transcription factors to bind and activate their target genes. In agreement with this, computational simulations suggest that H3K27me3 demethylase activity during replication does favor bistability switching to the active state (Sneppen and Ringrose, 2019). Determining whether the EFL6/REF6/JMJ13 homologs also participate in such replication-coupled transcriptional reprogramming awaits direct investigations.

In addition, differentiation of ESCs is enhanced by ex14D-EZH2, a splicing variant of EZH2 with reduced catalytic activity (Mu et al., 2018). This indicates that the presence of tightly regulated variants of PRC2 may facilitate differentiation by impeding rapid H3K27me3 spreading in nascent chromatin at specific loci.

Finally, the equilibrium between the kinetics of H3K27 trimethylation and the mitotic rate may strongly influence the ability of a cell to perpetuate PRC2-mediated silencing through mitosis. Intuitively, if the cell cycle length is shorter than the time required for full H3K27me3 restoration, then H3K27me3 could be gradually lost within few cell divisions. In Arabidopsis, a coupling between the regulation of cell division timing and replication-dependent dilution of H3K27me3 has been proposed to control the termination of the stem cell pool during floral development (Sun et al., 2014). This coupling fine-tunes the number of floral organs produced by the meristem and thus conditions the reproductive fitness of the plant. Interestingly, this mechanism might be conserved in other dicots such as

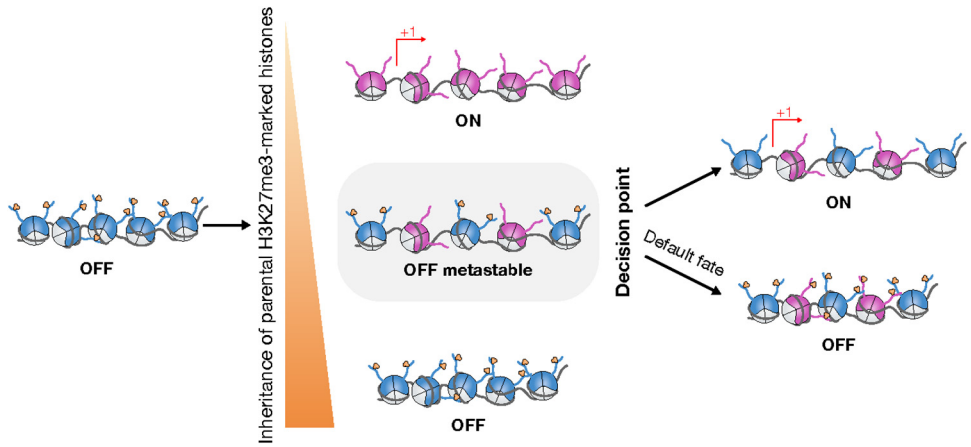

FIGURE 3 | Chromatin replication can potentiate cell fate transitions. During chromatin replication, asymmetric inheritance of parental H3K27me3 can lead to transcriptional reactivation in only one daughter cell **(Middle, Top, Bottom)**. In case of symmetric inheritance of parental H3K27me3, repressive chromatin is switched from a stable repressive state to a metastable state that is permissive for epigenetic reprogramming **(Middle)**. By default, H3K27me3 landscapes are restored such that repressive chromatin remains silent **(Right, Bottom)**. Nevertheless, local disruption of the restoration of repressive chromatin can trigger specific changes in gene expression **(Right, Top)**.

tomato (Bollier et al., 2018) and monocots such as the rice (Conrad et al., 2014).

Chromatin Replication Can Potentiate PRC2-Mediated Silencing

Whereas cells can take advantage of chromatin destabilization during the S-phase to unlock the transcription of specific PRC2 target genes, chromatin replication was also reported to potentiate PRC2-mediated silencing. In ESCs, proper establishment of H3K27me3 at pluripotency genes such as Nanog, Oct4, and Sox2 is likely to be critical for pluripotency exit and rely on the local recruitment of PRC2 by CAF1 in S-phase (Cheng et al., 2019).

Whereas earlier studies in Arabidopsis showed that the repression of *FLC* established during the vernalization process is not maintained in post-mitotic cells of mature leaves (Finnegan and Dennis, 2007), replication was recently confirmed to be required for H3K27me3 spreading and the establishment of long-term silencing of *FLC* (Jiang and Berger, 2017; Sharif and Koseki, 2017; Yang et al., 2017). In keeping with this, mathematical modeling revealed that the sharp switch of *FLC* to the silent state is consistent with a replication-dependent spreading of H3K27me3 at the locus, suggesting that the coupling between PRC2-mediated silencing and chromatin replication can generate a quantitative integrator of environmental signals (Angel et al., 2011).

CONCLUSION

The S-phase is particularly challenging for the maintenance of transcriptional programs, hence for cell identity. Cell identity is safeguarded during chromatin replication by the inheritance of the H3K27me3 landscape, which enables the perpetuation of PRC2-mediated transcriptional repression. H3K27me3 inheritance relies on both the accurate re-deposition of parental H3K27me3-marked H3 (**Figure 1**) and the spreading of H3K27me3 downstream of the replication fork (**Figures 2**, **3**). Recent advances provide new evidence that cell identity switches during developmental processes are intrinsically coupled with chromatin replication and the regulation of PRC2-mediated silencing (**Figure 3**). These findings strongly support the hypothesis that the S-phase opens a window of opportunity for transcriptional reprogramming and cell fate decisions.

While our understanding of the molecular mechanisms underlying H3K27me3 inheritance is gradually increasing and points toward overall conservation between organisms, differences have also emerged in plants. Thus, separation of H3K27me1 from H3K27me3 catalysis into different pathways illustrates a plant-specific innovation that might directly impact on the kinetics of H3K27me3 re-establishment during replication. In addition, developmental processes more specific to plant biology, such as continuous growth or widespread endoreplication, could introduce additional differences in the mechanistic and developmental impacts of H3K27me3 inheritance. Further investigation of PRC2 interactions within the micro-environment of the replication fork will provide key insights to understand how H3K27me3 inheritance is modulated at specific genomic loci in order to fine-tune developmental processes in space and time.

AUTHOR CONTRIBUTIONS

AH and FR designed the outline of the manuscript with additional input from CJ. All authors contributed to the writing of the manuscript and approved the final manuscript. AH contributed to all figure designs.

ACKNOWLEDGMENTS

Research in the Roudier Laboratory was supported by a starting grant from the Programme Avenir Lyon Saint Etienne (ANR-11-IDEX-0007) and additional core funding from the Ecole Normale Supérieure de Lyon as well as the Agence Nationale de la Recherche to FR. CJ was the recipient of a doctoral grant from the French Ministère de l'Enseignement Supérieur, de la Recherche et de l'Innovation.

REFERENCES

Alabert, C., Barth, T. K., Reverón-Gómez, N., Sidoli, S., Schmidt, A., Jensen, O. N., et al. (2015). Two distinct modes for propagation of histone PTMs across the cell cycle. *Genes Dev.* 29, 585–590. doi: 10.1101/gad.256354.114

Alabert, C., Bukowski-Wills, J.-C., Lee, S.-B., Kustatscher, G., Nakamura, K., de Lima Alves, F., et al. (2014). Nascent chromatin capture proteomics determines chromatin dynamics during DNA replication and identifies unknown fork components. *Nat. Cell Biol.* 16, 281–293. doi: 10.1038/ncb2918

Anderson, A. E., Karandikar, U. C., Pepple, K. L., Chen, Z., Bergmann, A., and Mardon, G. (2011). The enhancer of trithorax and polycomb gene Caf1/p55 is essential for cell survival and patterning in drosophila development. *Dev. Camb. Engl.* 138, 1957–1966. doi: 10.1242/dev.058461

Angel, A., Song, J., Dean, C., and Howard, M. (2011). A Polycomb-based switch underlying quantitative epigenetic memory. *Nature* 476, 105–108. doi: 10.1038/nature10241

Annunziato, A. T. (2015). The fork in the road: histone partitioning during DNA replication. *Genes* 6, 353–371. doi: 10.3390/genes6020353

Barrero, J. M., González-Bayón, R., del Pozo, J. C., Ponce, M. R., and Micol, J. L. (2007). INCURVATA2 encodes the catalytic subunit of DNA polymerase α and interacts with genes involved in chromatin-mediated cellular memory in *Arabidopsis thaliana*. *Plant Cell* 19, 2822–2838. doi: 10.1105/tpc.107.054130

Benoit, M., Simon, L., Desset, S., Duc, C., Cotterell, S., Poulet, A., et al. (2019). Replication-coupled histone H3.1 deposition determines nucleosome composition and heterochromatin dynamics during *Arabidopsis* seedling development. *New Phytol.* 221, 385–398. doi: 10.1111/nph.15248

Berger, N., Dubreucq, B., Roudier, F., Dubos, C., and Lepiniec, L. (2011). Transcriptional regulation of Arabidopsis leafy cotyledon2 involves RLE, a cis-Element that regulates trimethylation of histone H3 at Lysine-27[W]. *Plant Cell* 23, 4065–4078. doi: 10.1105/tpc.111.087866

Berry, S., Dean, C., and Howard, M. (2017). Slow chromatin dynamics allow polycomb target genes to filter fluctuations in transcription factor activity. *Cell Syst.* 4, 445–457.e8. doi: 10.1016/j.cels.2017.02.013

Bollier, N., Sicard, A., Leblond, J., Latrasse, D., Gonzalez, N., Gévaudant, F., et al. (2018). At-MINI ZINC FINGER2 and Sl-INHIBITOR OF MERISTEM ACTIVITY, a conserved missing link in the regulation of floral meristem termination in *Arabidopsis* and Tomato. *Plant Cell* 30, 83–100. doi: 10.1105/tpc.17.00653

Brand, M., Nakka, K., Zhu, J., and Dilworth, F. J. (2019). Polycomb/Trithorax antagonism: cellular memory in stem cell fate and function. *Cell Stem Cell* 24, 518–533. doi: 10.1016/j.stem.2019.03.005

Cheloufi, S., Elling, U., Hopfgartner, B., Jung, Y. L., Murn, J., Ninova, M., et al. (2015). The histone chaperone CAF-1 safeguards somatic cell identity. *Nature* 528, 218–224. doi: 10.1038/nature15749

Cheloufi, S., and Hochedlinger, K. (2017). Emerging roles of the histone chaperone CAF-1 in cellular plasticity. *Curr. Opin. Genet. Dev.* 46, 83–94. doi: 10.1016/j.gde.2017.06.004

Cheng, L., Zhang, X., Wang, Y., Gan, H., Xu, X., Lv, X., et al. (2019). Chromatin assembly factor 1 (CAF-1) facilitates the establishment of facultative heterochromatin during pluripotency exit. *Nucleic Acids Res.* 47, 11114–11131. doi: 10.1093/nar/gkz858

Clémot, M., Molla-Herman, A., Mathieu, J., Huynh, J.-R., and Dostatni, N. (2018). The replicative histone chaperone CAF1 is essential for the maintenance of identity and genome integrity in adult stem cells. *Dev. Camb. Engl.* 145:dev161190. doi: 10.1242/dev.161190

Coleman, R. T., and Struhl, G. (2017). Causal role for inheritance of H3K27me3 in maintaining the OFF state of a drosophila HOX gene. *Science* 356:eaai8236. doi: 10.1126/science.aai8236

Conrad, L. J., Khanday, I., Johnson, C., Guiderdoni, E., An, G., Vijayraghavan, U., et al. (2014). The polycomb group gene EMF2B is essential for maintenance of floral meristem determinacy in rice. *Plant J.* 80, 883–894. doi: 10.1111/tpj.12688

del Olmo, I., López, J. A., Vázquez, J., Raynaud, C., Piñeiro, M., and Jarillo, J. A. (2016). Arabidopsis DNA polymerase ϵ recruits components of Polycomb repressor complex to mediate epigenetic gene silencing. *Nucleic Acids Res.* 44, 5597–5614. doi: 10.1093/nar/gkw156

del Olmo, I., López-González, L., Martín-Trillo, M. M., Martínez-Zapater, J. M., Piñeiro, M., and Jarillo, J. A. (2010). EARLY IN SHORT DAYS 7 (ESD7) encodes the catalytic subunit of DNA polymerase epsilon and is required for flowering repression through a mechanism involving epigenetic gene silencing. *Plant J. Cell Mol. Biol.* 61, 623–636. doi: 10.1111/j.1365-313X.2009.04093.x

Derkacheva, M., Steinbach, Y., Wildhaber, T., Mozgová, I., Mahrez, W., Nanni, P., et al. (2013). Arabidopsis MSI1 connects LHP1 to PRC2 complexes. *EMBO J.* 32, 2073–2085. doi: 10.1038/emboj.2013.145

Escobar, T., Oksuz, O., Descostes, N., Bonasio, R., and Reinberg, D. (2018). Precise re-deposition of nucleosomes on repressive chromatin domains sustain epigenetic inheritance during DNA replication. *BioRxiv* [Preprint], doi: 10.1101/418707

Feng, J., and Lu, J. (2017). LHP1 Could Act as an Activator and a Repressor of Transcription in Plants. *Front. Plant Sci.* 8:2041. doi: 10.3389/fpls.2017.02041

Finnegan, E. J., and Dennis, E. S. (2007). Vernalization-induced trimethylation of histone H3 lysine 27 at FLC is not maintained in mitotically quiescent cells. *Curr. Biol. CB* 17, 1978–1983. doi: 10.1016/j.cub.2007.10.026

Förderer, A., Zhou, Y., and Turck, F. (2016). The age of multiplexity: recruitment and interactions of Polycomb complexes in plants. *Curr. Opin. Plant Biol.* 29, 169–178. doi: 10.1016/j.pbi.2015.11.010

Francis, N. J., Follmer, N. E., Simon, M. D., Aghia, G., and Butler, J. D., (2009). Polycomb proteins remain bound to chromatin and DNA during DNA replication *in vitro*. *Cell* 137, 110–122. doi: 10.1016/j.cell.2009.02.017

Gan, H., Serra-Cardona, A., Hua, X., Zhou, H., Labib, K., Yu, C., et al. (2018). The Mcm2-Ctf4-Polα axis facilitates parental histone H3-H4 transfer to lagging strands. *Mol. Cell* 72, 140.e–151.e. doi: 10.1016/j.molcel.2018.09.001

Hammond, C. M., Strømme, C. B., Huang, H., Patel, D. J., and Groth, A. (2017). Histone chaperone networks shaping chromatin function. *Nat. Rev. Mol. Cell Biol.* 18, 141–158. doi: 10.1038/nrm.2016.159

Hansen, K. H., Bracken, A. P., Pasini, D., Dietrich, N., Gehani, S. S., Monrad, A., et al. (2008). A model for transmission of the H3K27me3 epigenetic mark. *Nat. Cell Biol.* 10, 1291–1300. doi: 10.1038/ncb1787

He, H., Li, Y., Dong, Q., Chang, A.-Y., Gao, F., Chi, Z., et al. (2017). Coordinated regulation of heterochromatin inheritance by Dpb3–Dpb4 complex. *Proc. Natl. Acad. Sci.* 114, 12524–12529. doi: 10.1073/pnas.1712961114

Højfeldt, J. W., Laugesen, A., Willumsen, B. M., Damhofer, H., Hedehus, L., Tvardovskiy, A., et al. (2018). Accurate H3K27 methylation can be established de novo by SUZ12-directed PRC2. *Nat. Struct. Mol. Biol.* 25, 225–232. doi: 10.1038/s41594-018-0036-6

Huang, H., Strømme, C. B., Saredi, G., Hödl, M., Strandsby, A., González-Aguilera, C., et al. (2015). A unique binding mode enables MCM2 to chaperone histones H3–H4 at replication forks. *Nat. Struct. Mol. Biol.* 22, 618–626. doi: 10.1038/nsmb.3055

Hyun, Y., Yun, H., Park, K., Ohr, H., Lee, O., Kim, D.-H., et al. (2013). The catalytic subunit of *Arabidopsis* DNA polymerase α ensures stable maintenance of histone modification. *Dev. Camb. Engl.* 140, 156–166. doi: 10.1242/dev.084624

Jacob, Y., Bergamin, E., Donoghue, M. T. A., Mongeon, V., LeBlanc, C., Voigt, P., et al. (2014). Selective methylation of histone H3 variant H3.1 regulates heterochromatin replication. *Science* 343, 1249–1253. doi: 10.1126/science.1248357

Jiang, D., and Berger, F. (2017). DNA replication–coupled histone modification maintains Polycomb gene silencing in plants. *Science* 357, 1146–1149. doi: 10.1126/science.aan4965

Kalb, R., Latwiel, S., Baymaz, H. I., Jansen, P. W. T. C., Müller, C. W., Vermeulen, M., et al. (2014). Histone H2A monoubiquitination promotes histone H3 methylation in Polycomb repression. *Nat. Struct. Mol. Biol.* 21, 569–571. doi: 10.1038/nsmb.2833

Kanhere, A., Viiri, K., Araújo, C. C., Rasaiyaah, J., Bouwman, R. D., Whyte, W. A., et al. (2010). Short RNAs are transcribed from repressed polycomb target genes and interact with polycomb repressive complex-2. *Mol. Cell* 38, 675–688. doi: 10.1016/j.molcel.2010.03.019

Kaya, H., Shibahara, K. I., Taoka, K. I., Iwabuchi, M., Stillman, B., and Araki, T. (2001). FASCIATA genes for chromatin assembly factor-1 in arabidopsis maintain the cellular organization of apical meristems. *Cell* 104, 131–142. doi: 10.1016/s0092-8674(01)00197-0

Klose, R. J., Cooper, S., Farcas, A. M., Blackledge, N. P., and Brockdorff, N. (2013). Chromatin sampling–an emerging perspective on targeting polycomb repressor proteins. *PLoS Genet.* 9:e1003717. doi: 10.1371/journal.pgen.1003717

Laprell, F., Finkl, K., and Müller, J. (2017). Propagation of Polycomb-repressed chromatin requires sequence-specific recruitment to DNA. *Science* 356, 85–88. doi: 10.1126/science.aai8266

Lee, L. R., Wengier, D. L., and Bergmann, D. C. (2019). Cell-type–specific transcriptome and histone modification dynamics during cellular reprogramming in the *Arabidopsis* stomatal lineage. *Proc. Natl. Acad. Sci. U.S.A.* 116, 21914–21924. doi: 10.1073/pnas.1911400116

Li, H., and Luan, S. (2011). The cyclophilin AtCYP71 interacts with CAF-1 and LHP1 and functions in multiple chromatin remodeling processes. *Mol. Plant* 4, 748–758. doi: 10.1093/mp/ssr036

Lynch, M. D., Smith, A. J. H., De Gobbi, M., Flenley, M., Hughes, J. R., Vernimmen, D., et al. (2012). An interspecies analysis reveals a key role for unmethylated CpG dinucleotides in vertebrate Polycomb complex recruitment. *EMBO J.* 31, 317–329. doi: 10.1038/emboj.2011.399

Margueron, R., Justin, N., Ohno, K., Sharpe, M. L., Son, J., Drury, W. J., et al. (2009). Role of the polycomb protein EED in the propagation of repressive histone marks. *Nature* 461, 762–767. doi: 10.1038/nature08398

Margueron, R., and Reinberg, D. (2011). The Polycomb Complex PRC2 and its Mark in Life. *Nature* 469, 343–349. doi: 10.1038/nature09784

Masai, H., and Foiani, M. (2018). *DNA Replication: From Old Principles to New Discoveries*. Berlin: Springer.

Mendenhall, E. M., Koche, R. P., Truong, T., Zhou, V. W., Issac, B., Chi, A. S., et al. (2010). GC-rich sequence elements recruit PRC2 in mammalian ES cells. *PLoS Genet.* 6:e1001244. doi: 10.1371/journal.pgen.1001244

Michieletto, D., Chiang, M., Colì, D., Papantonis, A., Orlandini, E., Cook, P. R., et al. (2018). Shaping epigenetic memory via genomic bookmarking. *Nucleic Acids Res.* 46, 83–93. doi: 10.1093/nar/gkx1200

Mikulski, P., Hohenstatt, M. L., Farrona, S., Smaczniak, C., Stahl, Y., Kalyanikrishna, et al. (2019). The chromatin-associated protein PWO1 interacts with plant nuclear lamin-like components to regulate nuclear size. *Plant Cell* 31, 1141–1154. doi: 10.1105/tpc.18.00663

Mozgova, I., and Hennig, L. (2015). The polycomb group protein regulatory network. *Annu. Rev. Plant Biol.* 66, 269–296. doi: 10.1146/annurev-arplant-043014-115627

Mu, W., Starmer, J., Yee, D., and Magnuson, T. (2018). EZH2 variants differentially regulate polycomb repressive complex 2 in histone methylation and cell differentiation. *Epigenet. Chromat.* 11:71. doi: 10.1186/s13072-018-0242-9

Oksuz, O., Narendra, V., Lee, C.-H., Descostes, N., LeRoy, G., Raviram, R., et al. (2018). Capturing the onset of PRC2-mediated repressive domain formation. *Mol. Cell* 70, 1149–1162.e5. doi: 10.1016/j.molcel.2018.05.023

Pedroza-Garcia, J.-A., De Veylder, L., and Raynaud, C. (2019). Plant DNA Polymerases. *Int. J. Mol. Sci.* 20:4814. doi: 10.3390/ijms20194814

Petruk, S., Cai, J., Sussman, R., Sun, G., Kovermann, S. K., Mariani, S. A., et al. (2017). Delayed accumulation of H3K27me3 on nascent DNA is essential for recruitment of transcription factors at early stages of stem cell differentiation. *Mol. Cell* 66, 247–257.e5. doi: 10.1016/j.molcel.2017.03.006

Petryk, N., Dalby, M., Wenger, A., Stromme, C. B., Strandsby, A., Andersson, R., et al. (2018). MCM2 promotes symmetric inheritance of modified histones during DNA replication. *Science* 361, 1389–1392. doi: 10.1126/science.aau0294

Ramachandran, S., Ahmad, K., and Henikoff, S. (2017). Capitalizing on disaster: establishing chromatin specificity behind the replication fork. *Bioessays* 39:1600150. doi: 10.1002/bies.201600150

Ramachandran, S., and Henikoff, S. (2015). Replicating nucleosomes. *Sci. Adv.* 1:e1500587. doi: 10.1126/sciadv.1500587

Reinberg, D., and Vales, L. D. (2018). Chromatin domains rich in inheritance. *Science* 361, 33–34. doi: 10.1126/science.aat7871

Reverón-Gómez, N., González-Aguilera, C., Stewart-Morgan, K. R., Petryk, N., Flury, V., Graziano, S., et al. (2018). Accurate recycling of parental histones reproduces the histone modification landscape during DNA replication. *Mol. Cell.* 72, 239–249.e5. doi: 10.1016/j.molcel.2018.08.010

Riising, E. M., Comet, I., Leblanc, B., Wu, X., Johansen, J. V., and Helin, K. (2014). Gene silencing triggers polycomb repressive complex 2 recruitment to CpG islands genome wide. *Mol. Cell* 55, 347–360. doi: 10.1016/j.molcel.2014.06.005

Rutowicz, K., Lirski, M., Mermaz, B., Teano, G., Schubert, J., Mestiri, I., et al. (2019). Linker histones are fine-scale chromatin architects modulating developmental decisions in *Arabidopsis*. *Genome Biol.* 20:157. doi: 10.1186/s13059-019-1767-3

Saxena, M., Roman, A. K. S., O'Neill, N. K., Sulahian, R., Jadhav, U., and Shivdasani, R. A. (2017). Transcription factor-dependent "anti-repressive" mammalian enhancers exclude H3K27me3 from extended genomic domains. *Genes Dev.* 31, 2391–2404. doi: 10.1101/gad.308536.117

Saxton, D. S., and Rine, J. (2019). Epigenetic memory independent of symmetric histone inheritance. *eLife* 8:e51421. doi: 10.7554/eLife.51421

Schorderet, P., Lonfat, N., Darbellay, F., Tschopp, P., Gitto, S., Soshnikova, N., et al. (2013). A genetic approach to the recruitment of PRC2 at the HoxD Locus. *PLoS Genet.* 9:e1003951. doi: 10.1371/journal.pgen.1003951

Schuettengruber, B., Bourbon, H.-M., Croce, L. D., and Cavalli, G. (2017). Genome regulation by polycomb and trithorax: 70 Years and counting. *Cell* 171, 34–57. doi: 10.1016/j.cell.2017.08.002

Serra-Cardona, A., and Zhang, Z. (2018). Replication-coupled nucleosome assembly in the passage of epigenetic information and cell identity. *Trends Biochem. Sci.* 43, 136–148. doi: 10.1016/j.tibs.2017.12.003

Sharif, J., and Koseki, H. (2017). No winter lasts forever: polycomb complexes convert epigenetic memory of cold into flowering. *Dev. Cell* 42, 563–564. doi: 10.1016/j.devcel.2017.09.004

Sharif, J., and Koseki, H. (2018). Rewriting the past: de novo activity of PRC2 restores global H3K27 methylation patterns. *Nat. Struct. Mol. Biol.* 25:197. doi: 10.1038/s41594-018-0039-33

Snedeker, J., Wooten, M., and Chen, X. (2017). The inherent asymmetry of DNA replication. *Annu. Rev. Cell Dev. Biol.* 33, 291–318. doi: 10.1146/annurev-cellbio-100616-060447

Sneppen, K., and Ringrose, L. (2019). Theoretical analysis of Polycomb-Trithorax systems predicts that poised chromatin is bistable and not bivalent. *Nat. Commun.* 10, 1–18. doi: 10.1038/s41467-019-10130-2

Sun, B., Looi, L.-S., Guo, S., He, Z., Gan, E.-S., Huang, J., et al. (2014). Timing Mechanism Dependent on Cell Division Is Invoked by Polycomb Eviction in Plant Stem Cells. *Science* 343:1248559. doi: 10.1126/science.1248559

Teves, S. S., and Henikoff, S. (2014). DNA torsion as a feedback mediator of transcription and chromatin dynamics. *Nucleus* 5, 211–218. doi: 10.4161/nucl.29086

Veluchamy, A., Jégu, T., Ariel, F., Latrasse, D., Mariappan, K. G., Kim, S.-K., et al. (2016). LHP1 regulates H3K27me3 spreading and shapes the three-dimensional conformation of the *Arabidopsis* genome. *PLoS One* 11:e0158936. doi: 10.1371/journal.pone.0158936

Woo, C. J., Kharchenko, P. V., Daheron, L., Park, P. J., and Kingston, R. E. (2010). A region of the human HOXD cluster that confers polycomb-group responsiveness. *Cell* 140, 99–110. doi: 10.1016/j.cell.2009.12.022

Wooten, M., Snedeker, J., Nizami, Z. F., Yang, X., Ranjan, R., Urban, E., et al. (2019). Asymmetric histone inheritance via strand-specific incorporation and biased replication fork movement. *Nat. Struct. Mol. Biol.* 26, 732–743. doi: 10.1038/s41594-019-0269-z

Xiao, J., Jin, R., and Wagner, D. (2017). Developmental transitions: integrating environmental cues with hormonal signaling in the chromatin landscape in plants. *Genome Biol.* 18:88. doi: 10.1186/s13059-017-1228-9

Xu, M., Wang, W., Chen, S., and Zhu, B. (2012). A model for mitotic inheritance of histone lysine methylation. *EMBO Rep.* 13, 60–67. doi: 10.1038/embor.2011.206

Yan, W., Chen, D., Smaczniak, C., Engelhorn, J., Liu, H., Yang, W., et al. (2018). Dynamic and spatial restriction of Polycomb activity by

plant histone demethylases. *Nat. Plants* 4:681. doi: 10.1038/s41477-018-0219-5

Yang, H., Berry, S., Olsson, T. S. G., Hartley, M., Howard, M., and Dean, C. (2017). Distinct phases of Polycomb silencing to hold epigenetic memory of cold in *Arabidopsis*. *Science* 357, 1142–1145. doi: 10.1126/science.aan1121

Yee, W. B., Delaney, P. M., Vanderzalm, P. J., Ramachandran, S., and Fehon, R. G. (2019). The CAF-1 complex couples hippo pathway target gene expression and DNA replication. *Mol. Biol. Cell* 30, 2929–2942. doi: 10.1091/mbc.E19-07-0387

Yu, C., Gan, H., Serra-Cardona, A., Zhang, L., Gan, S., Sharma, S., et al. (2018). A mechanism for preventing asymmetric histone segregation onto replicating DNA strands. *Science* 361, 1386–1389. doi: 10.1126/science.aat8849

Yu, J.-R., Lee, C.-H., Oksuz, O., Stafford, J. M., and Reinberg, D. (2019). PRC2 is high maintenance. *Genes Dev.* 33, 903–935. doi: 10.1101/gad.325050.119

Zhou, Y., Romero-Campero, F. J., Gómez-Zambrano, Á, Turck, F., and Calonje, M. (2017a). H2A monoubiquitination in *Arabidopsis thaliana* is generally independent of LHP1 and PRC2 activity. *Genome Biol* 18:69. doi: 10.1186/s13059-017-1197-z

Zhou, Y., Tergemina, E., Cui, H., Förderer, A., Hartwig, B., Velikkakam James, G., et al. (2017b). Ctf4-related protein recruits LHP1-PRC2 to maintain H3K27me3 levels in dividing cells in *Arabidopsis thaliana*. *Proc. Natl. Acad. Sci. U.S.A.* 114, 4833–4838. doi: 10.1073/pnas.1620955114

Zhou, Y., Wang, Y., Krause, K., Yang, T., Dongus, J. A., Zhang, Y., et al. (2018). Telobox motifs recruit CLF/SWN-PRC2 for H3K27me3 deposition via TRB factors in *Arabidopsis*. *Nat. Genet.* 50, 638–644. doi: 10.1038/s41588-018-0109-9

Conflict of Interest: The authors declare that the research was conducted in the absence of any commercial or financial relationships that could be construed as a potential conflict of interest.

1.4 The Arabidopsis root as a model of cell differentiation

Root development relies on a highly-organised structure that undergoes stereotypical cell divisions to allow continuous growth (Fig. 3). Within the meristem, the stem cell niche is organized around the quiescent center with contacting stem cells or initials. These initials asymmetrically divide to produce transit-amplifying cells which then undergo rapid divisions before reaching the transition zone to begin elongation and acquire their final identity. This continuous process creates an apico-basal differentiation gradient, with the stem cell niche at the tip of the root and the end-differentiated cells on the opposite side. Another shorter differentiation gradient is present distal to the stem cell niche, which leads to the formation of the root cap.

The relative simplicity of root organogenesis has led to its use as a model of choice to address developmental biology questions and in particular understand how gene networks interact in each cell type as the organ develops. For example, FACS-sorted cells transcriptomics assayed the dynamics of gene expression (Brady et al., 2007), and the use of alternative splicing on a genome-wide scale (Li et al., 2016). More recently, single-cell RNA-seq analysis have identified transitional states between cell identities (Ryu et al., 2019; Zhang et al., 2019; Denyer et al., 2019; Shulse et al., 2019; Jean-Baptiste et al., 2019) and ultimately have provided evidence challenging the current dogmas on cell identity, possibly overly dependent on morphological and identity markers (Ye and Sarkar, 2018; Shulse et al., 2019).

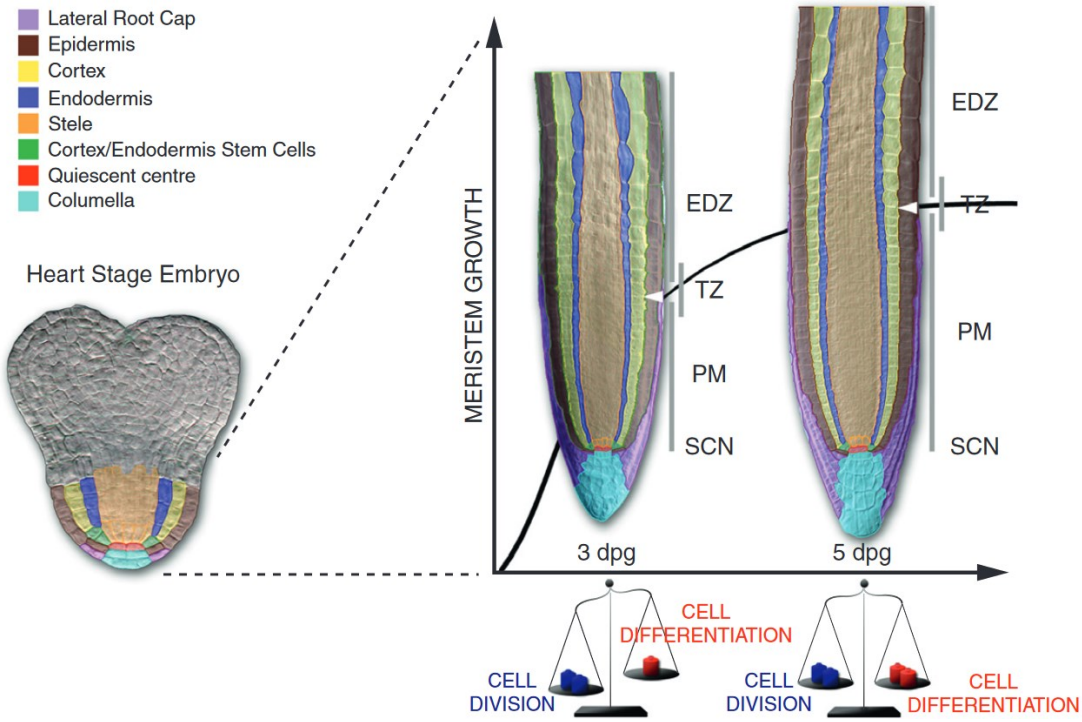

Figure 3 The development of the Arabidopsis root meristem. **(Left)** Heart stage Arabidopsis embryo showing the origin of the root meristem. **(Right)** Roots at 3 and 5 days post germination (dpg). Cell types are indicated via false colouration. Upon germination, the root undergoes rapid divisions to expand the meristem (size indicated by white arrowhead). At 5dpg, the balance between cell division rate and cell differentiation rate equilibrates and the size of the meristem is constant. SCN : stem cell niche; PM: proximal meristem; TZ: transition zone; EDZ: elongation/differentiation zone *Adapted from Perilli et al., 2011*

2. Objectives

The essential role of PRC2 activity in regulating root development has been previously illustrated by the phenotypic alterations triggered by partial or total PRC2 deficiency (de Lucas et al., 2016; Aichinger et al., 2011). Furthermore, the dynamic nature of H3K27me3 between different cell types in the root has been reported (de Lucas et al., 2016; Deal and Henikoff, 2010). Coupled with the inherent accessibility and transparency of the root, this makes an excellent model to study the effects of PRC2 complexes along a differentiation gradient.

My first aim is to determine the overlapping and specific roles of SWN- and CLF-PRC2 complexes in roots. Next, to understand how PRC2 controls root growth, I investigate its role both in maintaining root stem cell niche homeostasis and the impact of PRC2 regulation as cells exit the stem cell niche. I present my results in the two following sections organised as manuscript drafts, each containing their dedicated introduction, and discussion.

In section 3, I present the results of the work I conducted to understand the respective role of SWN and CLF that provide evidence supporting a complex cooperation between SWN and CLF subunits within the same cells in the regulation of H3K27me3 levels over genes.

In section 4, I address the role of PRC2 regulation in the QC on SCN activity, and further investigate how this regulation also shapes gene expression patterning as cells change identity from QC to mature cell types.

3. Quantitative tuning of plant PRC2 complexes controls H3K27me3 deposition during development

3.1 Introduction

Our team is interested in understanding the different roles that SWN- and CLF-PRC2 have during early stages of development. Ana Gonzales Morao, a previous PhD student in the team, characterised the expression patterns of *SWN* and *CLF* in the root tip (de Lucas et al., 2016) and initiated the characterisation of the developmental and molecular defects triggered by the absence of SWN or CLF on root development. She found that *clf* mutant roots grow slightly faster than WT, while *swn* roots were indistinguishable from the wild type (Fig. 4a-b). To see if this may be linked to levels of H3K27me3 in roots, she assayed global levels of the histone mark by Western Blot and found a massive loss of H3K27me3 in *clf* but not *swn* (Fig. 4c). This confirms the role of CLF as the major catalyst of H3K27me3 post-germination, but leaves the role of *SWN* unclear. In accordance with observed redundancy between the subunits, *swn clf* double mutants have very short roots while losing all H3K27me3 (Fig. 4a-c).

To investigate further the role of SWN and CLF, I have analysed their expression pattern in the root tip and established their respective repertoire of targets in the genome by checking AtE(z) occupancy, as well as determining H3K27me3 distribution in *swn* and *clf*. A similar epigenomic dataset in whole seedling was published by another team last year (Shu et al., 2019) and provides an interesting point of comparison with our data.

Thus, we first show that *SWN* and *CLF* are expressed ubiquitously, albeit with varying levels of CLF from cell to cell. Genome-wide protein occupancy and H3K27me3 distribution data indicate that SWN-PRC2 and CLF-PRC2 globally target the same loci across the Arabidopsis genome. However, the absence of SWN- or CLF-PRC2 shows starkly contrasting effects on H3K27me3 distribution with either a global increase or a decrease in H3K27me3 levels, respectively. In addition, we show that overexpression of SWN interferes with PRC2 activity, possibly by affecting CLF stability. Collectively, our analyses provide evidence for a cooperative

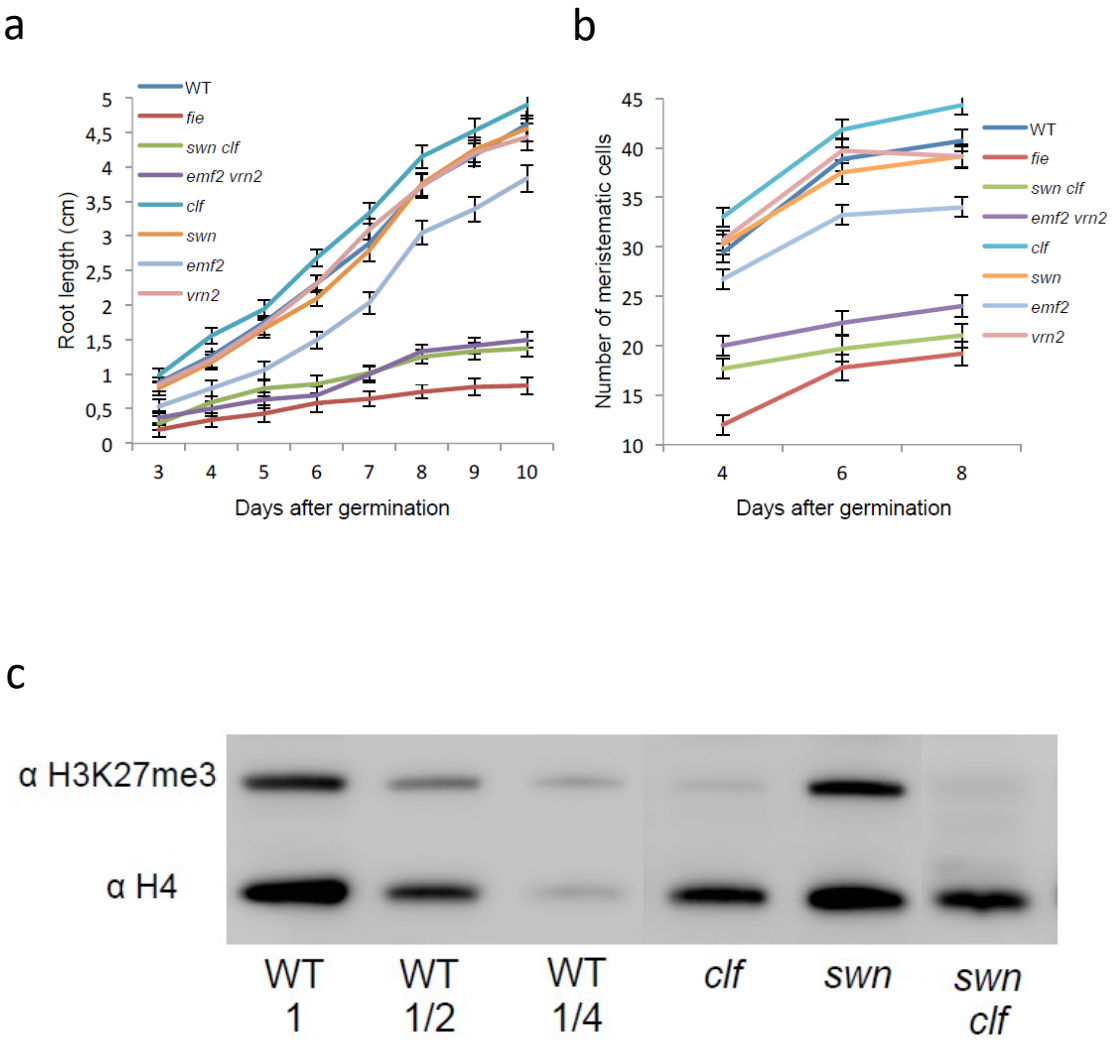

Figure 4 CLF is the major subunit responsible for H3K27me3 levels in roots. **(a-b)** Root growth kinetics in mutants of PRC2 subunits, as measured by root length (a) or meristem length (b). N > 30 for each genotype at each time point. **(c)** Immunoblot of H3K27me3 levels in WT, *swn, clf,* and *swn clf* root tip ecxtratcs. Histone H4 is used as a loading control. *Reproduced from Ana Karina Morao PhD thesis.*

albeit antagonistic role of the two AtE(z) homologues in regulating the maintenance of H3K27me3 levels in Arabidopsis.

3.2 Results

3.2.1 SWN and CLF are present in the same cells but at different ratios

In order to gain insight into the role of SWN and CLF during root development, we first aimed to determine the expression pattern and localisation of SWN and CLF in the primary root tip.

We generated a reporter line expressing both *pSWN::SWN-mCherry* and *pCLF::CLF-GFP* in the same root in the *clf swn* background. At early developmental stages, independent transformants showed a wild-type phenotype indicating an efficient complementation of the double mutant (Fig. S1a-c). A later stages, we quantified flowering time of *pCLF::CLF-GFP* or *pSWN::SWN-mCherry* lines in *swn-7 -/- clf-28 -/-* individuals (Fig. S1d). While *pCLF::CLF-GFP swn-7 clf-28* plants phenocopied *swn-7* plants with a wild-type phenotype, *pSWN::SWN-TAG swn-7 clf-28* plants showed a flowering time shift either similar or more severe than the one observed for *clf-29* plants. This could indicate that the mutant complementation by the SWN-TAG fusion protein may be less efficient than the endogenous SWN for late developmental stages.

Using confocal microscopy imaging, we found that both proteins are detectable in most cell types and developmental zones from meristematic tissue to mature cells (Fig. 5a-b), except for the columella, where CLF-GFP appears to be much more diffuse than SWN-mCherry (Fig. 5d-f). In addition, the CLF-GFP protein was detected as both nuclear and cytoplasmic, whereas SWN-mCherry was only observed in nuclei. Higher exposure revealed that CLF-GFP is weakly detectable in the cytoplasm of CSC and daughter cells, while nuclear CLF-GFP can be detected in the fourth, more mature columella layer (Fig. 5g). Thus, while the two E(z) are present simultaneously in most root cells, subtle variations in their distribution exist and a range of CLF/SWN ratios can be observed among different cell types (Fig. 5c&f), that would need to be quantified using a ratiometric approach. The localisation of the two proteins was similar in root tips expressing either CLF-GFP or SWN-mCherry.

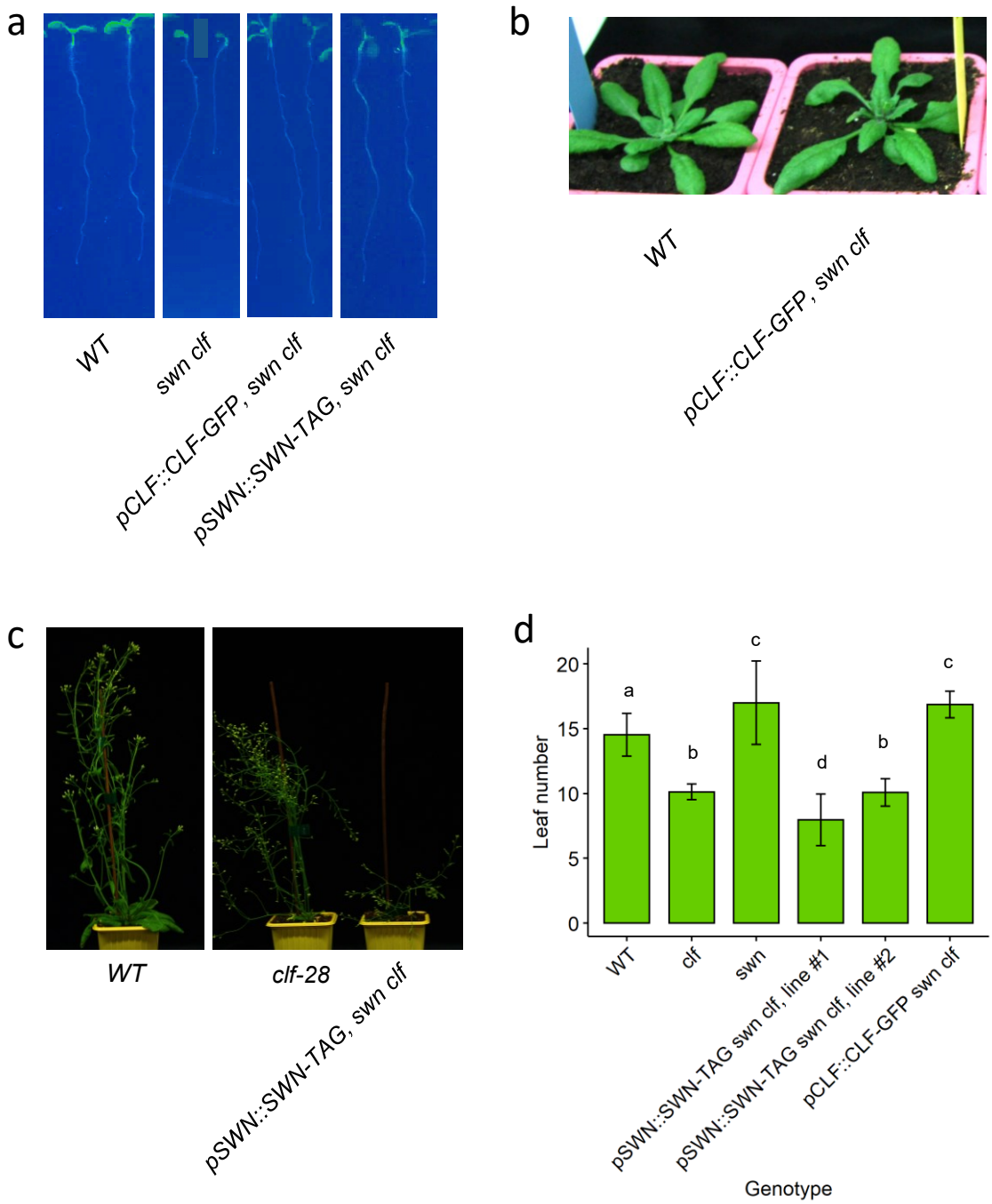

Figure S1 Validation of the functionality of the tagged AtE(z) constructions in plants devoid of endogenous AtE(z). **(a**) 5-day old seedlings. *swn clf* cotyledons are still folded and first leaves are not visible macroscopically; roots are shorter. **(b)** Images of 3 week old plants. **(c)** Images of 8-week old plants. **(d)** Flowering time phenotyping and comparison between WT, clf, and *swn* plants. *swn clf* double mutants do not produce aerial organs and do not survive outside of *in vitro* conditions. Letters above bars regroup significantly different phenotypic classes as determined by pairwise t-test ($p<0.05$). 28 plants per genotype were analysed for flowering time phenotyping.

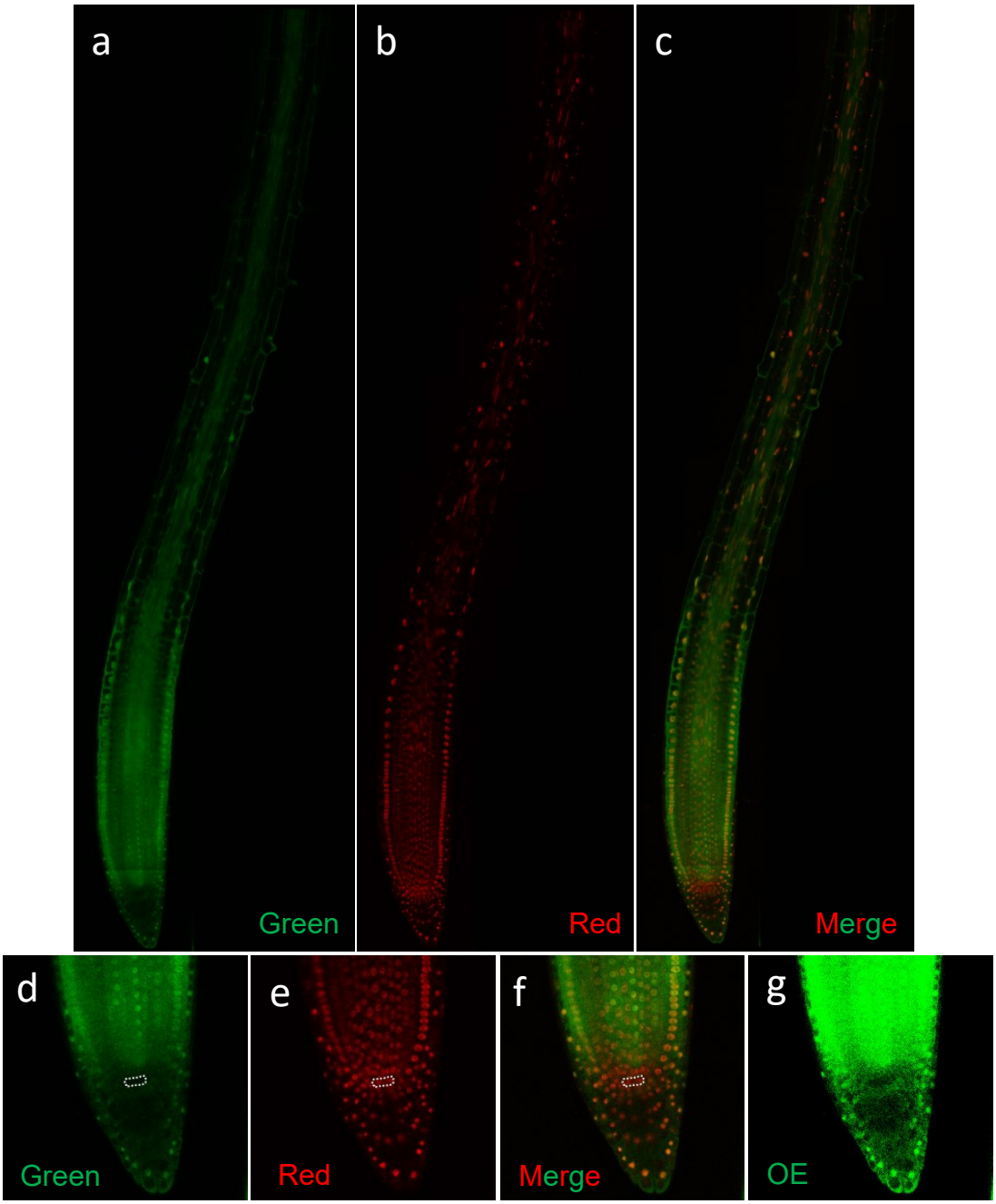

Figure 5 SWN and CLF proteins are ubiquitous along the primary roots. **(a-c)** Composite image of a representative root of *CLF-GFP SWN-mCherry swn-7 clf-28* line; green channel (a), red channel (b) and merge (c). **(d-g)** Zoom of root tip in (a-c). The quiescent center is highlighted by the dotted line in (d), (e) and (f). (g) Overexposure of the green channel in (d) showing depletion of the GFP signal in QC cells. Observations were confirmed in 10 roots for each of two *CLF-GFP SWN-mCherry swn-7 clf-28* lines analysed.

3.2.2 SWN- and CLF-PRC2 complexes target the same gene sets along the genome

We next aimed at determining the genomic loci targeted by SWN-PRC2 and CLF-PRC2 complexes in the root tips of SWN, CLF and FIE GFP-tagged lines (de Lucas et al, 2016). ChIP-seq experiments were thus performed in these lines using the same anti-GFP antibody. Since FIE enrichment sites should be representative of all PRC2 complexes along the genome, we analyzed the distribution of SWN and CLF around the 3950 FIE peak coordinates (Fig. 6). Overall, similar enrichment was found for the two E(z) at FIE peaks and no significant enrichment of any E(z) was found on loci showing no FIE enrichment (Fig. 6a-b).

As SWN and CLF appear to have a very similar repertoire of targets within root cells, we then aimed at determining if genes regulated by PRC2 may be preferentially dependent on one of the two E(z) subunits for H3K27me3 marking. Previous whole-seedling analyses of H3K27me3 distribution in *swn* and *clf* mutants led to conflicting reports, in which differential H3K27me3 marking in the single mutants was observed at either very few loci (Shu et al., 2019) or at very many in *clf* mutants (Wang et al., 2016). However, the methods used in these studies did not permit the detection of global changes in distribution of H3K27me3, which require spike-in normalisation for correcting ChIP efficiency and library preparation biases (Chen et al., 2016).

Thus, we performed H3K27me3 ChIP-seq with Drosophila chromatin spike-in on whole root tips to determine the relative levels of H3K27me3 in WT, *clf* and *swn* mutants over regions marked by H3K27me3 in WT (Fig. 6c). In WT, 6,164 regions were significantly enriched in H3K27me3. In *clf*, H3K27me3 levels at these genomic coordinates were reduced by a global median factor of 0.72 (IQR = 0.59). Enrichment analysis revealed 84 peaks with an increased H3K27me3 level by at least 2-fold, and 1,700 peaks that show at least a 2-fold reduced signal (1.3% and 27.6% of WT peaks respectively). The observation of both increase and decrease in H3K27me3 level in *clf* single mutants has been previously reported in whole seelings (Wang et al., 2016), with different proportions though with a 2-fold gain of H3K27me3 over 871 genes and 2-fold loss of H3K27me3 over 1385 genes.

Interestingly, in *swn* mutants a general increase in H3K27me3 levels was observed (Fig. 6c), by a median factor of 3.08 (IQR=0.92), with about 6000 peaks (97.3% of WT peaks) showing over a 2-fold increase in H3K27me3 level. Similar results were observed when monitoring H3K27me3 -marked genes, be it over TSS regions or over whole gene bodies (Fig. S3a-b).

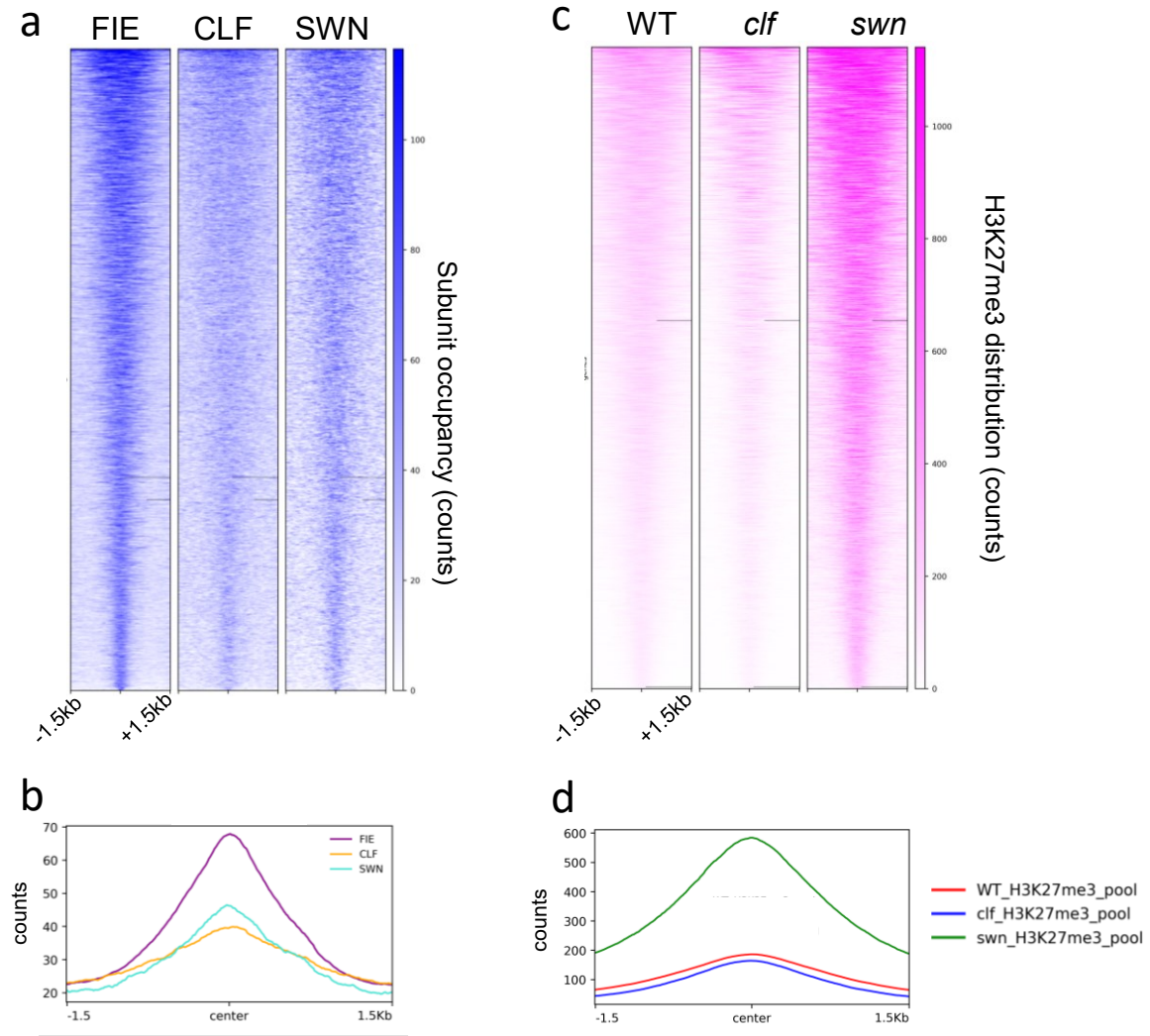

Figure 6 SWN and CLF are enriched at the same loci. **(a)** FIE-GFP, CLF-GFP and SWN-GFP distributions over a 3-kb window centered on each FIE peak (a). Average distribution of PRC2 subunits over FIE peaks are shown as metagenes in (b). **(c-d)** H3K27me3 levels over WT peaks in WT, *swn* and *clf* mutants. Levels between H3K27me3-ChIP samples in (c-d) are normalised by spike-in and library size (see Methods). Metagene representation of average H3K27me3 distribution per region for the three genotypes in (c) are shown in (d).

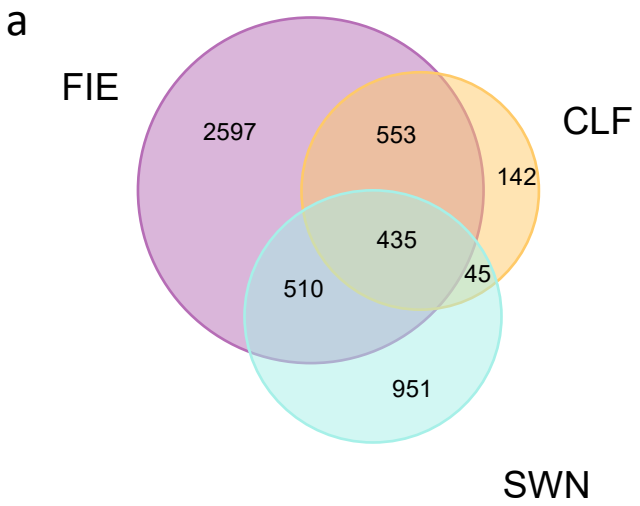

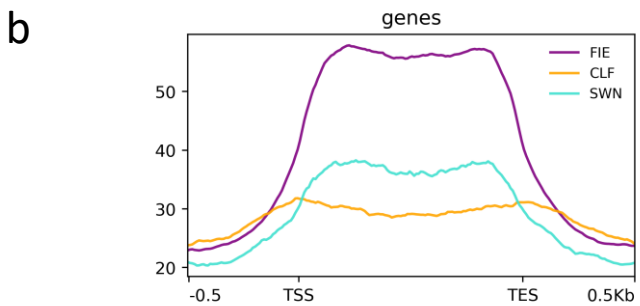

Figure S2 CLF and SWN are only detected at a subset of FIE targets. **(a)** Venn diagram representing the overlap of genes called as bound by FIE, CLF and SWN. The number of genes in each overlap is indicated. **(b)** Metagene representation of the average distribution of FIE, SWN and CLF over the 4,095 FIE-occupied genes.

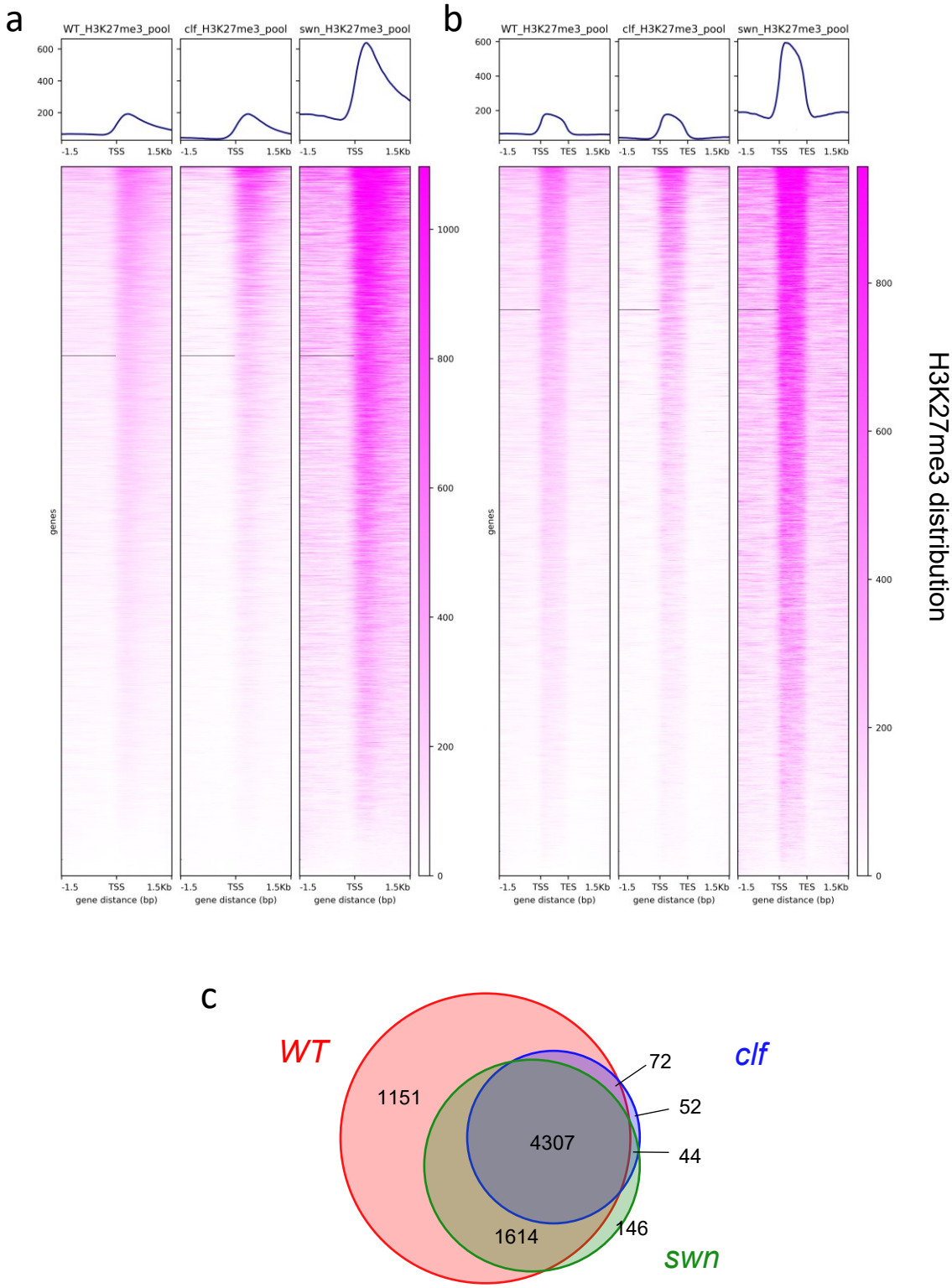

Figure S3 Supplementary analysis of H3K27me3 in AtE(z). **(a-b)** Spike-in-normalised H3K27me3 distribution over TSS (a) and whole gene body (b) of the 6,164 H3K27me3-marked genes in WT and *clf* or *swn* single mutants. Scale indicates read count per bin of 50 bases. **(c)** Venn diagram representation of genes marked by H3K27me3 in *WT*, *clf* and *swn* mutants. Spike-in normalisation is not taken into account during this analysis, and peaks are determined based on local background levels.

Peak calling analysis on the same data revealed less peaks of H3K27me3 in both *swn* and *clf* than in WT. Association of peaks with overlapping genes shows that *swn* and *clf* apparently lose H3K27me3 on many loci (Fig. S3c). It is likely that there would be a strong confounding effect of the observed global changes of H3K27me3 levels in both *swn* and *clf*, making peak calling an unsuitable method to compare these samples.

We conclude that SWN- and CLF-PRC2 target the same regions across the genome and share a similar enrichment pattern over target genes, which suggests a cooperation between the two complexes. Furthermore, the data from *clf* mutants indicate that while this AtE(z) appears to be the major catalysing subunit contributing to most of H3K27me3 in root cells, SWN-PRC2 is able to maintain a basal level of H3K27me3, at least in the absence of CLF. The overall increase in H3K27me3 levels in *swn* suggest that SWN may have a role in attenuating H3K27me3 levels instead of directly catalysing it.

3.2.3 Increased SWN expression causes abnormal development in Arabidopsis roots and shoots

The observations a presented above led us to hypothesise that SWN may regulate CLF-PRC2 activity, possibly by competing with the CLF subunit either for interaction with other PRC2 components or with target locus, thereby reducing the amount of the catalytically active CLF-PRC2 at PRC2-regulated genes. To test this hypothesis, we sought to increase the amount of endogenous SWN by expressing a *pSWN::SWN-mCherry* or *pSWN::SWN-GFP* (thereafter referred to *pSWN::SWN-TAG)* in different *swn* backgrounds.

Out of 7 independent *pSWN::SWN-TAG swn-7* lines, 4 were WT-like throughout the development cycle while the remaining 3 segregated *clf*-like phenotypes (referred to *clf*-inducing lines) showing typical leaf curling, reduced rosette diameter, and early flowering phenotypes (Fig. 7a). The *clf*-like aerial phenotypes were transmitted recessively since plants needed both alleles of the *pSWN::SWN-TAG* transgene to display these phenotypic alterations. The fact that this was observed for the three independent lines indicates that the *clf*-like phenotype is likely linked to the transgene itself. In addition, 4 of 8 wild-type plants transformed with the same transgene displayed the same *clf*-life phenotypes, also transmitted in a recessive manner. We also found minor root growth variations in the SWN-TAG lines, (Fig. S5). Phenotypic and molecular analysis of untagged SWN lines is ongoing to determine whether

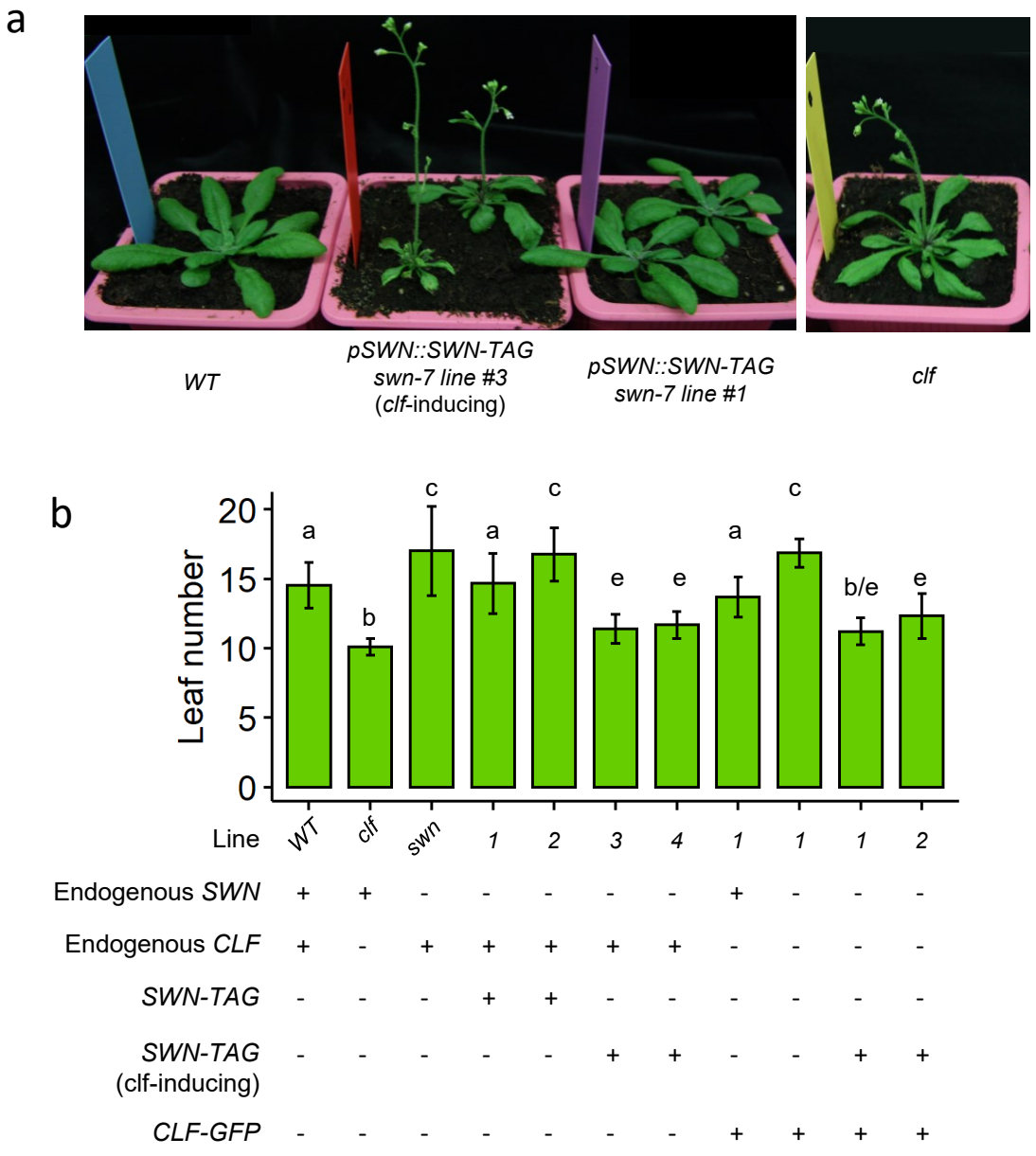

Figure 7 *SWN* expression level correlates with *clf-like* phenotypic alterations. **(a)** 24-day old plants of *WT*, *pSWN::SWN-TAG* in *swn-7* with line 3 showing early flowering, curled leaves and reduced rosette size while line 1 resembles WT, and *clf-29*. **(b)** Quantification of leaf number at bolting initiation in different genetic backgrounds. Statistical difference between mean leaf number per genotype (pairwise t-test). "+" and "-" signs indicate the presence or absence of the indicated *AtE(Z)* allele. Letters above bars regroup significantly different phenotypic classes as determined by pairwise t-test ($p<0.05$). Flowering time quantification was performed on 28 plants per genotype.

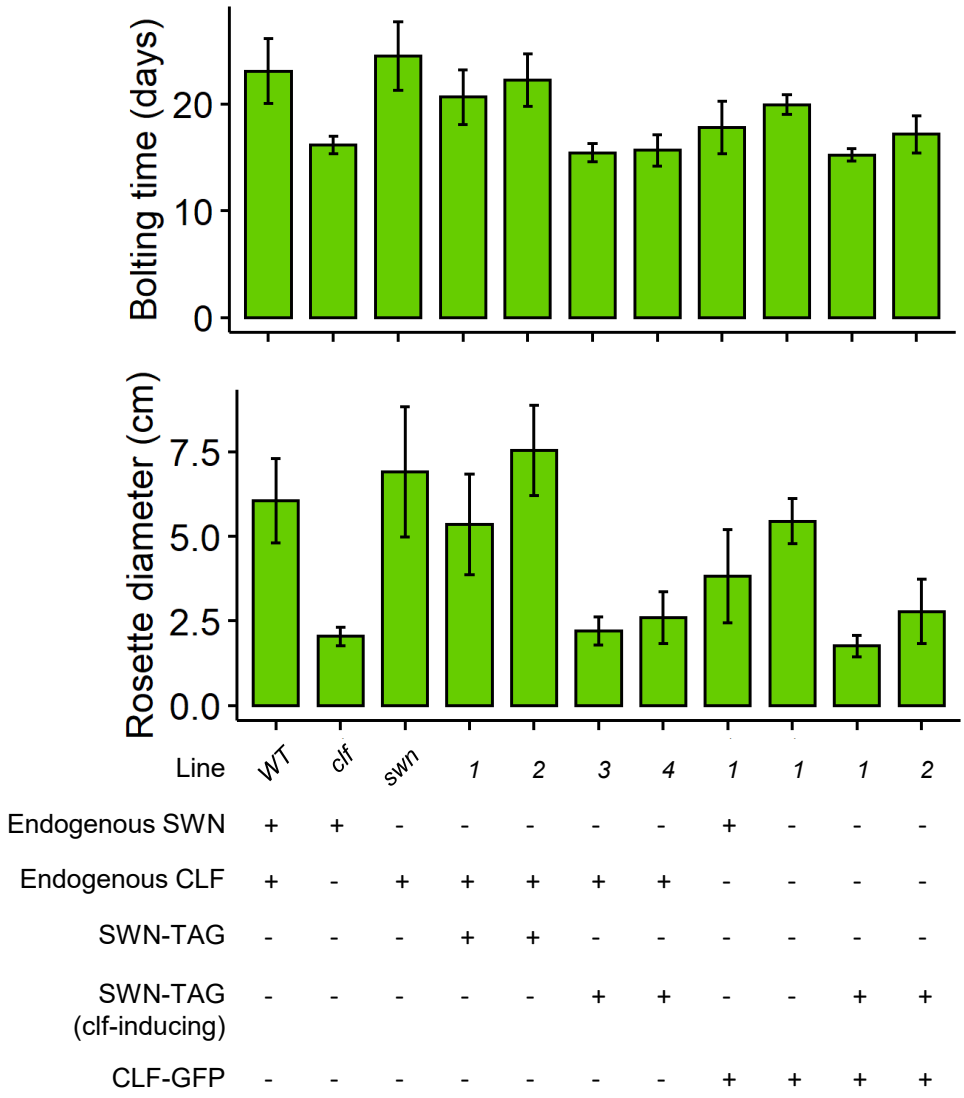

Figure S4 Phenotypic traits in genetic backgrounds with different copies of *AtE(z)*. Graphs show the quantification of rosette diameter and plant age at initiation of bolting, complementing leaf number counts in Fig. 3. "+" and "-" signs indicate the presence or absence of the indicated *AtE(z)* allele. 28 plants were analysed per genotype

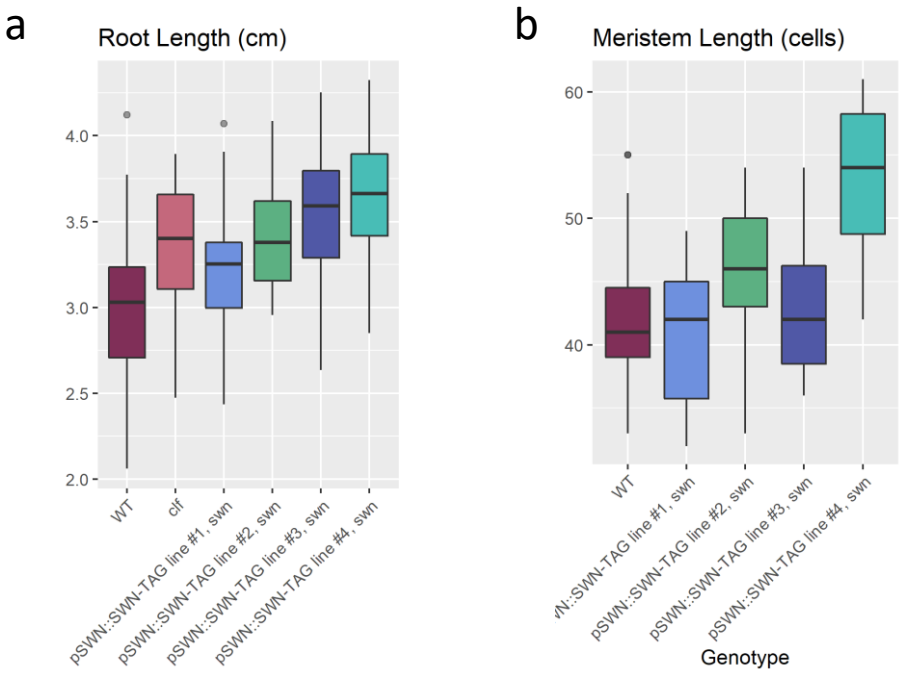

Figure S5 Root growth phenotyping of SWN-TAG lines. **(a)** Root length at 5 DAG. All genotypes have significantly longer roots than WT. N > 40 for each genotype. **(b)** Meristem length at 5 DAG. Only pSWN::SWN-TAG #4 has significantly longer meristem than WT. N = 20 for each genotype for meristem measurements. Statistics tested by t-test.

these alterations are linked to the fusion of the FP tag or not, despite the fact that the same tag, at the same position doesn't impair CLF activity.

One expectation of the competition hypothesis is that different levels of SWN should yield different levels of interference with PRC2 activity. To demonstrate this, we used flowering time as a quantitative readout, since flowering time is dependent on *FLC* regulation by PRC2 and functions as a quantitative switch at the whole-organism level (Angel et al., 2011). Pilot experiments verified that *clf-29* mutants are early flowering in our growth condition as measured by leaf number, age or rosette size at the time of bolting initiation (Fig. 7b, Fig. S4), and that the opposite was true for *swn-7*. The same flowering time traits were quantified in four of the *pSWN::SWN-TAG* lines, two which appeared WT (line #1 and #2) and two that were *clf*-inducing (line #3 and #4). Lines #1/2 had flowering time traits resembling WT or swn-7 mutants (Fig. 7b, Fig. S4), while lines #3/4 were early flowering though not as severely as *clf-29.* Root length analysis on these lines at 5 days after germination (DAG) revealed that all the lines had significantly increased length compared to WT, though only pSWN::SWN-TAG line #4 showed increased meristem length (Fig. S5).

We then performed qRT-PCR to quantify *SWN* and *CLF* mRNA levels in plants homozygous for *pSWN::SWN-TAG* construction, in the *clf*-inducing and 'normal' lines, analysing two independent lines of each. *SWN-TAG* expression levels in *clf*-inducer lines were found to be 16- and 32-fold higher than in wild-type plants, while those that did not induce *clf*-like phenotypes expressed *SWN-TAG* at 2- and 8-fold higher (Fig. S6a). Endogenous *CLF* expression level was similar to WT irrespective of the genetic background considered (Fig. S6b).

In order to explain the recessive nature of the *clf*-like phenotype, we then asked if the WT level of SWN depends on the biallelic expression of the *SWN* gene. Since homozygous *swn-7* plants have relatively subtle phenotypic alterations when compared to WT, we chose to test this hypothesis in a sensitized PRC2 genetic background using *clf-28 -/-* plants. If the number of *SWN* alleles present in the plant is important for the level of SWN and its function, one expects that plants that are *swn-7 +/- clf-28 -/-* have less SWN and therefore less functional PRC2 than *swn-7 +/+ clf-28 -/-* plants. In agreement with this, phenotypic analyses revealed a correlation between flowering time traits and the number of functional *SWN* alleles in *clf* mutant plants (Fig. S7a). Conversely, we noted a delay in bolting when comparing *swn-7 -/- clf-28 +/+* and *swn-7 -/- clf-28 +/-* plants (Fig. S7b). These observations suggest that the recessive nature of

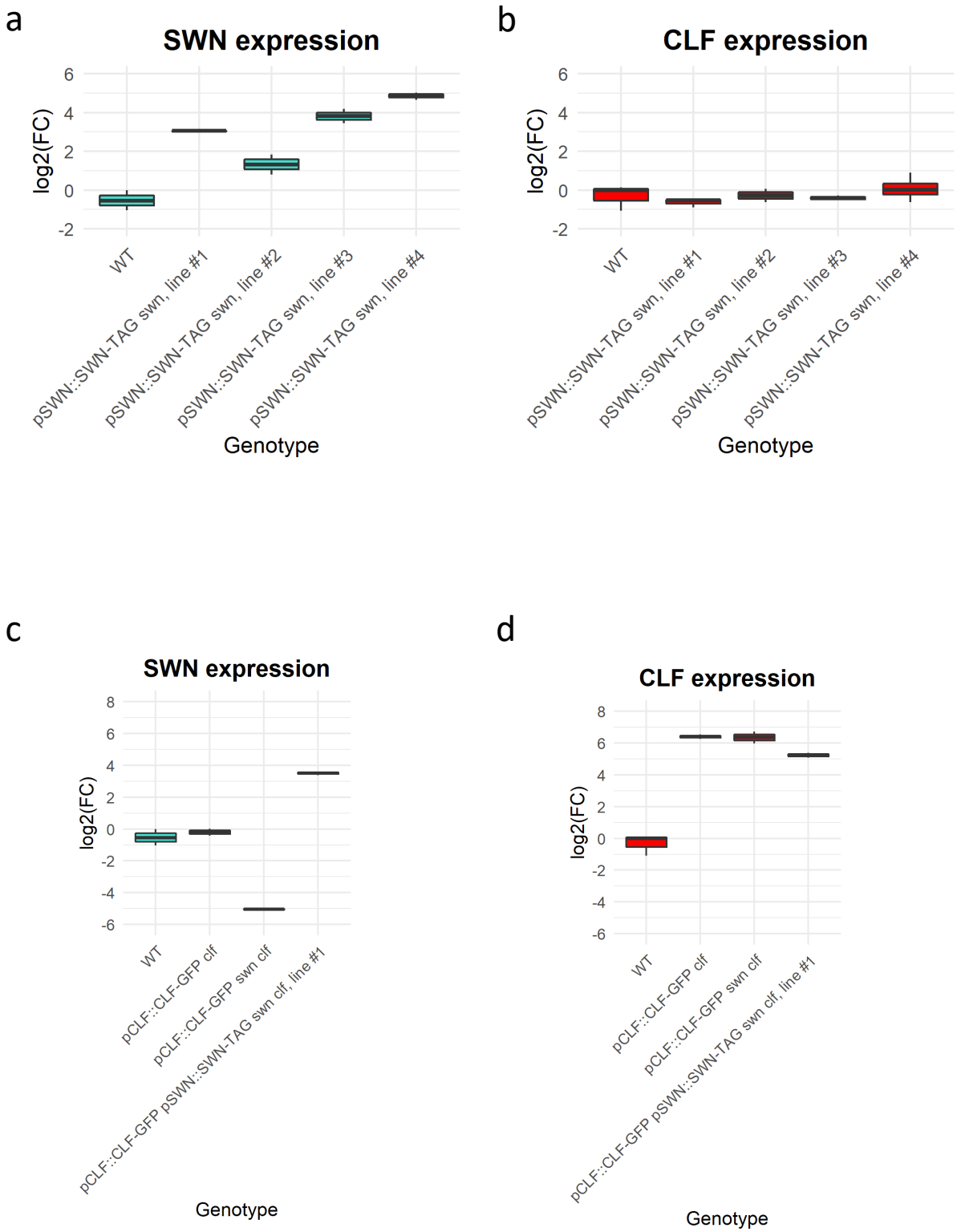

Figure S6 Increased *SWN* expression correlates with *clf-like* phenotypic alterations. qRT-PCR quantification of *SWN* (a,c) and *CLF* (b,d) expression levels in rosette leaves of *pSWN::SWN-TAG* lines (a,b) and *pCLF::CLF-GFP* lines (c,d). Fold change is the percentage enrichment normalised to input in the sample compared to that of WT. All qRT-PCR were performed in technical triplicates for each of 2 biological replicates.

a

WT | *clf-28 -/-* (N=7) | *swn-7 +/- clf-28 -/-* (N=7)

b

WT N=8 | *swn-7 -/-* *N=7* | *swn-7 -/- clf-28 +/-* *N=9*

Figure S7 Flowering time and rosette size in sensitised backgrounds are dependent on biallelic expression of *AtE(z)*. **(a)** Comparison of WT (left), *clf* with two (middle) or one (right) allele of *SWN*. Note the difference in rosette size between genotypes. **(b)** Comparison of WT (left) and *swn-7* with two (middle) or one (right) allele of *CLF*. Note the difference in bolting time.

the *clf*-like phenotype in SWN-TAG expressing lines is related to the amount of SWN mRNA and protein levels. Curiously, increasing of the amount of CLF in *clf* mutant lines overexpressing *pCLF::CLF-GFP* up to 64-fold in comparison to WT levels did not affect flowering time (Fig. 7b; Fig. S6d). We found normal endogenous *SWN* expression levels in the *CLF-GFP* overexpression line (Fig. S6c).

To test the effects of simultaneous *CLF* and *SWN* overexpression, we transformed the *CLF-GFP swn-7 clf-28* lines with the *SWN-TAG* construct. In contrast to the *pSWN::SWN-TAG swn-7* transformants described above, with only 3 out of 7 lines showing *clf*-like alterations, all 48 lines expressing both E(z) were *clf*-inducing at the T2 stage. We verified in one of the transformants that *SWN-TAG* was overexpressed (Fig. S6c). Quantification of flowering time showed that overexpression of *SWN-TAG* along with *CLF-GFP* overexpression resulted in an acceleration of flowering time that is similar to that measured in *clf*-inducer lines (Fig. 7b). Thus, while overexpression of *SWN* alone can induce early flowering, restoration of SWN/CLF mRNA ratio by overexpressing CLF did not rescue this change in flowering time.

To check if CLF-GFP levels were constant with varying quantities of SWN expression, we observed pCLF::CLF-GFP in roots without functional *SWN*, with endogenous *SWN* and in roots overexpressing *SWN-TAG*. In the lines overexpressing *SWN-TAG,* a noticeable drop in CLF-GFP fluorescence was observed (Fig. S8a-c). Quantification of signal density in nuclei confirmed this observation (Fig. S8d). In addition, these measurements showed a slight but significant drop in CLF-GFP levels between *swn-7 -/-* and *SWN +/+* roots. Taken together, the observations suggest that the dose of SWN negatively affects CLF protein levels, in a direct or indirect manner.

3.3 Discussion

3.3.1 SWN and CLF are partially redundant

SWN and CLF have been long considered as redundant or partially redundant, though little data has demonstrated the mechanisms underlying this genetic redundancy since the first molecular study of *SWN* in Chanvivattana et al., 2004. A previous report indicates that *SWN* is preferentially expressed in the epidermal and cortical cell layers, whereas *CLF* is mainly present in the meristem and vascular tissues of roots (de Lucas et al., 2016). While our studies also show that *CLF* expression or CLF stability appears strongest or higher in meristematic cells, we

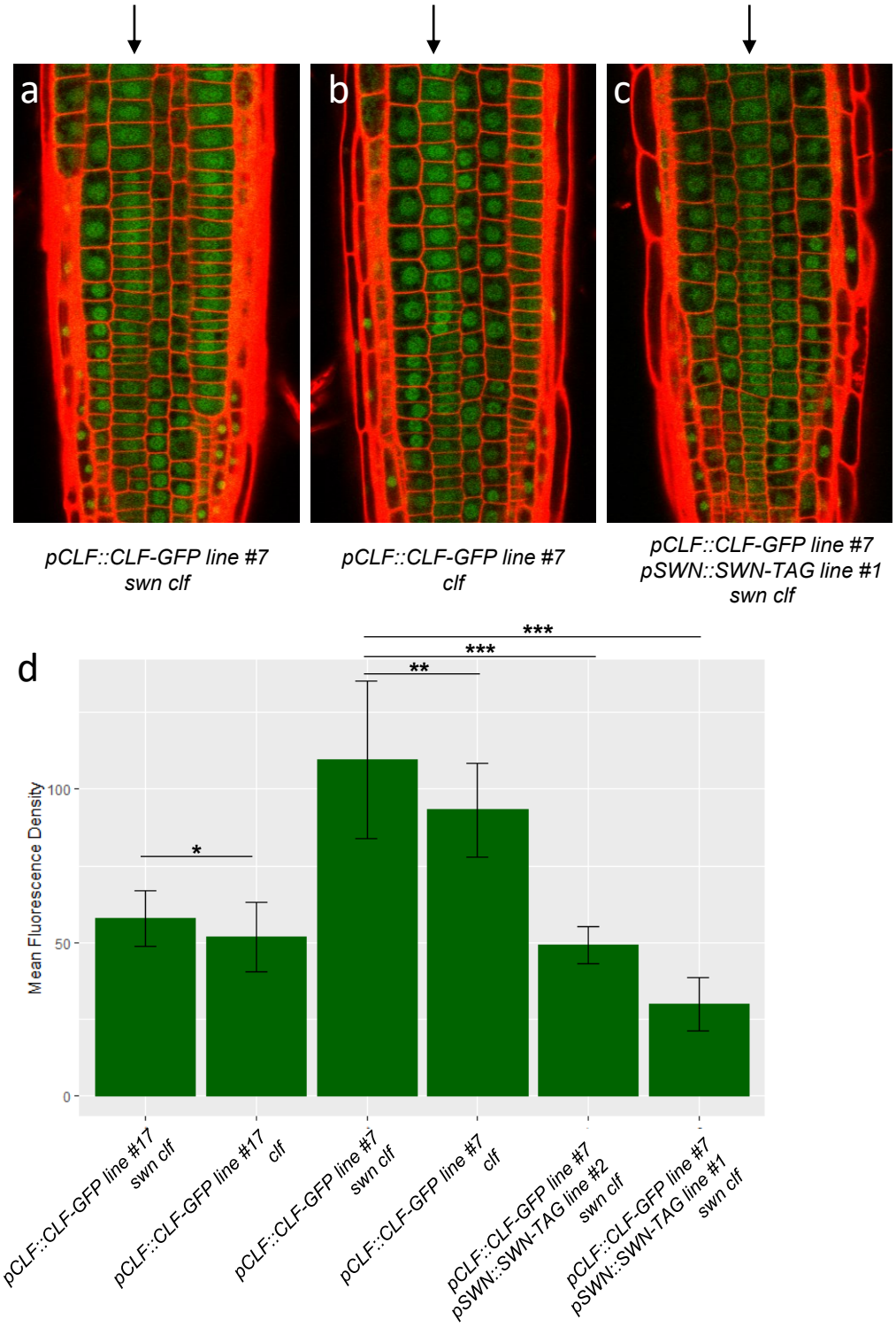

Figure S8 Preliminary results indicating that SWN may regulate CLF protein levels. **(a-c)** Confocal micrographs of roots at 5 DAG. Cell membranes are stained red by propidium iodide. Examples of cortical cell~~s~~ file used for quantification in (c) are indicated by the arrow. **(d)** Average nuclear fluorescence density in 8 meristematic and 8 elongating cortical cells per root for 4 roots per genotype indicated. * = p-value < 0.05; ** = p-value < 0.001; *** = p-value < 1e-5.

find that *SWN* is ubiquitously expressed in the root tip. Interestingly, overlapping expression domain between SWN and MEA has been reported (Qiu et al., 2017) and the *swn* mutation also enhanced the *mea*-associated fertilisation independent ovule development phenotype (Wang et al., 2006). Thus, the ability of the ubiquitously expressed *SWN* to compensate for the loss of another E(z), while by itself having no effect on root meristem size (de Lucas et al., 2016), vegetative phase change (Xu et al., 2016) or fertilisation independent seed (Wang et al., 2006) appears to be a common trend among unrelated developmental programs.

Protein-protein interaction assays based on yeast two-hybrid show that both *CLF* and *SWN* have the capacity to interact with the core PRC2 components *EMF2, VRN2* and *FIS2* (Chanvivattana et al., 2004) as well as PRC2 interacting proteins such as *ENHANCER OF LHP1 1 (EOL1)* and *TELOMERE BINDING PROTEIN 1-3 (TRB1,2,3)* (Zhou et al., 2017; Zhou et al., 2018), further supporting the idea that they may act redundantly but may also compete if some of these subunits and associated proteins become limiting.

Our ChIP-seq data suggests that SWN and CLF mainly target the same loci in the genome, an observation also noted in Shu et al., 2019. While the reported number of loci marked by H3K27me3 ranges from 5000 to 8000 regions (this work; Lafos et al., 2011; Shu et al., 2019; Deng et al., 2013), in both our work and in Shu et al., 2019 the number of loci associated with direct SWN or CLF binding remains under 2000 regions. This might reflect a technical difficulty of immunoprecipitating the AtE(z) subunits *in vivo*, possibly in relation with a relative instability or to their mode of interaction with nucleosomes. Indeed, E(z) subunits do not directly bind to chromatin and likely have more transient protein-chromatin interaction than the FIE protein that contains a WD domain allowing direct binding to H3K27me3 (Mozgova and Hennig, 2015; Hugues et al., 2020). Therefore, it is a reasonable prediction that we only detect AtE(z) occupancy over the loci that are regulated by PRC2 in most cells at the time of cross-linking or those that are constantly targeted by PRC2. A different method such as DamID might bring another a more comprehensive map of AtE(z) localisation.

Our data support a role of SWN and CLF in the catalysis of H3K27me3 over the same target genes, in the same cells. Nevertheless, the redundancy is merely partial since in the absence of CLF-PRC2, SWN-PRC2 is insufficient to regulate flowering time (Chanvivattana et al., 2004), or to maintain H3K27me3 levels over loci such as *AG* and *STM* (Schubert et al., 2006). We and others (Wang et al., 2016; Shu et al., 2019) show that many loci in *clf* mutants have

reduced H3K27me3 levels. The reasons for the incapacity of SWN to maintain H3K27me3 levels remains unclear, and could include differences in catalytic activity or differential affinities with auxiliary PRC2 subunits. Another hypothesis could be more mechanistic since the preferential expression of CLF in dividing cells could indicate that CLF would be more important during replication than SWN. Interestingly, recent reports have shown that the onset of regulation of *FLOWERING LOCUS C (FLC)* by PRC2 is coupled with cell division (Finnegan and Thomas, 2007; Yang et al., 2017; Jiang and Berger, 2017) and the replication-coupled histone variant, H3.1 (Jiang and Berger, 2017). These observations would support a model in which the primary role of CLF-PRC2 is to catalyse H3K27me3 at the replication fork (reviewed in Hugues et al., 2020; in introduction).

The developmental roles of SWN remains a mystery however, with few clues pointing to the origin of the selection pressure maintaining its existence in Brassicaceae (Qiu et al., 2017) and in many other angiosperms including rice and maize (Chanvivattana et al., 2004; A. Vialette, unpublished data). An interesting hypothesis is that a ubiquitously expressed, but less active SWN-PRC2 may be more energetically and metabolically efficient to ensure the basal maintenance of gene regulatory patterns in mature tissues, in which replication and large transcriptional switches are much less frequent. Investigating a role of SWN in these mature cells should perhaps be explored, even in a perennial Brassicaceae to complement the *A. thaliana* studies.

3.3.2 SWN may regulate the overall PRC2 activity by antagonizing CLF-PRC2

Our work suggests a novel, somewhat unexpected role of SWN in antagonising CLF-PRC2 activity. We find that increasing SWN levels *in vivo* results in plants phenocopying CLF-deficient phenotypes including leaf curling, reduced rosette size and early flowering time. These phenotypes have been associated with numerous weak or null mutants of core PRC2 subunits such as *CLF* or *EMF2* (Chanvivattana et al., 2004; Schubert et al., 2006; Lafos et al., 2011). Combination of the null *vrn2-1* mutant with the weak *emf2-10* mutant shows reduced global H3K27me3 levels in whole seedlings without apparent flowering time defects (Lafos et al., 2011). Furthermore, the *clf* phenotype has been associated with the upregulation of just *AG* and *SEP3*, of which a mutant apparently rescues flowering time defects and curly leaves (Lopez-Vernaza et al., 2012). These examples illustrate that flowering time is dependent on a handful of genes in the vernalisation or photoperiodic pathways (reviewed in Perrella et al.,

2020) and may not completely reflect global H3K27me3 levels. Molecular characterisation of H3K27me3 levels in *clf*-inducing lines will be essential to conclude about how PRC2 is affected in these lines.

Interestingly, we noted that root length increases slightly with increasing SWN dose in the same lines, also phenocopying *clf* mutants (Fig 4a, Fig. S5). All the *SWN-TAG* lines tested showed this variation while the aerial *clf*-like phenotypes required SWN-TAG to be expressed at least 16-fold to manifest themselves. This leads to the interesting hypothesis that root growth is more sensitive than flowering time to variation SWN levels.

The convergence of our genetic and genomic results suggests that SWN may play a role in attenuating CLF-PRC2 activity on a genome-wide scale. A potential explanation for such an attenuation could rely on a competitive mechanism. The fact that SWN and CLF share partners and genomic targets, in the same cells, is consistent with this competition hypothesis and may explain the effects observed with increasing or decreasing doses of SWN (SWN OE lines and *swn-7* line) on flowering time. However, a classical competitive interaction would imply that the restoration of the nuclear SWN and CLF stoichiometry in cells would suffice to rescue flowering time defects. Two independent lines overexpressing both SWN and CLF did not show differences in flowering time compared lines overexpressing SWN with normal levels of CLF (Fig. 7b. Some unpublished evidence against competition between subunits for Su(z) found by Ana Morao was that H3K27me3 levels at well-known PRC2 targets determined by ChIP-qRTPCR in *clf* and *clf vrn2* backgrounds are very similar. The same was true between *emf2* and *swn emf2*. These data support a minimal role for VRN2 and SWN in catalysing H3K27me3, and also further weaken a hypothesis based on a mechanism of SWN regulating CLF by competition.

Interestingly, we found that SWN levels may actually affect that of CLF. Direct mechanisms of regulation could be transcriptional, post-transcriptional or even post-translational via SWN methyl-transferase activity. The endosperm-specific AtE(z), *MEA,* is regulated by H3K27me3 to maintain parent-of-origin dependent regulation (Jullien et al., 2006). However, the *CLF* locus is not marked by H3K27me3 in whole seedlings (Qiu et al., 2016). Post-translational regulation has been shown in mammalian systems where PRC2 auto-methylation is an important mechanism (Lee et al., 2019; Wang et al., 2019) leading to conformational changes activating PRC2 activity. Though in our evidence, such a mechanism would have to

reduce protein stability. In spite of these examples, it is important to note that the apparent SWN regulation of CLF could be indirect.

Further complexity is implied by our preliminary results showing that CLF and SWN ratios vary between cell types and developmental phase. Examples in the animal field have shown an antagonistic role between E(z) homologues in regulating a developmental switch during hematopoiesis where the onset of later stages of differentiation favours a EZH1-PRC2 (Xu et al., 2015). Another study has also reported of EZHIP, a PRC2 accessory protein which when absent, causes a massive increase in H3K27me3 levels in mice (Razzagini et al., 2019).

Our data opens novel avenues to understanding how PRC2 activity is fine-tuned in Arabidopsis, which may point to a convergent evolution of mechanisms antagonising PRC2 activity directly in multicellular organisms.

3.4 Materials and Methods

Plant materials and growth conditions

All the lines used are in the Col-0 accession. The *swn-7* (SALK_139371), *clf-29* (SALK_021003) and *clf-28* lines (SALK_109121) have been described previously (Doyle et al., 2009; Bouveret et al., 2006; Wang et al., 2006) and the absence of full mRNA expression has been validated by RNA-seq (this work). *pFIE::FIE-GFP* and *pCLF::CLF-GFP* lines have been described previously (de Lucas et al., 2016). *pSWN::SWN-GFP* used in ChIP-seq experiments was described previously in Wang et al., 2006.

All plants were grown in long day conditions cycling 22.5°C for 16 hours in light, and 18.5°C for 8 hours in darkness. For all experiments, seeds were surface sterilised, stratified in water at 4°C for 3 days in darkness, sown on agarose plates (½MS, 1% sucrose, 1% agarose) and grown vertically under the same photoperiodic conditions.

Cloning strategy

The *pSWN::SWN-GFP* and *pSWN::SWN-mCherry* lines were generated using the Golden Gate strategy (Engler et al., 2014). Briefly, 5' and 3' regulatory sequences were obtained by amplifying genomic DNA using the primer pairs SWN_5' and SWN_3' (see Table 2 of the Annexe

section), and purified PCR products were cloned into pICH41295 and pICH41276 (Addgene) vectors respectively. eGFP and mCherry fluorescent tags were cloned into pICSL5008 and pAGM1301 (Addgene) respectively. The full length 5,408 bp genomic sequence of the *SWN* gene was obtained by direct DNA synthesis and cloned in pUC57 (Genewiz). *pSWN::SWN-GFP* or *-mCherry* was assembled using the plasmids containing SWN 5' regulatory sequence, genomic sequence, the respective fluorescent tag and 3' regulatory sequences into pICH47811 (Addgene), in a single cloning step. The assembled product was then cloned into pAGM4673 (Addgene) with a BASTA resistance cassette, and an end linker (in pICH41744). Plasmids were then introduced into *Agrobacterium tumefaciens* by electroporation and subsequently transformed into *WT*, *swn-7 -/- clf-28 +/-* or the *pCLF::CLF-GFP* lines *Arabidopsis* plants using the floral dip method.

Chromatin immunoprecipitation (ChIP) and library preparation

ChIP was performed according to Morao et al 2018 with minor modifications.

For H3K27me3 ChIP, roots tips were harvested and cross-linked with 1% formaldehyde in vacuum for 15 minutes. For GFP-ChIP, a double cross-linking was performed by treating roots with disuccinimidyl glutarate (DSG) for 45 minutes at root remperature followed by 1% formaldehyde for 7 minutes. Extracted chromatin was sonicated using a Covaris S220 ultra-sonicator to generate DNA fragments with an average length of 250 bp. A small proportion of sonicated chromatin of each replicate was kept as INPUT, while the rest was incubated overnight with an excess of anti-H3K27me3 (Millipore, 07-449) or anti-GFP (Abcam, ab290) antibodies coupled to magnetic beads. For spike-in normalised replicates, 25 µg of sample chromatin (concentration determined with BCA protein assay kit, Sigma-Aldrich) was mixed with 2 µg of Drosophila chromatin (Active Motif Catalog No. 53083), and an additional spike-in antibody was included during overnight incubation with anti-H3K27me3. Purified DNA fragments were used for qPCR testing for enrichment level of histone mark over known loci compared to INPUT. 1ng of immunoprecipitated DNA was used for library preparation (Diagenode MicroPlex v2).

At least two replicates were obtained for each dataset. Spike-in experiment was performed on one replicate.

Validation of ChIP experiment quality was performed by qPCR on typical H3K27me3-marked (*AT3G11260, AT1G28300, AT5G12330, AT5G49520, AT5G10140*) or -unmarked (*AT5G13440*, *AT3G18780*) loci using primers described in Annexe Table 2.

Analysis and integration of ChIP-seq replicates

High-quality reads were mapped to the TAIR10 *Arabidopsis* genome using bowtie2 (Langmead and Salzberg, 2012) with the –very-sensitive option. Reads with a maximum of one mismatch were kept, and PCR duplicates were removed. Peak calling analysis was performed using MACS2 (Zhang et al., 2008) which uses a model-based approach to define peaks based on background levels of signal within a sample. H3K27me3 replicates were integrated using IDR (Li et al., 2011). Genes were annotated as marked by a histone mark when a peak overlapped by at least one bp with an annotated gene (annotated genes are a list of 28 363 TAIR-10-defined genes filtered for loci prone to mapping biases, often due to repeating elements). Robust FIE-GFP and CLF-GFP peaks were determined by intersection between replicates, while SWN-GFP peaks were determined by pooling replicates.

For spike-in replicates, reads were also mapped to the *Drosophila* genome (Release 6). The total number of reads mapping to the Drosophila genome was used as the normalising factor for correction of count levels. The median ratio between the median 50 peaks by significance was used to correct levels of non-spiked replicates. Our spiked and un-spiked replicates showed similar profiles after correction.

Heatmaps and metagenes were made using deepTools (Ramirez et al., 2016) using “bamCompare”, “computeMatrix”, “plotHeatmap” and “plotProfile” functions.

RNA extraction and qRT-PCR

RNA extractions were prepared using the Spectrum Plant Total RNA kit (Sigma). Genomic DNA contamination was eliminated using Ambion TURBO DNA-free. Reverse transcription was performed using SuperScript IV VILO (Thermo Fischer). qRT-PCR was performed using a Quant Studio 6 Flex Real-Time PCR System, SYBR green detection chemistry and 384-well plates (Roche). qPCR experiments were performed in at least biological duplicate, with technical

triplicates, on *SWN* and *CLF* genes, using three housekeeping genes for normalisation (Annexe Table 1).

Meristem length quantification

For meristem length quantification, *in vitro* grown seedlings at 5 DAG were cleared with chloral hydrate solution (chloral hydrate 40g/L, glycerol 30%) and images of the root sagittal plane were taken using a Zeiss AxioImager microscope equipped with a Differential Interference Contrast (DIC) optics. The number of cortical cells was counted from the cortex-endodermis initial to the final meristematic cortex cell for each image.

Confocal microscopy of root tips and quantification of pixel density

All imaging was performed using a Zeiss LSM710 confocal microscope. Laser intensity and photo-multiplicator transmitter was modified between reporter lines to optimise dynamic range of the signal while reducing background noise and over-exposure.

For images in Fig. 5, roots were mounted in water between a glass slide and coverslip without counterstaining. ImageJ was used to produce the composite image with the “stitching” plug-in.

For quantification of GFP signal in Fig. S8, dissected roots were immersed in propidium iodide solution (20 µg/L) for 10 minutes before mounting in water between a glass slide and coverslip. Images were taken of the meristematic cortical cells. ImageJ was used to measure pixel density in 8 meristematic and cortical cells per root for 4 roots per genotype.

4. PRC2 regulation in the root stem cell niche orchestrates cell differentiation timing during development

4.1 Introduction

Development of multicellular organisms involves the differentiation of cells from stem cell pools to mature cell types, encompassing successive transcriptome changes. The Arabidopsis root provides a unique opportunity to study an organ in continuous growth, with a stem cell niche and tractable cell types with accessible clonal information. Two differentiation gradients can be distinguished, the columella and lateral root cap, distal to the stem cell niche, and the proximally-located epidermal, ground and vascular tissues. Transcriptomic changes along these two root gradients have been investigated in numerous studies using bulk-sequenced sorted cells (Brady et al., 2009; Li et al., 2016) or more recently by single cell RNA sequencing (scRNA-seq) (Ryu et al., 2019; Denyer et al., 2019; Zhang et al., 2019; Jean-Baptiste et al., 2019; Shulse et al., 2019). Together, these studies have provided insight into the transcriptional transitions during the acquisition of cell identity, at high resolution, and the intricate patterning of gene networks during differentiation trajectories such as cortex, endodermis and trichoblast cells have been described (Shulse et al., 2019; Denyer et al., 2019; Jean-Baptiste et al., 2019).

The quiescent centre (QC) at the heart of the root stem cell niche maintains the stemness of surrounding initials, each giving rise to a specific root cell file (Pi et al., 2015). Furthermore, the QC maintains a low mitotic activity, a quiescent state, which can be lifted in stress-inducing conditions or in the presence of hormonal agents (Heyman et al., 2013; Planas-Riverola et al., 2019). Thus, the QC population has an important role as an intermediate between the proximal and distal root differentiation gradients, integrating signals impacting stem cell niche activity (Rahni et al., 2016; Choe et al., 2017). Numerous studies have sought to determine the clonal relationship between the QC and the different initials, but this has been challenging due to the inherent quiescence of QC cells. While the QC parental origin of columella stem cells has been clearly demonstrated (Cruz-Ramirez et al., 2013), this remains disputed for the stele and ground tissue initials (Kidner et al., 2000; Rahni and Birnbaum, 2019). Thus, the unique characteristics

of the QC cell population provide an opportunity to simultaneously study a relatively homogenous cell type and a potential primordial state of root differentiation pathways.

The role of epigenetic regulation to maintain transcriptional patterns across cell divisions has been demonstrated across many model species. In plants, numerous studies have investigated how changes in chromatin states may play a role in regulating waves of transcriptional patterning in processes such as flowering transition (Engelhorn et al., 2017; You et al., 2017) or tissue regeneration (Rymen et al., 2019). While correlation between histone marks such as H3K4me3 and active transcription is clear in these studies, the effects of H3K27me3, catalysed by Polycomb Repressive Complex 2 (PRC2), on gene expression are less obvious, possibly due to the lack of cell-type specificity in these studies.

In this section, we investigated the chromatin states of genes specifically within the QC cell population. Integrating epigenomic profiling with publicly available single cell transcriptomic dataset revealed that PRC2 regulation within the QC represses a subset of genes that are dynamically activated during subsequent stages of cell fate acquisition. By reconstructing root developmental trajectories, we show that PRC2 activity in the QC likely fine-tunes the regulation of late-activated genes along the columella, cortex and endodermis differentiation pathways. In addition, we demonstrate that PRC2 activity in the QC is required and possibly sufficient to maintain meristem homeostasis and ensure proper root development.

4.2 Results

In order to purify QC cells, we used the Isolation of Nuclei in Tagged Cell Types (INTACT) method (Morao et al, 2018) using lines expressing nuclear-anchored GFP under the *WOX5* promoter (Fig. 8a). This *pWOX5::NTF* line shows QC-specific GFP signal. The enrichment level achieved by the INTACT method was validated by comparing the intensity of H3K27me3 and H3K4me3 chromatin marks from QC-purified nuclei and from whole root, over the 25 most significant QC-specific marker genes determined by scRNA-seq data (Methods). We found that these markers had similar H3K4me3 marking between QC and whole root chromatin data, but had less H3K27me3 normalised counts on average in the QC than in whole roots (Fig. 8b). H3K27me3 was similarly dynamic at *AGL42* and *WOX5*, two well-known marker genes of QC identity (Fig. 8c). These chromatin-based results will be complemented by qRT-PCR assays.

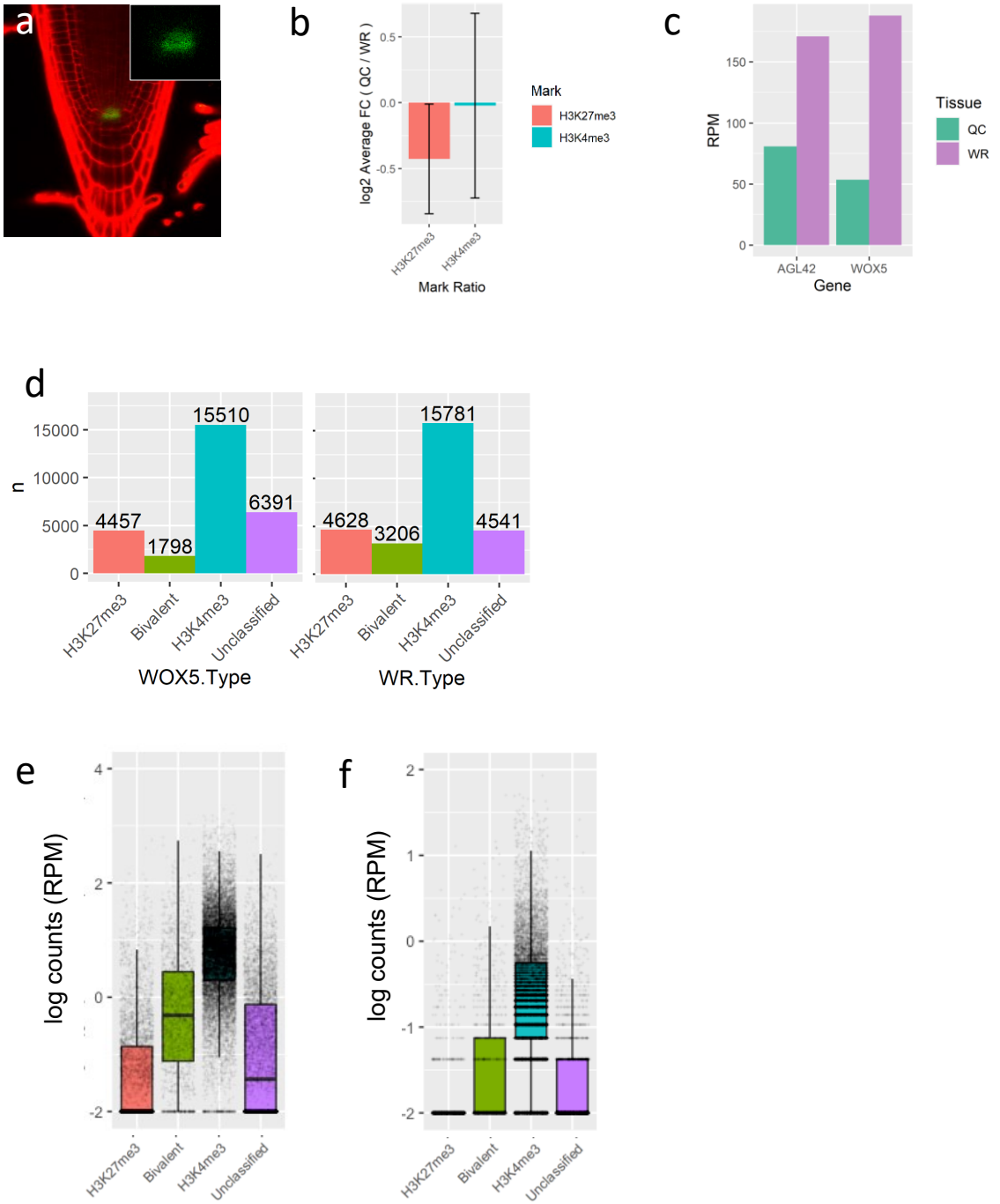

Figure 8: QC-specific chromatin data correlates with expression levels in the QC. **(a)** Representative confocal image of pWOX5::NTF root, stained with propidium iodide (left), and magnified, without red channel (inset). **(b)** Average log2 of fold change for H3K27me3 and H3K4me3 replicates at QC identity markers (Denyer, Ma, et al., 2019). **(c)** H3K27me3 levels at two well-known QC marker genes, AGL42 and WOX5, in QC and whole roots. **(d)** Number of genes per chromatin type within the QC and Whole Roots. **(e-f)** Expression levels of genes in the QC transcriptome per QC chromatin type using transcriptomic data from FACS-sorted QC cells (Li et al., 2016) or scRNA-seq (Denyer et al., 2019).

4.2.1 The QC chromatin landscape largely resembles that of the whole root

We assessed the chromatin state of genes within the QC cell population by measuring the distributions of H3K27me3 and H3K4me3 in QC nuclei. In parallel, the histone mark distributions were also measured in whole roots. Robust peaks over replicates were determined yielding similar numbers in whole root and QC samples (6,164 H3K27me3 peaks and 19,584 H3K4me3 peaks in whole roots compared to 5,449 and 16,541 respectively in QC). Peaks were associated to genes and genes were assigned to four classes based on their chromatin state within the QC: H3K27me3- or H3K4me3-marked genes, bivalent genes that present the two marks in this homogeneous cell population, and genes unmarked by either histone modification. Global proportions of genes were similar between the two cell populations, with small differences in the numbers of bivalently-marked and unmarked genes in the QC as compared to whole root (Fig. 8d; unmarked genes are denoted as "Unclassified" in all figures).

To analyse the differences between gene classification in the two cell populations, we categorised gene classes between whole root and QC samples (Supplementary Table), along with enriched GO terms for each category. As expected, most genes do not change class between the QC and whole root datasets. For instance, H3K4me3 genes marked in both samples are enriched in housekeeping genes necessary in all cells, while H3K27me3 marked genes in both samples are enriched with genes associated to non-root functions such as seed metabolic pathways or floral organ development. Among the genes that do change category, the largest groups are genes which are co-marked by H3K4me3 and H3K27me3 in whole root but are associated to only one of the two histone modification in the QC, and many marked genes in whole roots that are unmarked in the QC. These appear to be enriched in important functions in root development such as chemical response, cell cycle regulation and differentiation.

To investigate the relationship between the four chromatin states and expression level within the QC cell population, we used available cell-type specific datasets (Li et al, 2016) (Fig. 8e). As previously reported, we found that H3K27me3- and H3K4me3-marked genes correlated respectively with low and high gene expression levels, whereas the bivalently marked and unmarked genes appeared to be expressed at intermediate levels.

We then took advantage of recently published single-cell RNA-seq datasets to refine the resolution of our analyses. We chose to use the single cell transcriptomic data from Denyer, Ma et al. (2019) due to the higher number of QC cells that were reported in this dataset (reanalysis details and results in Supplementary Text 1). A cluster of cells correlating with the QC transcriptome was identified, and high-confidence QC cells within the cluster were selected by filtering cells that expressed over 50% of the QC-specific identity marker genes as determined by Identity Correlation Index (ICI) scores (Efroni et al., 2015). The transcriptomes of these cells were pooled together to recreate a QC-specific transcriptome. We found similar trends in the relationship between gene expression and chromatin category (Fig. 8f).

4.2.2 PRC2 regulates QC biological function

In order to investigate the role of PRC2 in regulating QC cell identity, we aimed to determine which genes are dynamically regulated between the QC and other root cell types. We reanalysed the scRNA-seq dataset using the Seurat R package to identify QC cells (Methods, Fig. 9a) and find QC marker genes (hereby referred to as QC DEGs, for Differentially Expressed Genes), of which 1126 genes showed preferential expression in QC cells and 1320 genes were specifically depleted in the QC cluster compared to most other cell types. A small proportion of these genes are targeted by PRC2 (44 H3K27me3 and 131 bivalent genes), and these included both QC-enriched and QC-depleted genes (Fig. 9b).

In order to assess the importance of PRC2 in maintaining the expression pattern of these genes, we assayed the expression levels of these genes in the root transcriptome of *swn clf* double mutants (Ana Morao, unpublished), which are completely deficient in PRC2 activity. We found that the expression of both QC-depleted and QC-enriched H3K27me3-only genes are upregulated by 2.5-fold on average (Fig. 9c), with a lesser increase in bivalent genes.

We then investigated the biological functions associated with PRC2-mediated gene regulation within the QC DEGs. GO-term analysis revealed significant enrichment for functions including root meristem growth, regulation of cell proliferation, hormone response and response to hypoxia for the groups of QC-enriched H3K27me3 and QC-depleted bivalent genes. This suggests that PRC2 is important in orchestrating QC functions by regulating both detection of endogenous signals (hormones or metabolic) as well as developmental response (growth and

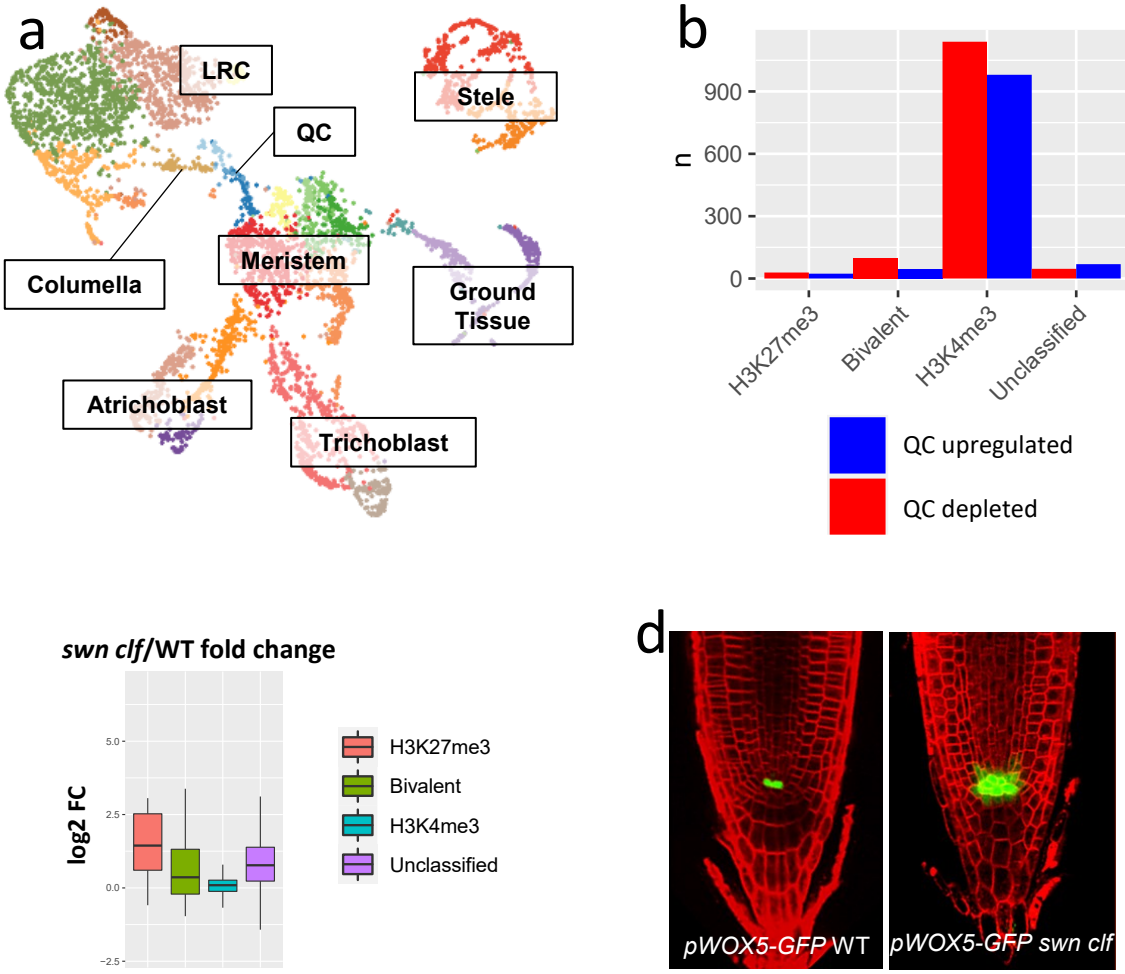

Figure 9 PRC2 regulation in the root stem cell niche. **(a)** UMAP representation of reanalyzed scRNA-seq data from Denyer, Ma et al,. 2019. Cells are positioned according to their transcriptional similarity and identities assigned to cell clusters. **(b)** Number of genes up- and down-regulated in QC in comparison with other cell identity clusters and according to chromatin type in the QC. **(c)** Average **f**old-change expression variation of genes between WT and *swn clf* according to QC chromatin type, based on whole root transcriptomic data. **(d)** Representative *pWOX5::NTF* expression pattern in WT and *swn clf* root tip, showing 4-5 QC cells in *swn clf* instead of 2 visible in WT. N > 10 roots for each genotype.

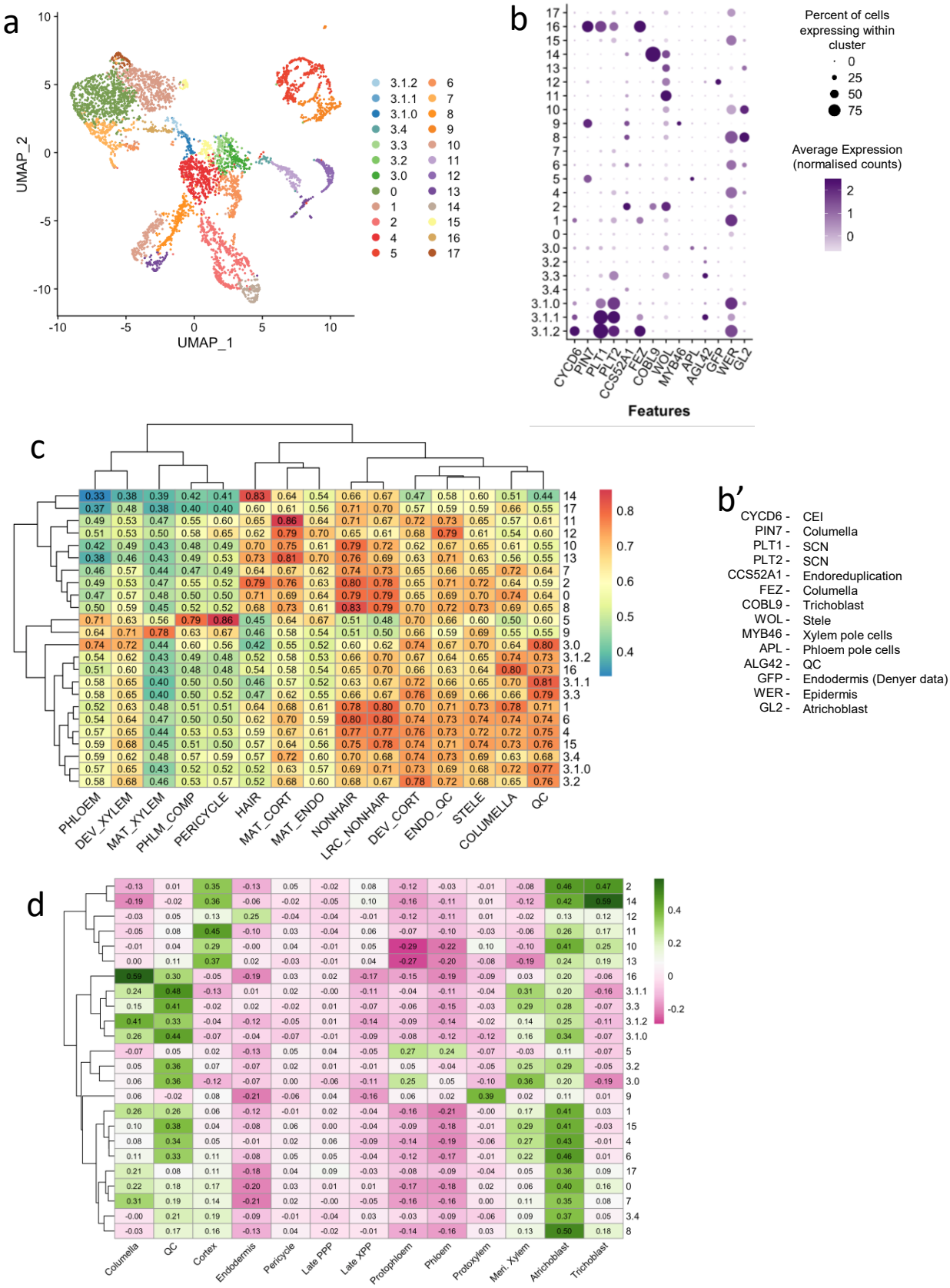

Figure S9 Assignement of cluster cell identities. Analysis of results are in Supplementary Text 1. **(a)** UMAP representation of reanalyzed scRNA-seq data from Denyer, Ma et al,. 2019. Cells are positioned according to their transcriptional similarity. **(b)** Expression of a selection of established identity markers in distinct cell types. Precisions on marker identities in (b'). **(c)** Spearman correlation analysis between scRNA-seq cluster transcriptome and data obtained from cell sorting bulk RNA-seq data (Li et al., 2016). Numbers within boxes contain the exact correlation values. **(d)** Spearman correlation of clusters correlating clusters with Spec scores used for identification of cell identity in Denyer, Mao et al., 2019.

cell proliferation). In agreement with this, severe perturbations of the pattern and number of QC divisions were observed in *swn clf* mutant. Introgression of a *pWOX5::GFP* reporter line in the *swn clf* background confirmed both the enlarged QC, as well as the QC identity of this supernumerary cell population (Fig. 9d). These together indicate that PRC2 is involved in maintaining quiescence within the QC.

4.2.3 Chromatin states in the QC correlate with expression levels and timing during cellular transitions along differentiation gradients

We then aimed at examining the association of PRC2 regulation in the QC with the transcriptional control of genes in cells along distinct differentiation trajectories. We chose to analyse three developmental trajectories from QC to columella cells, cortical cells and endodermal cells as these transitions were the most clearly identified from scRNA-seq data (Fig. S9, Methods).

QC-columella trajectory

Our reanalysis of the Denyer, Ma et al. (2019) dataset identified a total of 128 cells in clusters with QC or columella identity, from which we identified genes dynamically regulated during columella differentiation. Developmental timing of each cell was mapped using pseudotime analysis, with the cell with maximal *AGL42* expression, a marker gene for QC identity (Nawy et al., 2005), as the initiation point of the trajectory. UMAP visualisation of cell transcriptomes resulted in a continuous group of cells (Fig. 10a) displayed along a linear, unbranched developmental trajectory, suggesting that columella differentiation involves smooth transitions of transcriptional states. Clustering analysis on the 128 transcriptomes of unique cells belonging to the columella path identified groups of QC and columella identity at the two extremities of the trajectory, with transient identities located between them along the developmental trajectory (Fig. S10a-c).

For simplification in downstream analysis, cells were binned by pseudotime value into three groups corresponding to early, mid and late differentiation stages, containing 42, 34 and 52 cells respectively. DEG analysis between pseudotime bins uncovered 1,681 genes with significantly dynamic expression patterns along the trajectory. In order to analyse the patterns of expression dynamics among the 1,681 DEGs, these genes were separated into eight clusters

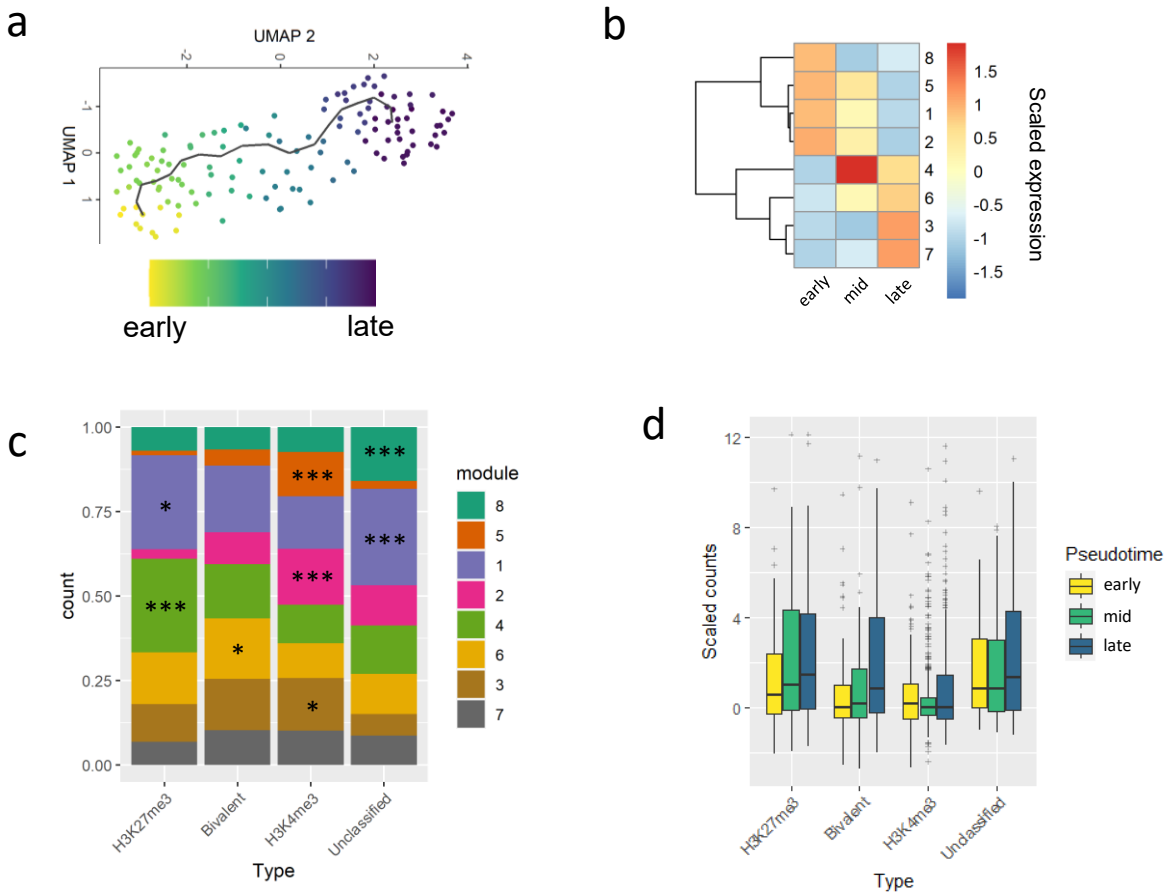

Figure 10 PRC2 activity in the QC regulates late activating genes during columella differentiation. **(a)** UMAP visualization of the 128 cells in the QC and columella clusters, colored by pseudotime. **(b)** Clustering analysis of gene co-expression among dynamic genes along developmental pseudotime. Cells were binned into 3 groups of equal size based on pseudotime value. **(c)** Distribution of the 7 co-expression clusters among each chromatin type. Asterisks indicate which individual clusters are enriched in genes of the corresponding chromatin type. Chi-test; * = 95% confidence, *** = 99.9% confidence. **(d)** Average scaled expression counts for the different classes of genes and chromatin types according to pseudotime.

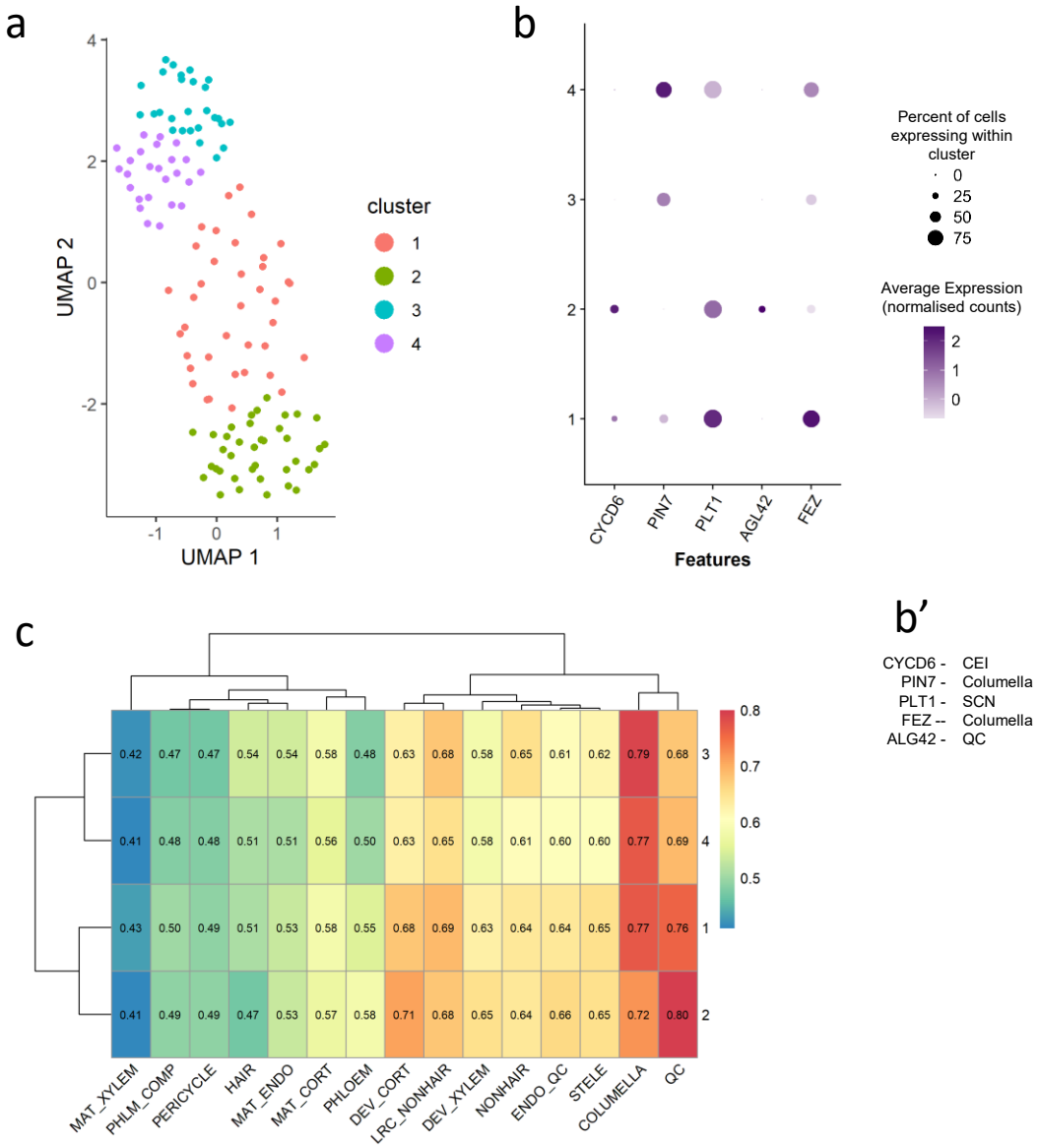

Figure S10: QC-Columella pseudotime analysis separates cells by developmental time and reveals discrete transition states between QC and Columella identities. **(a)** Reclustering of cells in Fig. 3a shows four clusters of cells. **(b)** Expression of established identity markers of QC, Columella Stem Cells and Columella identity within each cluster. Precisions on marker identities in (b'). **(c)** Spearman correlations of clusters transcriptomes with cell type specific bulk RNA-seq data sorted by FACS (Li et al., 2016).

of co-expression patterns along pseudotime groups (Fig. 10b), each containing between 133 and 291 genes. Hierarchical clustering of the patterns separated clusters 1, 2, 5 and 8 from clusters 3, 4, 6 and 7, forming two groups containing genes with peak expression at the start or at later stages of the trajectory (called QC maximum or post-QC maximum).

We were then interested in the relationship between PRC2 regulation in the QC and gene activation timing along the differentiation path. The genes differentially regulated along the QC-columella trajectory correspond to 4.3% QC-H3K27me3, 6.3% QC-bivalent, 81.9% QC-H3K4me3 and 7.5% QC-unmarked genes. Post-QC maximum genes were overrepresented among H3K27me3- and bivalently-marked genes in the QC (Fig. 10c) at 61.1% and 59.4% (chi-squared test, expected proportion is 48.3%). In addition, average gene expression over pseudotime showed similar trends as it increased for QC-H3K27me3 and QC-bivalent genes, while a limited change was observed for the QC-H3K4me3 and -unclassified genes (Fig. 10d-e). Taken together, these observations suggest that genes regulated by PRC2 in the QC are activated later during columella cell differentiation than the genes belonging to the other chromatin states identified in the QC. When analysing individual co-expression patterns in PRC2-regulated genes, clusters 1 and 4 were enriched with H3K27me3-marked genes (6.9% and 9.4% respectively compared to 4.3% expected by chance) while cluster 6 was enriched in bivalent genes with 10.2% instead of 6.3% expected by chance (Fig. 10c). Average expression in cluster 1 was the lowest of the early expressed clusters, whereas PRC2-regulated genes in clusters 4 and 6 have a larger expression range than clusters 3 and 7 (Fig. S11). Therefore, though H3K27me3 may be associated with a class of QC-enriched genes, these are not among the highest expressed. In contrast, it would appear that later expressed clusters which undergo the most PRC2 regulation appear to contain the most dynamic genes.

Developmental functions associated with PRC2-regulation along the columella differentiation trajectory were enriched in biological functions including auxin efflux, auxin homeostasis and cell differentiation (Fig. 11a). To directly test the functional relevance of this regulation, auxin distribution was assayed in the wild type and *swn clf* background using a *pRPS5A::DII-Venus* marker (Vernoux et al., 2011; Brunoud et al., 2012). The DII domain is degraded in the presence of auxin and therefore Venus fluorescence reports the absence of auxin (Galvan-Ampudia et al., 2020). In the WT background, in agreement with previous work, Venus fluorescence is highest in the proximal meristem, with weaker signal in the more exterior layers of the

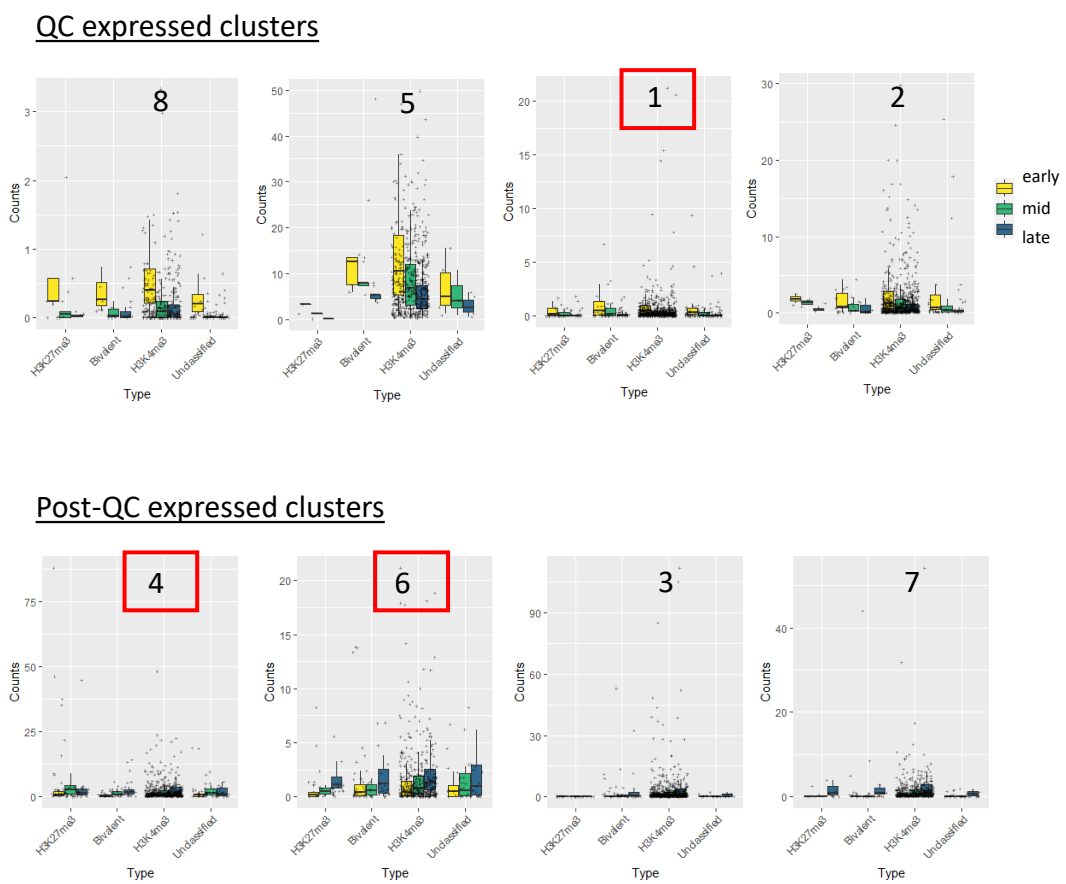

Figure S11 QC-Columella trajectory co-expression cluster analysis. Graphs show average expression level within co-expression clusters along pseudotime

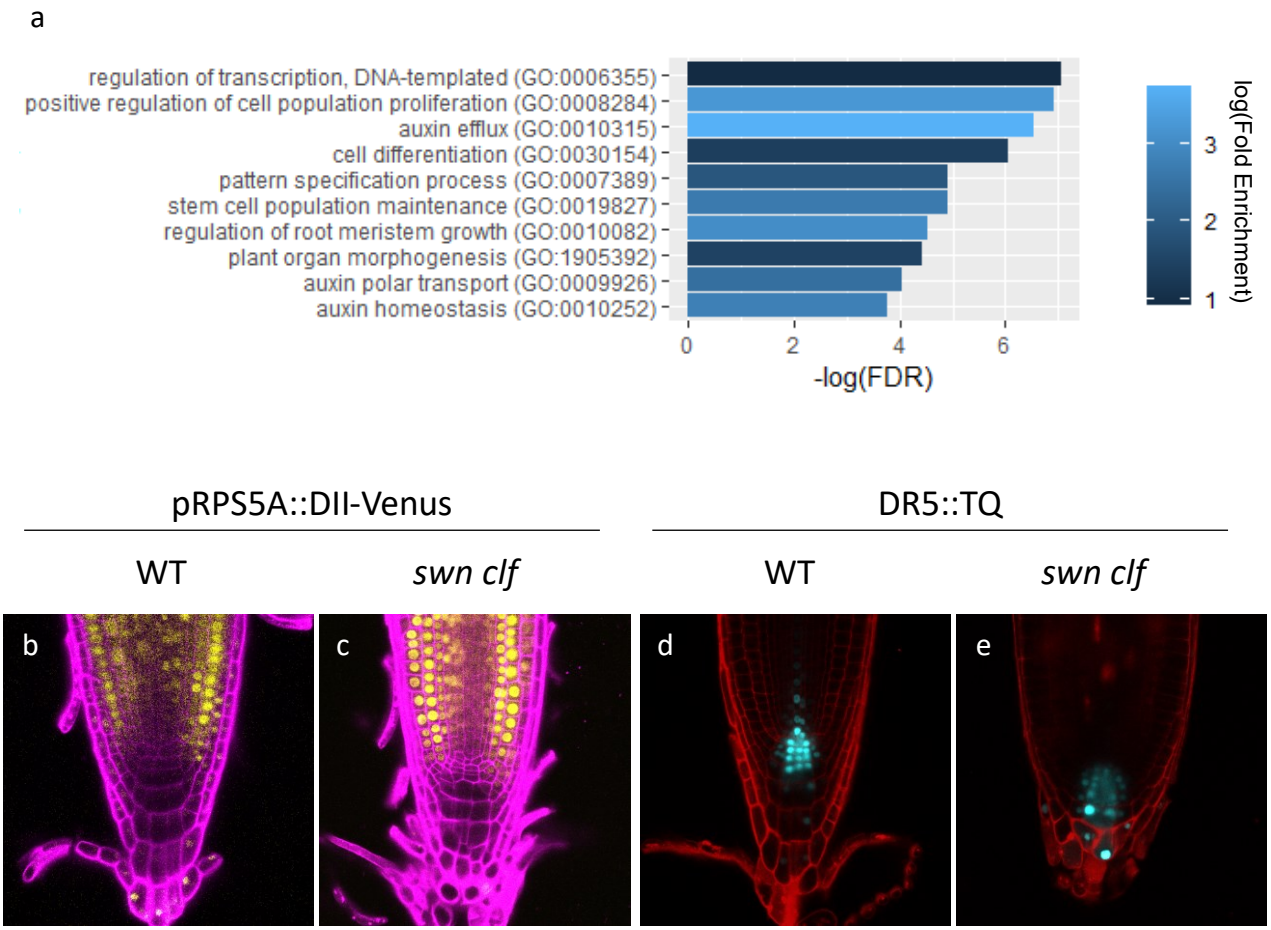

Figure 11 PRC2 activity regulates auxin accumulation and response within the columella. **(a)** GO terms enrichment analysis for genes marked by H3K27me3 in the QC and expressed at late stages during columella development. **(b-c)** Confocal micrographs of *DII-Venus* distribution in WT (b) and *swn clf* (c) root tip revealing cells with low levels of auxin. Note that the fluorescent signal in distant columella and lateral root cap cells observed in WT is absent in *swn clf*. N=5 per genotype **(d-e)** Confocal micrographs of the DR5::TQ marker reporting auxin transcriptional response in WT (d) and *swn clf* (e) root tip. Note the distal shift of auxin response in mature collumella cells observed in absence of PRC2 activity. N= 10 per genotype

columella and lateral root cap (Fig. 11b). In absence of PRC2 activity, Venus fluorescence is unaffected and potentially increased in the proximal meristem, but the signal in the columella and lateral root cap cells is completely absent (Fig. 11c). These observations suggest that auxin accumulates more within the columella/LRC of *swn clf* roots. To support this observation, we also assayed auxin transcriptional response using a *DR5::3xNLS-TQ* containing repeats of the auxin response element motif (Friml et al., 2003; Sabatini et al., 1999; Ulmasov et al., 1997). In WT, we observed a maximum of fluorescence signal in the QC, with progressively weaker signal in Columella Stem Cells (CSC) and their daughter cells (Fig. 11d). In the absence of PRC2, DR5-reported auxin response was stronger in the columella, with a shift of the fluorescence maxima from the QC towards columella-differentiated cells (Fig. 11e).

QC-ground tissue trajectory

To determine how PRC2 regulation is associated with gene expression timing along the longer differentiation gradient, we analysed cortex and endodermis developmental trajectories. Cortical and endodermal cell files both derive from the cortical endodermal initial (CEI) (Petricka et al., 2012). To perform a similar analysis as for columella differentiation in the previous section, we would ideally need to separate cortical from endodermal meristematic cells and analyse them separately with their respective terminal cell identity clusters. However, the UMAP of all cortical and endodermal cells revealed that they are indistinguishable in the meristematic zone, and do not branch into separate clusters before leading to the two ground tissue types (Fig. 9a, Supplementary Text 1). Therefore, while we individually analysed QC to cortical and QC to endodermal cell types, we had to use the entire pool of transcriptionally similar meristematic cells in our analyses.

Interestingly, the cellular paths from QC to mature cortical or endodermal identity show a rupture between transcriptional transitions (Fig. S12a, Fig. S13a). While a technical cause such as a lack of resolution in the single-cell data cannot be ruled out, this disconnection could also reflect a drastic transcriptional shift taking place in cells exiting the meristem. The latter does have some biological grounding as cell at the elongation zone undergo endoreduplication (Bourdon et al., 2012; Bhosale et al., 2018) and may begin to express more cell type-specific genes during specialisation, while reducing their overall mRNA pool (Jean-Baptiste et al., 2019).

Trajectory analysis of cortex differentiation showed a single branch from QC until the aforementioned rupture, after which a late branching is observed (Fig. S12a). Branching may

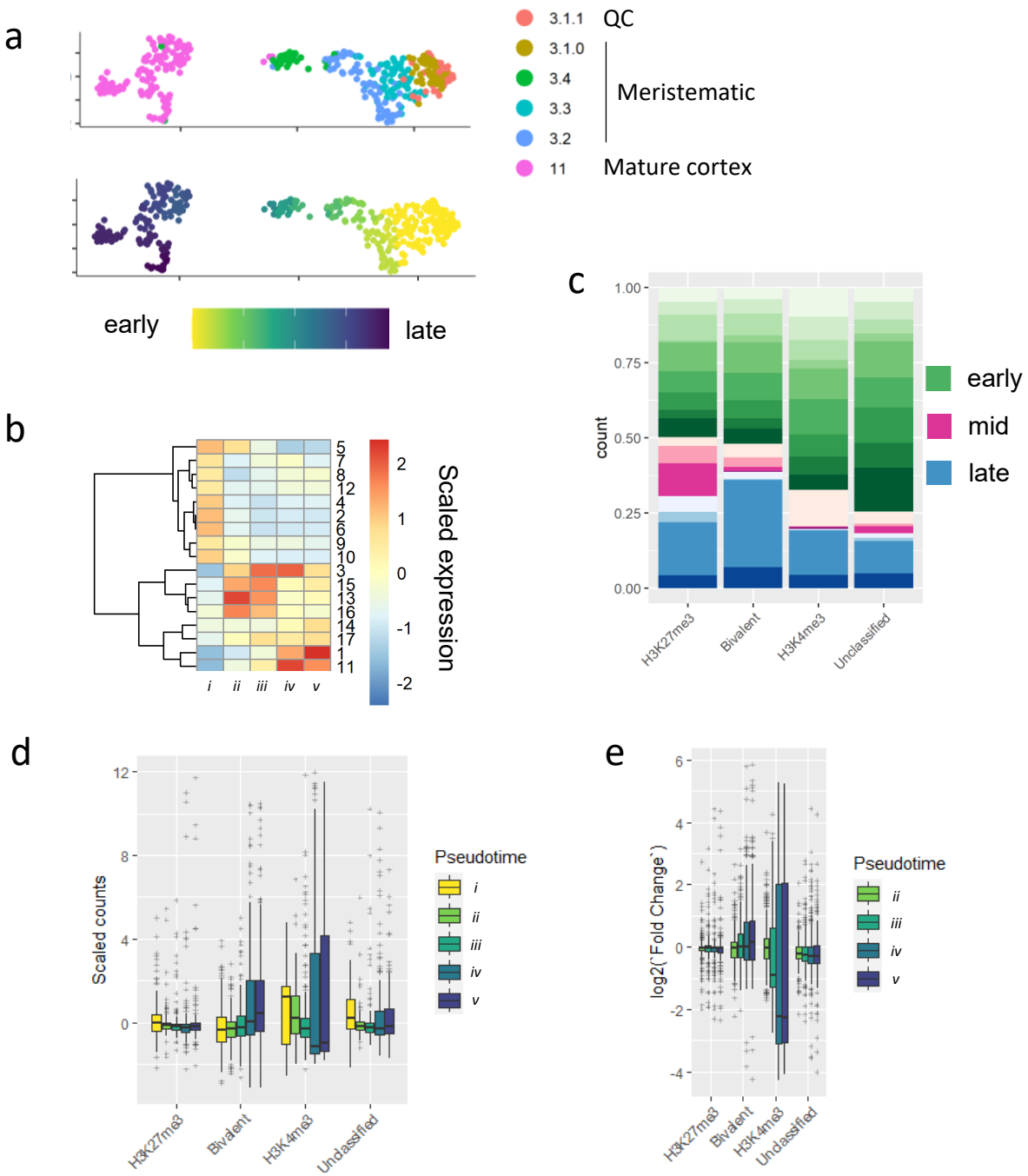

Figure S12 PRC2 activity in the QC is associated with the late expression of genes during cortical differentiation. **(a)** Top: UMAP representation of the 379 cells identified as QC (cluster 3.1.1), meristem (clusters 3.1.0, 3.2, 3.3, and 3.4) and cortex (cluster 11), bottom: UMAP colored by pseudotime along the cortex trajectory. **(b)** Clustering analysis of gene co-expression along developmental pseudotime. Cells were binned into 5 groups (*i*-*v*) of equal number based on pseudotime value. **(c)** Distribution of DEGs among each chromatin type. Early, mid and late are defined by the top three branches of the dendogram in (b). Expression clusters order are as in (b). **(d)** Average expression values for the top 200 DEGs along pseudotime and according to chromatin type in the QC. **(e)** Average fold-change expression per gene according to chromatin type in comparison to expression level in pseudotime bin *i* (i.e. QC/SCN).

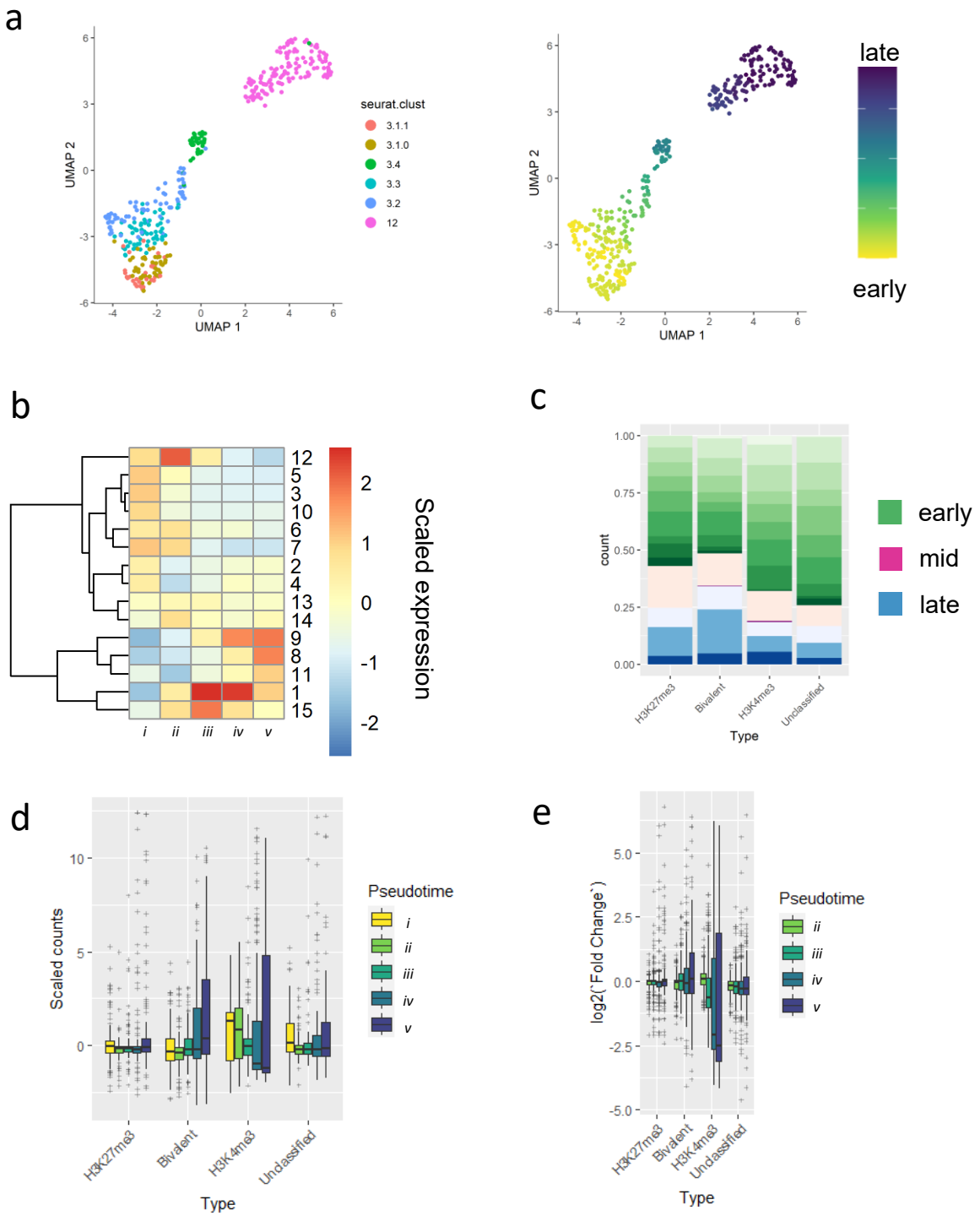

Figure S13 PRC2 activity in the QC is associated with the late expression of genes during endodermal differentiation. **(a)** Left: UMAP representation of the 368 cells identified as QC (cluster 3.1.1), meristem (clusters 3.1.0, 3.2, 3.3, and 3.4) and endodermins (cluster 12), right: UMAP colored by pseudotime along the endodermal development. **(b)** Clustering analysis of gene co-expression along developmental pseudotime. Cells were binned into 5 groups (*i*-*v*) of equal number based on pseudotime value. **(c)** Distribution of DEGs among each chromatin type. Early, mid and late are defined by the top three branches of the dendogram in (b). Expression clusters order are exactly as in (b). **(d)** Average expression values for the top 200 DEGs along pseudotime and according to chromatin type in the QC. **(e)** Average fold-change expression per gene according to chromatin type in comparison to expression level in pseudotime bin *i* (i.e. QC/SCN).

indicate two terminal cell types (Zhang et al., 2019) or a branch dedicated to cell division (Jean-Baptiste et al., 2019). Differential expression analysis over cortex developmental pseudotime was performed and a total of 9,560 dynamically expressed genes were identified along the cortex trajectory, with a low proportion of genes associated with QC-PRC2 regulation among these DEGs (87.6% H3K4me3, 2.2% H3K27me3, 4.4% bivalent and 5.8% unmarked genes). Binning of cells along pseudotime was performed over 5 bins to account for the length of the developmental trajectory, gene co-expression clusters were determined and hierarchical clustering was used to split the clusters into early, mid and late peaking genes (Fig. S12b). As for the columella trajectory, chi-squared enrichment testing found H3K27me3- and bivalently-marked genes in the QC to be more associated with late-expressed genes (30.6% and 38.7% than 20.8% expected by chance) and H3K27me3-marked genes were also slightly more associated with mid-trajectory peaking genes (19.6% instead of 12.6% by chance). Average gene expression over the trajectory did not reveal specific trends related to PRC2 regulation (Fig. S12d-e). Similar trends were observed in the analysis of the endodermal differentiation pathway (Supplementary Text 2, Fig. S13).

GO-term analysis for PRC2-regulated genes among ground tissue trajectories DEGs revealed enrichment in biological functions involving cell differentiation, phytohormone signalling, environmental response and metabolic processes (Fig. 12a-b). To further characterise the effects of PRC2 deficiency during ground tissue development, we introgressed the cortical and endodermal cell identity markers *CO2* and *EN7* reporter lines (Heidstra et al., 2014). In WT, *EN7* and *CO2* are expressed throughout the meristem, though *EN7* expression persists longer than *CO2* along the differentiation gradient. Both markers were expressed at low levels in *swn clf* with irregular and disjointed patterns (Fig. 12c-n), indicating defects in early ground tissue identity maintenance.

4.2.4 PRC2 activity in the SCN appears sufficient to ensure meristem homeostasis and root growth

We finally aimed at functionally testing the importance of PRC2 activity in the QC on overall root development. To this end, we measured root growth and meristem size at early stages of development in roots expressing the full genomic sequence of *CLF* fused to *GFP* under the QC-specific *WOX5* promoter in the *swn clf* background, using WT and *swn clf* seedlings as positive

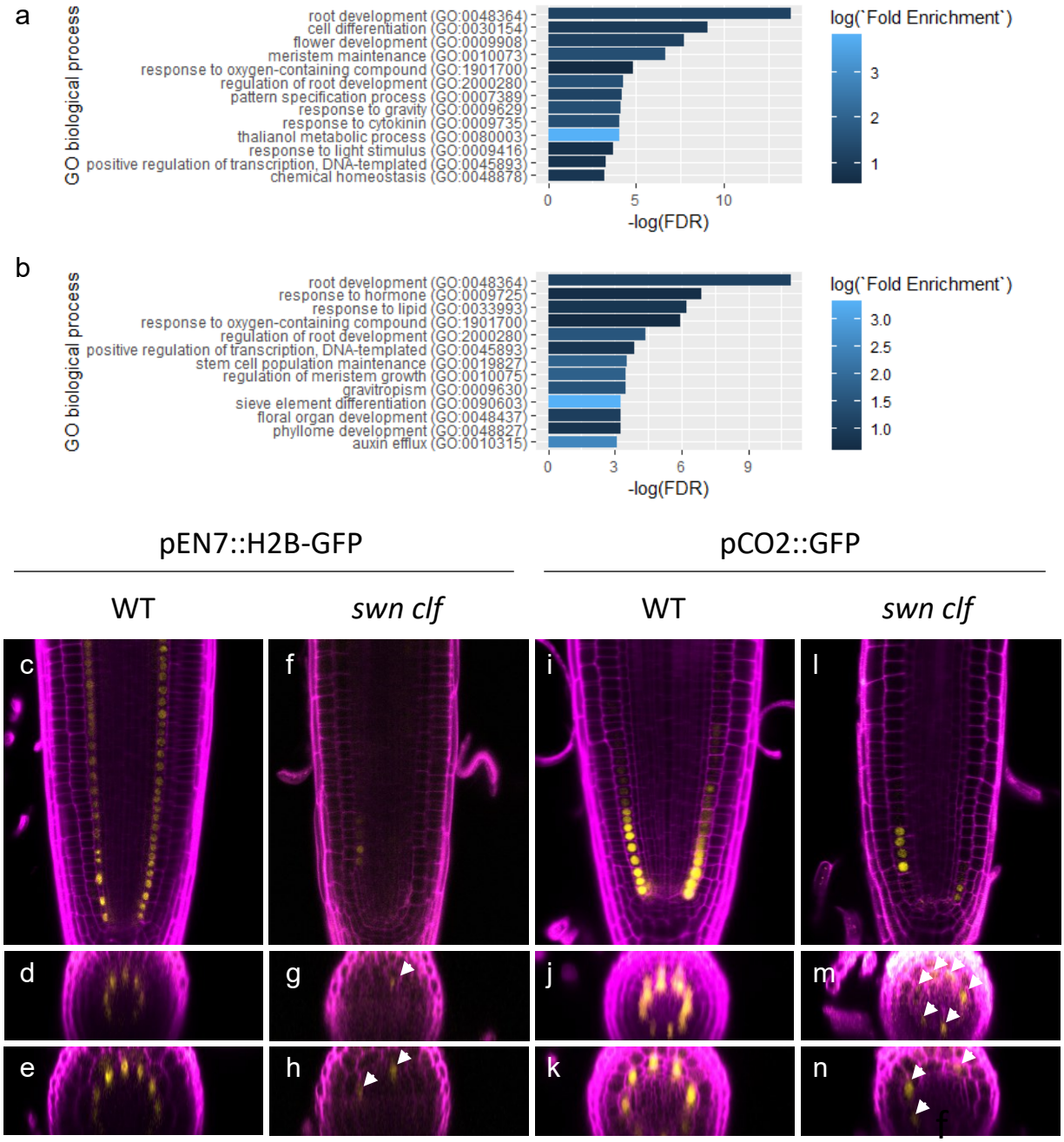

Figure 12 Loss of PRC2 function results in cortical and endodermal specification defects. **(a-b)** GO term enrichment analysis for PRC2-targeted genes among dynamically genes expressed along cortical (a) and endodermal (b) developmental trajectory. **(c-n)** Confocal micrographs of 6-d-old root tip expressing pEN7::H2B-GFP (a-f) and pCO2::GFP (g-l) reporting endodermal and cortical identity respectively. Representative longitudinal sections of the QC plane of WT and *clf swn* are shown in a, d, g, and j. Transverse sections of the same root tip at the Cortex-Endodermis Initial cell plane are shown in b, e, h and k, and at the plane of the eighth cortical meristematic cell in c, f, i and l. Arrowhead in g, h, m and n indicate where weak signal can be observed. At least 20 roots were observed for each genotype.

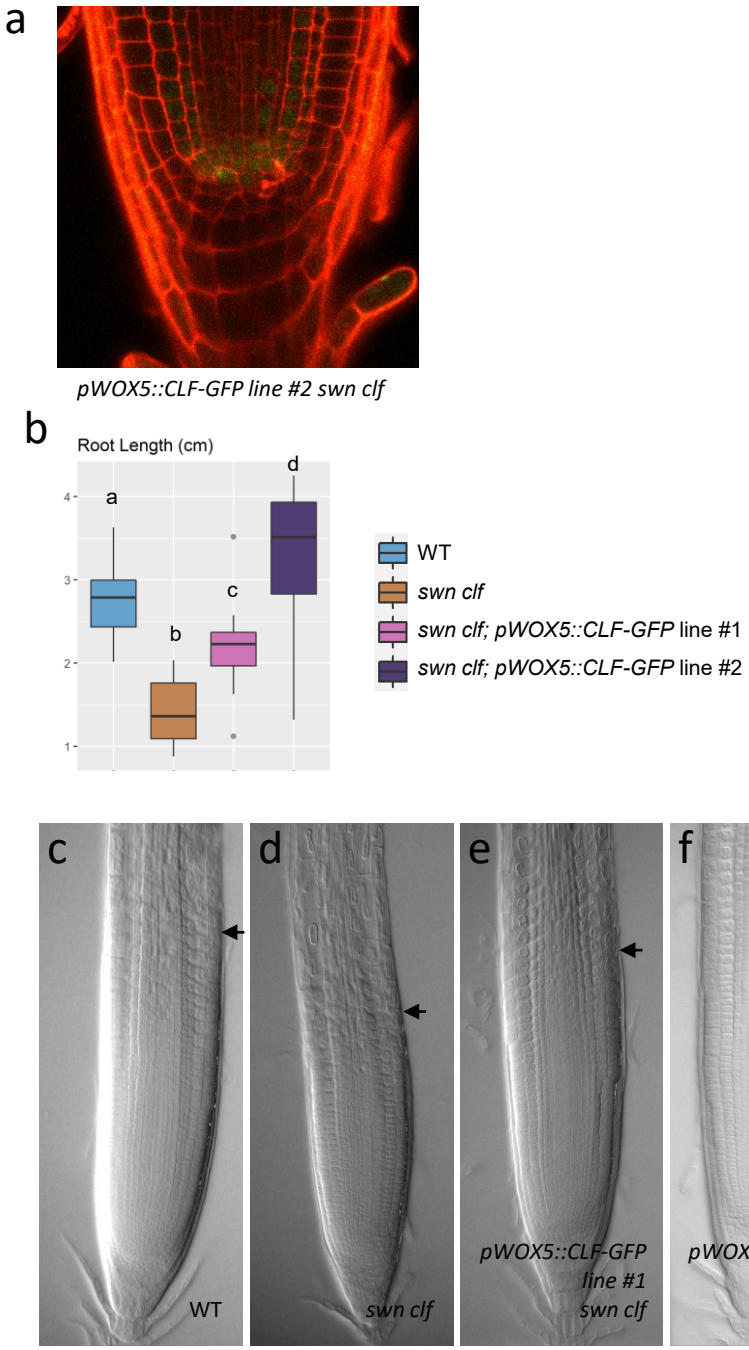

Figure 13 Restoration of PRC2 activity in the QC appears sufficient to rescue root development in *swn clf*. **(a)** Representative confocal micrograph of the pWOX5::CLF-GFP in *swn clf* root tip. **(b)** Quantification of root length of WT, *swn clf*, and two independent *pWOX5::CLF-GFP* lines at 6 DAG. At least 50 roots were measured for each genotype. **(c-f)** Root meristem of the lines analysed in (b). Black arrowheads mars the end of the meristematic zone as defined by cortical cell morphology. **(g)** Quantification of root meristem length among the genotypes. Colour code as in (b). At least 30 roots were measured for each genotype

and negative controls. The GFP signal was faintly visible within the QC and surrounding stem cells in the two independent lines of *pWOX5::CLF-GFP swn clf* analysed (Fig. 13a). As previously reported, root growth and meristem size in *swn clf* double mutants are reduced compared to WT seedlings at 5 days after germination (Fig. 13b-g) (Fig. 4; de Lucas et al., 2016). Strikingly, root growth and meristem size defects in the *swn clf* double mutant were at least partially rescued in these two lines. While these results would indicate that PRC2 activity in the SCN may be sufficient to ensure normal meristem development, more lines should be analysed to give further support to these observations.

4.3 Discussion

A large body of plant literature has shown that PRC2 activity is important in regulating phase transitions during the Arabidopsis life cycle, while leaving a gap about its direct role in cell differentiation. Integration of cell type-specific histone mark distributions with single cell transcriptomics in roots led us to uncover a role for PRC2 activity in regulating waves of transcriptional activation along the differentiation trajectories of at least three cell types. Furthermore, we provide evidence that this activity is required for root meristem homeostasis and proper timing of gene expression associated with cell identity and function.

4.3.1 Epigenomic analysis of a homogenous cell type

Most chromatin studies in plants have been performed on whole organs or complex populations of cells so far, which has been a clear limitation in determining the direct impact of chromatin dynamics on the regulation of developmental programs. Indeed, grinding whole organs leaves us with chromatin data that are averaged over the entire population of cell types. Nevertheless, cell type- or tissue- specific chromatin analysis in Arabidopsis have recently started (You et al., 2017; Engelhorn et al., 2017; Yan et al., 2019). Here, we analysed the QC epigenomic landscape, a significantly more homogenous cell population than in previous studies mainly owing to its ontology and low mitotic activity.

We report that the QC epigenomic landscape largely resembles that of whole root in this and past studies (Roudier et al., 2011). However, conclusions on the relationship between

chromatin types and expression levels in the QC can be more directly interpreted, providing solid evidence for the existence of bivalently marked genes and demonstrating that this particular state correlates with an intermediate expression level.

4.3.2 PRC2 activity in the QC controls meristem homeostasis

Our observations of increased QC divisions, alteration of division planes and expanded *WOX5*-expression domain in absence of PRC2 activity reflect defects in SCN function (Fig. 2d). Striking phenotypic alterations in root function occur once cells actively divide and begin to acquire their identity (Fig. 11b-e; Fig. 12c-n).

PRC2 activity in the QC likely plays an important role in the regulation of signalling pathways that are implicated in maintaining meristem homeostasis. Thus, key candidate PRC2 targets involved in such a regulatory network include *PLT1*, *PLT2*, *RGF1*, and *RGF4* (Ou et al., 2016; Yamada et al., 2020). In addition, we show that auxin signalling and response is defective in *clf swn*, which has also been reported in *clf* single mutant (Gu et al., 2014), with effects on meristem homeostasis (albeit the opposite effect, increasing growth rate and meristem size). Reintroduction PRC2 activity in the QC would then suffice to ensure normal levels of auxin related genes, and re-equilibrate the auxin/PLT/RGF gene network (Salvi et al., 2020; Ou et al., 2016; Yamada et al., 2020), thus rescuing root growth.

Defects beyond the QC could also be directly due to the lack of H3K27me3 in stem cell daughter cells, potentially as a cause of or in addition to the absence of the mark in the QC, notably since there is a clear transition in cellular behaviour from the relative quiescence to slow asymmetric division, and then to rapid mitosis at the very beginning of each cell differentiation pathways. PRC2 regulation having a role in the regulation of asymmetric division could explain the observations of defects in cortical and endodermal cell fate patterning (Hugues et al., 2020).

4.3.3 PRC2 is an important repressor of gene networks with high activation potential

We showed numerous correlations indicating that PRC2 is involved in spatial and temporal control of dynamically regulated genes during multiple differentiation pathways. We found that some PRC2 targets that are dynamically regulated during differentiation are already expressed in the QC while being still marked by H3K27me3, and usually the entire SCN. This adds to other

studies showing that the presence of H3K27me3 is not sufficient to predict the abolishment of transcription (Schubert et al., 2006) or transcriptional activation (Buzas et al., 2011), indicating that the presence of H3K27me3 and transcription are not completely incompatible.

PRC2 could be important not only in maintaining transcriptional repression, but also in the maintenance of a low expression levels of some genes. For instance, PRC2 activity was shown to attenuate *NRT2.1* expression during nitrate response (Bellegarde et al., 2018). This corroborates the notion that PRC2 limits gene expression for genes which are particularly sensitive when responding to cellular or environmental conditions, and require PRC2 regulation to filter out noise in activating signals (Bellegarde et al., 2018; Berry et al., 2017). The high proportion of PRC2 regulated genes among QC-enriched and -depleted genes showing upregulation in the absence of PRC2 (Fig. 9c) is particularly striking given that numerous studies have shown that H3K27me3 removal alone is insufficient to induce gene activation (Bouyer et al., 2011; Lafos et al., 2011; Rymen et al., 2019; Engelhorn et al., 2017; You et al., 2017). These dynamically expressed genes likely depend on PRC2-regulation for fine-tuning their expression along the root gradient, and more particularly in the QC, whose strategic position between the two differentiation gradients may represent a particularly contentious transcriptional environment (Choe et al., 2017; Rahni et al., 2016).

Of note, we show that within a given *swn clf* root, meristematic-cortical and -endodermal cell identity is lost at different distances from the SCN within the different cell files, even as early as in CEI daughter cells (Fig. 12 g, h, m, n). Since each cell is a result of anticlinal divisions of different initial cells, this may reflect a stochastic failure of specifying or maintaining cell identity in the cell files of these two cell types. Quantitative analysis of *CO2* and *EN7* expression patterning in the transgenic lines complementing PRC2 in the QC would further elucidate the role of PRC2 during the initial transitions of cells out of the SCN.

4.4 Materials and Methods

Plant materials and growth conditions

All the lines used are in the Col-0 accession. The *swn-7* (SALK_139371) and *clf-28*- lines (SALK_109121) have been described previously (Doyle et al., 2009; Wang et al., 2006) and the absence of full mRNA expression has been validated by RNA-seq. The pWOX5-NTF line was

described in Marquès-Bueno, Morao, Cayrel et al., (2016). *DR5::TQ* and *qDII-Venus* (Galvan-Ampudia et al., 2020) were kindly provided by Carlos Galvan-Ampudia. pEN7::H2B-GFP and pCO2::GFP were provided by the Ben Scheres lab (Heidstra et al., 2004). The pWOX5::CLF-GFP line was transformed into WT and *swn-7 -/- clf-28 +/-* backgrounds.

All plants were grown in long day conditions cycling 22.5°C for 16 hours in light, and 18.5°C for 8 hours in darkness. For all experiments, seeds were surface sterilised, stratified in water at 4°C for 3 days in darkness, sown on agarose plates (½MS, 1% sucrose, 1% agarose) and grown vertically under the same photoperiodic conditions.

Cloning strategy

The *pWOX5::CLF-GFP* line was generated using the Golden Gate strategy (Engler et al., 2014). Briefly, the promoter sequence of *WOX5* was obtained by amplifying genomic DNA using the primer pair WOX5_promoter (see Table 2 of the Annexe section), and the purified PCR product was cloned into the pICH47811 (Addgene) vector. eGFP was cloned into pICSL5008 (Addgene). The full length 5,295 bp genomic sequence of the *CLF* gene was obtained by direct DNA synthesis, and cloned in pUC57 (Genewiz). *pWOX5::CLF-GFP* was assembled using the plasmids containing the *WOX5* promoter, *CLF* genomic sequence, eGFP and a terminator in pICH77901 into the destination vector pICH47811 (Addgene), in a single cloning step. The assembled product was then cloned into pAGM4673 with a BASTA resistance cassette, and an end linker (in pICH41744). All purifications in between cloning steps were performed using Nucleospin Gel and PCR Clean-up (Macherey-Nagel).

The plasmid containing *pWOX5::CLF-GFP* was then introduced into *Agrobacterium tumefaciens* by electroporation and subsequently transformed into *swn-7 -/- clf-28 +/- Arabidopsis* plants using the floral dip method.

INTACT purification of QC nuclei, Chromatin immunoprecipitation (ChIP) and library preparation

INTACT experiments were perfomed according to Morao et al., 2018. Briefly, roots from *in vitro* grown *pWOX5::NTF* seedlings were harvested and cross-linked with 1% formaldehyde for 15 minutes. After stopping cross-linking, roots were frozen in liquid nitrogen and ground to a fine

powder. Nuclei were isolated using a Dounce tissue grinder. GFP-labelled nuclei were then purified using magnetic beads that were loaded with anti-GFP antibodies (Abcam, Ab290). Multiple washes were performed to remove cellular debris and unlabelled nuclei to obtain a purified nuclei suspension. For whole root ChIP, WT roots were harvested and cross-linked with 1% formaldehyde in vacuum for 15 minutes. Following extraction, chromatin was sonicated using a Covaris S220 ultra-sonicator to generate DNA fragments with an average length of 250 bp. A small proportion of solubilised chromatin of each replicate was kept as INPUT, while the rest was incubated overnight with an excess of anti-H3K27me3 or anti-H3K4me3 antibodies (Millipore 07-449 and 07-473). Purified DNA fragments were used for qPCR testing for enrichment level of histone mark over known loci compared to INPUT and validate the purity of the nuclei population. Purified DNA fragments from multiple INTACT-ChIP experiments were pooled together to produce a single INTACT replicate, owing to the low amount of QC cells per root and thus recovered DNA. 1ng of immunoprecipitated DNA was used for library preparation (Diagenode MicroPlex v2).

Two biological replicates were obtained for whole root H3K27me3 and QC H3K4me3 samples. Three were obtained for QC H3K27me3, and one was produced for whole root H3K4me3.

Analysis and integration of ChIP-seq replicates

High-quality reads were mapped to the TAIR10 Arabidopsis genome using bowtie2 (Langmead and Salzberg, 2012) with the –very-sensitive option. Reads with a maximum of one mismatch were kept, and PCR duplicates were removed. Peak calling analysis was performed using MACS2 (Zhang et al., 2008) which uses a model-based approach to define peaks based on background levels of signal within a sample. Multiple replicates were integrated using IDR (Li et al., 2011). Genes were annotated as marked by a histone mark when a peak overlapped by at least one bp with a gene.

Quantitative analysis of counts in Fig. 8b-c were produced by measuring average RPM-normalised read counts between replicates.

Analysis of bulk RNA-seq

High quality reads were mapped to the TAIR10 Arabidopsis genome using bowtie2 (Langmead and Salzberg, 2012) with the –very-sensitive option. Reads with a maximum of one mismatch were kept, and PCR duplicates were removed. Quantitative analysis of counts in Fig. 9c were produced by measuring average RPM-normalised read counts between replicates each gene. Two replicates were analysed for WT and one replicate was analysed for *swn clf*.

Reanalysis of pubically available single cell RNA-seq data

Denyer, Ma et al., 2019 single cell RNA-seq data were downloaded from the NCBI's Gene Expression Omnibus, under the reference GSE123818. The analysis pipeline was largely inspired from methods used in three papers analysing Arabidopsis roots by scRNA-seq (Shulse et al., 2019; Denyer, Ma et al., 2019; Jean-Baptiste et al., 2019).

Generation of a single cell expression matrix

The initial count table was generated exactly as in the original publication. Briefly, sequenced reads were aligned using CellRanger (Chromium 10X) to the TAIR10 Arabidopsis genome. A matrix of gene expression per cell was generated at this point, and PCR duplicates were removed. Valid cells were chosen with the following criteria: cell read count > 5% of 99th percentile of cells. Protoplasting-induced genes were removed using a list of genes in Supplementary Table 1 of the original publication.

Normalisation, dimensionality reduction and clustering analysis

The Seurat R package was used for normalisation of the data and relies on SCTransform, which is based on using regularised negative binomial regression, shown to be more efficient in correcting bias in read counts per cell (Hafemeister and Satija, 2019).

Variable genes were used to perform PCA analysis. 50 PCs were used as input for clustering cells by cell type using a resolution of 0.8, defining 18 clusters (numbered from 0-17) (Fig. S9a). The same 50 PCs were also used to perform Uniform Manifest Approximation and Projection (UMAP) dimensional reduction (McInnes et al., 2020).

Cell cluster identification

In order to identify clusters, a combination of three methods was used. Firstly, we determined the expression patterns of literature-derived markers in clusters using the DotPlot feature of the Seurat package. This allowed estimation of the percent of cells and the average levels of expression of a given gene within a cluster (Fig. S9b). A secondary approach evaluated cluster identity by using Spearman correlation to determine similarity of each cluster transcriptome with cell-sorted bulk-transcriptomes (Li et al., 2018) (Fig. S9c). Finally, we performed Spearman correlation between each cluster's transcriptome with the marker genes' specificity scores as specified in (Materials and Methods and Supplementary Table 2 in Denyer, Ma et al., 2019), based on the ICI method (Efroni et al., 2015). Results are discussed in Supplementary Text 1.

Differential gene expression analysis for QC cluster compared to other clusters

Differentially expressed genes of QC cells in Fig. 9b were found using the "FindMarkers" function in Seurat, using the Wilcox test with default parameters. A q-value cutoff of 0.05 was used to filter significant positive and negative QC marker genes.

Trajectory analysis using Monocle3

The count matrices for variable genes as determined by the SCTransform method in cells belonging to a given trajectory were used to perform pseudotime trajectory analysis with Monocle 3 (Cao et al., 2019). Cell counts were log-scale normalised before PCA analysis. 50 PCs were used as the input of UMAP dimensional reduction. Cells were then ordered using the cell with maximum *AGL42* expression as the root of the trajectory. Significantly differentially-expressed genes (q-value < 0.05) along the trajectory were determined using the "graph_test" function in Monocle3. Hierarchical clustering of genes was performed using "find_gene_modules" with a resolution of 0.05 for columella trajectory and 0.01 for ground tissue trajectories. Genes were binned by pseudotime and clustered to reduce computer calculation time.

Average gene expression levels per bin (Fig 10d-e, Fig. S12d-e and Fig. S13d-e) were calculated using SCTransform values of all genes of a given trajectory, within cells in each pseudotime bin.

Confocal microscopy of root tips

Roots at 5DAG of *in vitro* grown seedlings were immersed in propidium iodide solution (20 µg/L) for 10 minutes before mounting in water between a glass slide and coverslip. Imaging was performed using a Zeiss LSM710 confocal microscope. Laser intensity and photo-multiplicator transmitter was modified between reporter lines to optimise dynamic range of the signal while reducing background noise and over-exposure. The same parameters were used to generate all images of the same marker line.

Meristem length quantification

For meristem length quantification, *in vitro* grown seedlings at 5DAG were cleared with chloral hydrate solution (chloral hydrate 40g/L, glycerol 30%) and images of the root sagittal plane were taken using a Zeiss AxioImager microscope equipped with a Differential Interference Contrast (DIC) optics. The number of cortical cells was counted from the cortex-endodermis initial to the final meristematic cortex cell for each image.

4.5 Supplementary Information

Supplementary Text 1: Cell type identification of clusters during reanalysis of Denyer, Ma et al., 2019 dataset

Many cell types of interest were satisfactorily separated and defined by integrating expression patterns of literature-derived markers and global transcriptomic correlation approaches (Methods); our results strongly resemble that of the author's original analysis when dealing with the same cell type.

In order to perform trajectory analysis of different cell types, we required higher resolution into the meristematic cluster, cluster 3. We therefore isolated cluster 3 and repeated the PCA and clustering analysis on this group, an approach has been shown to yield further resolution into clusters of interest (Denyer, Ma et al., 2019). This yielded 5 sub-clusters of meristematic cells, with three showing clear identities, notably cluster 3.1 with the strongest QC identity, and 3.4 and 3.0 showing strong ground tissue and stele initial identity respectively (Fig. S9b-d). Further sub-clustering of the 99 cells in cluster 3.1 was performed to differentiate sub-clusters 3.1.1 (33 cells) and 3.1.2 (22 cells), which show high expression of the QC-marker *AGL42* and the CEI marker *CYCD6* respectively (Fig. S9b). Attempts to find sub-clusters of cluster 3.4 did not result in meaningful improvements in identity, possibly due to the already low number of cells (33 cells) within this cluster.

Supplementary Text 2: Details on the trajectory analysis of endodermal development

Trajectory analysis of endodermal development showed a single branch from the cells of the QC cluster to those of the endodermal cluster (Fig. S12a). DEG analysis over endodermis developmental pseudotime was performed and a total of 9,189 dynamically expressed genes along the trajectory were identified, with low levels of PRC2 regulation among dynamic genes (87.6% H3K4me3, 2.2% H3K27me3, 4.4% bivalent and 5.8% unmarked genes). Gene co-expression clusters were determined and hierarchical clustering split the clusters into early, mid and late peaking genes (Fig. S12b). As for columella and cortical trajectories, chi-squared enrichment testing found H3K27me3 and bivalently marked genes to be more associated with late peaking genes (24.8% and 34.25% than 19.3% expected by chance). H3K27me3 genes were also slightly more associated with mid-trajectory peaking genes (18.2% instead of 13.4% by

chance). As over cortex differentiation, average expression levels variation did not reveal specific trends related to PRC2 regulation (Fig. S12d-e).

Supplementary Table 1: Numbers and associated Gene Ontology biological function terms of different combinations of chromatin type within the QC and whole root based on peak calling and gene annotation.

Gene QC chromatin type	Gene whole root chromatin type	Number of genes	Associated GO terms
H3K27me3	H3K27me3	3,577	Fatty acid metabolic process; regulation of secondary cell wall biogenesis; response to stimulus; glucosinate catabolic process; suberin biosynthetic process; response to insect; cell-cell signaling involved in cell fate commitment; carbohydrate transport; positive regulation of proteasomal ubiquitin-dependent protein catabolic process; negative regulation of catalytic activity; floral organ development
H3K27me3	Co-marked	858	Maintenance of location; regulation of transcription
H3K27me3	H3K4me3	6	No significant enrichment
H3K27me3	Unmarked	18	No significant enrichment
Bivalent	H3K27me3	142	No significant enrichment
Bivalent	Co-marked	1,614	Respiratory burst; carotene catabolic process; stamen filament development; secondary metabolic process; shade avoidance; mRNA transcription; positive regulation of leaf senescence; asymmetric cell division; radial pattern formation; regulation of hormone metabolic process; phosphate ion transport; morphogenesis of a branching structure; induced systemic resistance; brassinosteroid metabolic process; cell wall macromolecule catabolic process; ethylene-activated signaling pathway olefinic compound biosynthetic process; immune effector process; pectin catabolic process; regulation of auxin mediated signaling pathway; response to nematode; response to chitin; response to jasmonic acid; auxin polar transport; cell wall modification; plant organ formation; leaf morphogenesis; response to brassinosteroid; amine metabolic process; meristem maintenance; terpenoid biosynthetic process; regulation of immune system process; negative regulation of molecular function; tropism; response to wounding; post-embryonic plant morphogenesis; cellular response to hypoxia; cellular response to lipid; defense response to fungus; negative regulation of transcription; cellular response to oxygen-containing compound; chemical homeostasis; regulation of post-embryonic development; root development; transmembrane transport

Supplementary Table 1: (continued)

Gene QC chromatin type	Gene whole root chromatin type	Number of genes	Associated GO terms
Bivalent	H3K4me3	41	tRNA threonylcarbamoyladenosine metabolic process; cellular response to hypoxia; response to chitin
Bivalent	Unmarked	1	No significant enrichment
H3K4me3	H3K27me3	38	No significant enrichment
H3K4me3	Co-marked	593	Response to chemical
H3K4me3	H3K4me3	14,650	Regulation of RNA splicing; response to endoplasmic reticulum stress; regulation of mRNA processing; nucleic acid phosphodiester bond hydrolysis; protein localization to endoplasmic reticulum; protein maturation; endosomal transport; ribosomal large subunit biogenesis; endoplasmic reticulum to Golgi vesicle-mediated transport; protein targeting to membrane; RNA 3'-end processing; nuclear-transcribed mRNA catabolic process; protein modification by small protein removal; mitochondrion organisation; membrane lipid biosynthetic process; rRNA processing; nuclear chromosome segregation; DNA-dependent DNA replication; vacuolar transport; establishment of protein localization to organelle; protein acylation; protein folding; protein-DNA complex assembly; glycerophospholipid biosynthetic process; chloroplast organization; intracellular protein transmembrane transport; mRNA splicing, via spliceosome; meiotic nuclear division; tRNA processing; ribonucleoprotein complex assembly; regulation of DNA metabolic process; positive regulation of cellular component organization; peptidyl-lysine modification; protein import; nucleocytoplasmic transport; translation; DNA recombination; nucleobase-containing compound transport; gene silencing; regulation of translation; response to cadmium ion; double-strand break repair; DNA conformation change; RNA modification; macromolecule methylation; histone modification; organelle assembly; alpha-amino acid biosynthetic process; regulation of chromosome organization; nucleotide biosynthetic process; membrane organization
H3K4me3	Unmarked	229	No significant enrichment
Unmarked	H3K27me3	872	Regulation of cell morphogenesis involved in differentiation
Unmarked	Bivalent	142	No significant enrichment
Unmarked	H3K4me3	1,084	Mitotic cell cycle process
Unmarked	Unmarked	4,293	Regulation of protein localisation to cell surface; regulation of double fertilisation forming a zygote and endosperm

5. Overall Discussion

My PhD work aimed at furthering our understanding about the role of PRC2 in regulating cellular transitions in the context of root development. Part of this work investigated the mechanistic differences between two homologues of the catalytic subunit of PRC2. We showed that these subunits cooperate to maintain H3K27me3 over target genes, though in apparently opposite means. We further show that increasing the levels of SWN within a cell results in phenotypic abnormalities, largely phenocopying the loss of its homologue, *CLF,* indicating a tight regulation of PRC2 activity exists and may be a factor in fine-tuning PRC2 activity.

To find the loci might that be responsible for the root growth defects observed in absence of PRC2, we have determined the repertoire of PRC2 targets within the QC cells. Our data suggests that PRC2 regulates well-known genetic pathways involved in controlling SCN activity. We also found that PRC2 tends to regulate genes expressed relatively late stages of cell differentiation. In agreement with these observations PRC2 deficiency leads to functional defects both in the QC and during cellular transitions along differentiation gradients.

5.1 PRC2, the lenient dictator

The key role of PRC2 in regulating plant development has been demonstrated in many instances by genetic approaches. By adding high-resolution genomic data, we show the role of PRC2 in controlling the timing and level of gene expression during the differentiation of root cell types. In particular, we find that PRC2 activity regulates two categories of genes during differentiation, the bivalently- and H3K27me3-marked genes, respectively expressed at intermediate and low levels. This resembles what has been observed in mammalian cell cultures (Bernstein et al., 2006).

This adds to increasing evidence that the presence of H3K27me3 does not exclude transcriptional activity at genes, as reported in the animal field (Young et al., 2011; Sanchez et al., 2013; Kar et al., 2017). Thus PRC2 activity may not completely silence its targets, but instead reduces the probability that genes may be transcribed (Berry et al., 2017). Relevance of this

probabilistic model may reflect in the stochastic nature of the phenotypes triggered by PRC2 loss of function, often with variable effects. Three classes of root phenotypes in absence of PRC2 are observed and their respective frequency according to the genetic background (Fig. 14a). During my work, I also encountered stochastic phenotypes in roots and shoot development (Fig. 12g,h,m,n; Fig. 14b). These observations point to a role of PRC2 in conferring robustness by filtering out transcriptional noise during the crosstalk of developmental gene networks.

At the cell population level, the sum of individual probabilistic events leads to an averaging likely resulting in the basal expression we observe among PRC2 targets. The intermediate expression levels observed over bivalently marked genes could correspond to genes for which transcription is activated due to factors that remain to be identified, and the balance between repressive and activating chromatin factors lead to the observed expression level. We found that the QC bivalent genes are enriched in functions related to signalling, a result which also has been observed among expressed Polycomb-regulated genes in murine cell culture (Kar et al., 2017), together reflecting a need for PRC2 repression to modulate, but not necessarily abolish, transcription specifically in these genes in multicellular organisms.

Interestingly, transcription may even be necessary for PRC2 recruitment. Human PRC2 has been shown not only to bind promiscuously to RNA (Zhao et al., 2010; Davidovich et al., 2015), but that nascent RNA contributes directly to PRC2 occupancy and H3K27me3 distribution in embryonic stem cells and induced pluripotent stem cells, via an RNA-interaction domain on the human E(z) homologue, EZH2 (Wei et al., 2016; Long et al., 2020).

Working on a parallel topic, we show that modifying SWN dose in plants perturbs PRC2 regulation of flowering time together with leaf shape. This phenotype is recurrently observed in PRC2-deficient plants and is directly attributed to PRC2 regulation of genes such as *AG* and *SEP3*, though we haven't confirmed this in our work. Nevertheless, the hypothesis that SWN may act, by an unknown mechanism, to activate these genes in spite of the presence of functional CLF within plants is a tempting one. An activating role of a PRC2 subunit was reported in humans, where EZH1 and SUZ, the human *E(z)* and *Su(z)* homologues, form a non-canonical complex binding to expressed genes that are not targeted by canonical human PRC2 (Xu et al., 2015). Whether or not gene activation by EZH1 is direct or simply correlative remains unclear. SWN distribution analysis by ChIP-seq experiments (this work and Shu et al. (2019)) did not

a

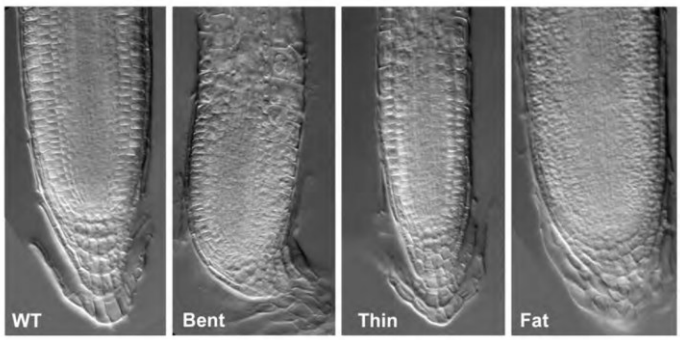

fie
emf2 vrn2
swn clf

b

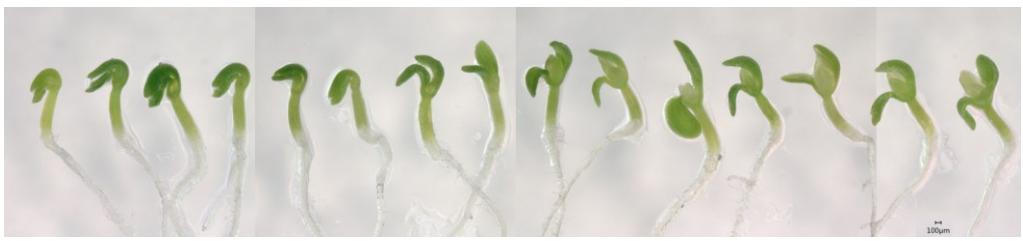

Figure 14 Stochasticity in absence of PRC2. **(a)** Variation in root morphological phenotypes at 5 DAG in absence of PRC2 in reported by Ana Morao (thesis). Root phenotyping work on *swn clf* mutants in this manuscript only considered "thin" roots, the major class in my conditions. **(b)** Variation in *swn clf* mutants shoot phenotypes at 5DAG, with highly variable degrees of cotyledon bending and secondary organ development.

reveal enrichment at non-PRC2 targets. Nevertheless, the evidence does not rule out a situation where SWN may play a role in the maintenance of low expression of a subset of PRC2 targets, conferring additional nuance in the idea of PRC2 as a strict silencer.

5.2 An Evo-devo perspective

Our work on both the mechanistic roles of different PRC2 complexes, as well as its impact on cell identity transitions, could greatly benefit from work in a simpler and more homogeneous system, such as *Physcomitrium patens*. *P. patens* (earthmoss) is a rising model for which an increasing amount of research tools and ressources are available (Rensing et al., 2020).

P. patens has only one copy of *PpE(z)*, called *PpCLF*, responsible for all PRC2 methyltransferase activity within the organism (Okano et al., 2009; Pereman et al., 2016). Complementation assays of *ppclf* with *AtSWN, AtCLF* and *AtMEA* could help determining which ancestral activities of *E(z)* are maintained in each *AtE(z)* copy, ultimately providing more clues about their functional differences and thus about the driving forces underlying their evolution, outside of expression patterning.

PRC2 activity is important for ensuring organogenesis in *P. patens*, a species in which its absence causes sporophyte-like organs to grow instead of gametophytic organs (Okano et al., 2009; Pereman et al., 2016). Furthermore, protonema, a filamentous organ which grows and branches from the germinated moss spore, grows much slower in *Pp-clf* and *Pp-fie* mutants than in WT (Pereman et al., 2016). This is strongly reminiscent of the perturbations in root and shoot organogenesis and identity specification observed in *A. thaliana* mutants lacking PRC2 activity (Chanvivattana et al., 2004; Bouyer et al., 2011; de Lucas et al., 2016; this work). A previous study working on three relatively close species of *A. thaliana, A. lyrata* and *Arabis alpina* who diverged about ~25M years ago, led to the finding that common PRC2 targets were genes with high selective pressure, for example those with reproduction- or development-related function. Meanwhile more variation between species was observed for PRC2 regulation over genes involved in environmental response (Chica et al., 2017). Studying PRC2 targets in the evolutionarily distant moss (diverged ~500M years ago) could allow for a further

understanding of the evolution of PRC2 repression implication in the green lineage, and also provide perspective on PRC2 control of development described in chapter 2.

6. References

Aichinger E, Villar CBR, Di Mambro R, Sabatini S, Köhler C. The CHD3 Chromatin Remodeler PICKLE and Polycomb Group Proteins Antagonistically Regulate Meristem Activity in the Arabidopsis Root[C][W]. *Plant Cell*. 2011;23(3):1047-1060. doi:10.1105/tpc.111.083352

Angel A, Song J, Dean C, Howard M. A Polycomb-based switch underlying quantitative epigenetic memory. *Nature*. 2011;476(7358):105-108. doi:10.1038/nature10241

Bannister AJ, Kouzarides T. Regulation of chromatin by histone modifications. *Cell Res*. 2011;21(3):381-395. doi:10.1038/cr.2011.22

Bellegarde F, Herbert L, Séré D, et al. Polycomb Repressive Complex 2 attenuates the very high expression of the Arabidopsis gene NRT2.1. *Scientific Reports*. 2018;8(1):7905. doi:10.1038/s41598-018-26349-w

Bernstein BE, Mikkelsen TS, Xie X, et al. A Bivalent Chromatin Structure Marks Key Developmental Genes in Embryonic Stem Cells. *Cell*. 2006;125(2):315-326. doi:10.1016/j.cell.2006.02.041

Berry S, Dean C, Howard M. Slow Chromatin Dynamics Allow Polycomb Target Genes to Filter Fluctuations in Transcription Factor Activity. *Cell Systems*. 2017;4(4):445-457.e8. doi:10.1016/j.cels.2017.02.013

Bhosale R, Boudolf V, Cuevas F, et al. A Spatiotemporal DNA Endoploidy Map of the Arabidopsis Root Reveals Roles for the Endocycle in Root Development and Stress Adaptation. *The Plant Cell*. 2018;30(10):2330-2351. doi:10.1105/tpc.17.00983

Bourdon M, Pirrello J, Cheniclet C, et al. Evidence for karyoplasmic homeostasis during endoreduplication and a ploidy-dependent increase in gene transcription during tomato fruit growth. *Development*. 2012;139(20):3817-3826. doi:10.1242/dev.084053

Bouveret R, Schönrock N, Gruissem W, Hennig L. Regulation of flowering time by Arabidopsis MSI1. *Development*. 2006;133(9):1693-1702. doi:10.1242/dev.02340

Bouyer D, Roudier F, Heese M, et al. Polycomb repressive complex 2 controls the embryo-to-seedling phase transition. *PLoS Genet*. 2011;7(3):e1002014. doi:10.1371/journal.pgen.1002014

Brady SM, Orlando DA, Lee J-Y, et al. A High-Resolution Root Spatiotemporal Map Reveals Dominant Expression Patterns. *Science*. 2007;318(5851):801-806. doi:10.1126/science.1146265

Brunoud G, Wells DM, Oliva M, et al. A novel sensor to map auxin response and distribution at high spatio-temporal resolution. *Nature*. 2012;482(7383):103-106. doi:10.1038/nature10791

Buzas DM, Robertson M, Finnegan EJ, Helliwell CA. Transcription-dependence of histone H3 lysine 27 trimethylation at the Arabidopsis polycomb target gene FLC. *The Plant Journal: For Cell and Molecular Biology*. 2011;65(6):872-881. doi:10.1111/j.1365-313X.2010.04471.x

Cao J, Spielmann M, Qiu X, et al. The single-cell transcriptional landscape of mammalian organogenesis. *Nature*. 2019;566(7745):496-502. doi:10.1038/s41586-019-0969-x

Chanvivattana Y, Bishopp A, Schubert D, et al. Interaction of Polycomb-group proteins controlling flowering in Arabidopsis. *Development*. 2004;131(21):5263-5276. doi:10.1242/dev.01400

Chen K, Hu Z, Xia Z, Zhao D, Li W, Tyler JK. The Overlooked Fact: Fundamental Need for Spike-In Control for Virtually All Genome-Wide Analyses. *Mol Cell Biol*. 2016;36(5):662-667. doi:10.1128/MCB.00970-14

Chen S, Jiao L, Shubbar M, Yang X, Liu X. Unique Structural Platforms of Suz12 Dictate Distinct Classes of PRC2 for Chromatin Binding. *Mol Cell*. 2018;69(5):840-852.e5. doi:10.1016/j.molcel.2018.01.039

Chica C, Louis A, Crollius HR, Colot V, Roudier F. Comparative epigenomics in the Brassicaceae reveals two evolutionarily conserved modes of PRC2-mediated gene regulation. *Genome Biology*. 2017;18(1):207. doi:10.1186/s13059-017-1333-9

Choe G, Lee J-Y. Push-pull strategy in the regulation of postembryonic root development. *Current Opinion in Plant Biology*. 2017;35:158-164. doi:10.1016/j.pbi.2016.12.005

Cruz-Ramírez A, Díaz-Triviño S, Wachsman G, et al. A SCARECROW-RETINOBLASTOMA Protein Network Controls Protective Quiescence in the Arabidopsis Root Stem Cell Organizer. Estelle M, ed. *PLoS Biol*. 2013;11(11):e1001724. doi:10.1371/journal.pbio.1001724

Davidovich C, Wang X, Cifuentes-Rojas C, et al. Towards a Consensus on the Binding Specificity and Promiscuity of PRC2 for RNA. *Mol Cell*. 2015;57(3):552-558. doi:10.1016/j.molcel.2014.12.017

Deal RB, Henikoff S. A simple method for gene expression and chromatin profiling of individual cell types within a tissue. *Dev Cell*. 2010;18(6):1030-1040. doi:10.1016/j.devcel.2010.05.013

Deng W, Buzas DM, Ying H, et al. Arabidopsis Polycomb Repressive Complex 2 binding sites contain putative GAGA factor binding motifs within coding regions of genes. *BMC Genomics*. 2013;14:593. doi:10.1186/1471-2164-14-593

Denyer T, Ma X, Klesen S, Scacchi E, Nieselt K, Timmermans MCP. Spatiotemporal Developmental Trajectories in the Arabidopsis Root Revealed Using High-Throughput Single-Cell RNA Sequencing. *Developmental Cell*. 2019;48(6):840-852.e5. doi:10.1016/j.devcel.2019.02.022

Doyle MR, Amasino RM. A single amino acid change in the enhancer of zeste ortholog CURLY LEAF results in vernalization-independent, rapid flowering in Arabidopsis. *Plant Physiology*. 2009;151(3):1688-1697. doi:10.1104/pp.109.145581

Efroni I, Ip P-L, Nawy T, Mello A, Birnbaum KD. Quantification of cell identity from single-cell gene expression profiles. *Genome Biol*. 2015;16(1):9. doi:10.1186/s13059-015-0580-x

Engelhorn J, Blanvillain R, Kröner C, et al. Dynamics of H3K4me3 Chromatin Marks Prevails over H3K27me3 for Gene Regulation during Flower Morphogenesis in Arabidopsis thaliana. *Epigenomes*. 2017;1(2):8. doi:10.3390/epigenomes1020008

Engler C, et al. A Golden Gate Modular Cloning Toolbox for Plants. ACS Synthetic Biology 3, n° 11 (21 novembre 2014): 839-43. https://doi.org/10.1021/sb4001504.

Ernst J, Kellis M. Discovery and characterization of chromatin states for systematic annotation of the human genome. *Nat Biotechnol*. 2010;28(8):817-825. doi:10.1038/nbt.1662

Filion GJ, van Bemmel JG, Braunschweig U, et al. Systematic Protein Location Mapping Reveals Five Principal Chromatin Types in Drosophila Cells. *Cell*. 2010;143(2):212-224. doi:10.1016/j.cell.2010.09.009

Finnegan EJ, Dennis ES. Vernalization-induced trimethylation of histone H3 lysine 27 at FLC is not maintained in mitotically quiescent cells. *Curr Biol*. 2007;17(22):1978-1983. doi:10.1016/j.cub.2007.10.026

Friml J, Vieten A, Sauer M, et al. Efflux-dependent auxin gradients establish the apical-basal axis of Arabidopsis. *Nature*. 2003;426(6963):147-153. doi:10.1038/nature02085

Galvan-Ampudia CS, Cerutti G, Legrand J, et al. Temporal integration of auxin information for the regulation of patterning. Kleine-Vehn J, Hardtke CS, eds. *eLife*. 2020;9:e55832. doi:10.7554/eLife.55832

Gendall AR, Levy YY, Wilson A, Dean C. The VERNALIZATION 2 Gene Mediates the Epigenetic Regulation of Vernalization in Arabidopsis. *Cell*. 2001;107(4):525-535. doi:10.1016/S0092-8674(01)00573-6

Goodrich J, Puangsomlee P, Martin M, Long D, Meyerowitz EM, Coupland G. A Polycomb-group gene regulates homeotic gene expression in Arabidopsis. *Nature*. 1997;386(6620):44-51. doi:10.1038/386044a0

Gu X, Xu T, He Y. A Histone H3 Lysine-27 Methyltransferase Complex Represses Lateral Root Formation in Arabidopsis thaliana. *Molecular Plant*. 2014;7(6):977-988. doi:10.1093/mp/ssu035

Hafemeister C, Satija R. Normalization and variance stabilization of single-cell RNA-seq data using regularized negative binomial regression. *Genome Biology*. 2019;20(1):296. doi:10.1186/s13059-019-1874-1

Heidstra R, Welch D, Scheres B. Mosaic analyses using marked activation and deletion clones dissect Arabidopsis SCARECROW action in asymmetric cell division. *Genes & Development*. 2004;18(16):1964-1969. doi:10.1101/gad.305504

Hennig L, Taranto P, Walser M, Schönrock N, Gruissem W. Arabidopsis MSI1 is required for epigenetic maintenance of reproductive development. *Development*. 2003;130(12):2555-2565. doi:10.1242/dev.00470

Heyman J, Cools T, Vandenbussche F, et al. ERF115 Controls Root Quiescent Center Cell Division and Stem Cell Replenishment. *Science*. 2013;342(6160):860-863. doi:10.1126/science.1240667

Hugues A, Jacobs CS, Roudier F. Mitotic Inheritance of PRC2-Mediated Silencing: Mechanistic Insights and Developmental Perspectives. *Frontiers in Plant Science*. 2020;11:262. doi:10.3389/fpls.2020.00262

Jean-Baptiste K, McFaline-Figueroa JL, Alexandre CM, et al. Dynamics of Gene Expression in Single Root Cells of *Arabidopsis thaliana*. *Plant Cell*. 2019;31(5):993-1011. doi:10.1105/tpc.18.00785

Jiang D, Berger F. DNA replication-coupled histone modification maintains Polycomb gene silencing in plants. *Science*. 2017;357(6356):1146-1149. doi:10.1126/science.aan4965

Jullien PE, Katz A, Oliva M, Ohad N, Berger F. Polycomb Group Complexes Self-Regulate Imprinting of the Polycomb Group Gene MEDEA in Arabidopsis. *Current Biology*. 2006;16(5):486-492. doi:10.1016/j.cub.2006.01.020

Kar G, Kim JK, Kolodziejczyk AA, et al. Flipping between Polycomb repressed and active transcriptional states introduces noise in gene expression. *Nature Communications*. 2017;8(1):36. doi:10.1038/s41467-017-00052-2

Kidner C, Sundaresan V, Roberts K, Dolan L. Clonal analysis of the Arabidopsis root confirms that position, not lineage, determines cell fate. *Planta*. 2000;211(2):191-199. doi:10.1007/s004250000284

Köhler C, Hennig L, Bouveret R, Gheyselinck J, Grossniklaus U, Gruissem W. Arabidopsis MSI1 is a component of the MEA/FIE Polycomb group complex and required for seed development. *EMBO J*. 2003;22(18):4804-4814. doi:10.1093/emboj/cdg444

Lafos M, Kroll P, Hohenstatt ML, Thorpe FL, Clarenz O, Schubert D. Dynamic Regulation of H3K27 Trimethylation during Arabidopsis Differentiation. *PLOS Genetics*. 2011;7(4):e1002040. doi:10.1371/journal.pgen.1002040

Langmead B, Salzberg SL. Fast gapped-read alignment with Bowtie 2. *Nature Methods*. 2012;9(4):357-359. doi:10.1038/nmeth.1923

Lee C-H, Yu J-R, Granat J, et al. Automethylation of PRC2 promotes H3K27 methylation and is impaired in H3K27M pediatric glioma. *Genes Dev*. 2019;33(19-20):1428-1440. doi:10.1101/gad.328773.119

Lee C-H, Yu J-R, Kumar S, et al. Allosteric Activation Dictates PRC2 Activity Independent of Its Recruitment to Chromatin. *Molecular Cell*. 2018;70(3):422-434.e6. doi:10.1016/j.molcel.2018.03.020

Li Q, Brown JB, Huang H, Bickel PJ. Measuring reproducibility of high-throughput experiments. *Ann Appl Stat*. 2011;5(3):1752-1779. doi:10.1214/11-AOAS466

Li S, Yamada M, Han X, Ohler U, Benfey PN. High-Resolution Expression Map of the Arabidopsis Root Reveals Alternative Splicing and lincRNA Regulation. *Developmental Cell*. 2016;39(4):508-522. doi:10.1016/j.devcel.2016.10.012

Long Y, Hwang T, Gooding AR, Goodrich KJ, Rinn JL, Cech TR. RNA is essential for PRC2 chromatin occupancy and function in human pluripotent stem cells. *Nat Genet*. 2020;52(9):931-938. doi:10.1038/s41588-020-0662-x

Lopez-Vernaza M, Yang S, Müller R, Thorpe F, Leau E de, Goodrich J. Antagonistic Roles of SEPALLATA3, FT and FLC Genes as Targets of the Polycomb Group Gene CURLY LEAF. *PLOS ONE*. 2012;7(2):e30715. doi:10.1371/journal.pone.0030715

Lucas M de, Pu L, Turco G, et al. Transcriptional Regulation of Arabidopsis Polycomb Repressive Complex 2 Coordinates Cell-Type Proliferation and Differentiation. *The Plant Cell*. 2016;28(10):2616-2631. doi:10.1105/tpc.15.00744

Margueron R, Justin N, Ohno K, et al. Role of the polycomb protein EED in the propagation of repressive histone marks. *Nature*. 2009;461(7265):762-767. doi:10.1038/nature08398

Margueron R, Reinberg D. The Polycomb complex PRC2 and its mark in life. *Nature*. 2011;469(7330):343-349. doi:10.1038/nature09784

Marquès-Bueno MM, Morao AK, Cayrel A, et al. A versatile Multisite Gateway-compatible promoter and transgenic line collection for cell type-specific functional genomics in Arabidopsis. *The Plant Journal*. 2016;85(2):320-333. doi:10.1111/tpj.13099

McInnes L, Healy J, Melville J. UMAP: Uniform Manifold Approximation and Projection for Dimension Reduction. *arXiv:180203426 [cs, stat]*. Published online September 17, 2020. Accessed October 9, 2020. http://arxiv.org/abs/1802.03426

Morao AK, Caillieux E, Colot V, Roudier F. Cell Type-Specific Profiling of Chromatin Modifications and Associated Proteins. In: Bemer M, Baroux C, eds. *Methods in Molecular Biology*. Vol 1675. Methods in Molecular Biology. Springer New York; 2018:111-130. doi:10.1007/978-1-4939-7318-7_8

Moritz LE, Trievel RC. Structure, mechanism, and regulation of polycomb-repressive complex 2. *J Biol Chem*. 2018;293(36):13805-13814. doi:10.1074/jbc.R117.800367

Nawy T, Lee J-Y, Colinas J, et al. Transcriptional Profile of the Arabidopsis Root Quiescent Center. *The Plant Cell*. 2005;17(7):1908-1925. doi:10.1105/tpc.105.031724

Nicoglou A, Merlin F. Epigenetics: A way to bridge the gap between biological fields. *Studies in History and Philosophy of Science Part C: Studies in History and Philosophy of Biological and Biomedical Sciences*. 2017;66:73-82. doi:10.1016/j.shpsc.2017.10.002

Okano Y, Aono N, Hiwatashi Y, et al. A polycomb repressive complex 2 gene regulates apogamy and gives evolutionary insights into early land plant evolution. *PNAS*. 2009;106(38):16321-16326. doi:10.1073/pnas.0906997106

Ou Y, Lu X, Zi Q, et al. RGF1 INSENSITIVE 1 to 5, a group of LRR receptor-like kinases, are essential for the perception of root meristem growth factor 1 in Arabidopsis thaliana. *Cell Res*. 2016;26(6):686-698. doi:10.1038/cr.2016.63

Pereman I, Mosquna A, Katz A, et al. The Polycomb group protein CLF emerges as a specific tri-methylase of H3K27 regulating gene expression and development in Physcomitrella patens. *Biochimica et Biophysica Acta (BBA) - Gene Regulatory Mechanisms*. 2016;1859(7):860-870. doi:10.1016/j.bbagrm.2016.05.004

Perilli S, Di Mambro R, Sabatini S. Growth and development of the root apical meristem. *Current Opinion in Plant Biology*. 2012;15(1):17-23. doi:10.1016/j.pbi.2011.10.006

Perrella G, Vellutini E, Zioutopoulou A, Patitaki E, Headland LR, Kaiserli E. Let it bloom: cross-talk between light and flowering signaling in Arabidopsis. *Physiol Plant*. 2020;169(3):301-311. doi:10.1111/ppl.13073

Petricka JJ, Winter CM, Benfey PN. Control of *Arabidopsis* Root Development. *Annual Review of Plant Biology*. 2012;63(1):563-590. doi:10.1146/annurev-arplant-042811-105501

Pi L, Aichinger E, van der Graaff E, et al. Organizer-Derived WOX5 Signal Maintains Root Columella Stem Cells through Chromatin-Mediated Repression of CDF4 Expression. *Developmental Cell*. 2015;33(5):576-588. doi:10.1016/j.devcel.2015.04.024

Planas-Riverola A, Gupta A, Betegón-Putze I, Bosch N, Ibañes M, Caño-Delgado AI. Brassinosteroid signaling in plant development and adaptation to stress. *Development*. 2019;146(5):dev151894. doi:10.1242/dev.151894

Qiu Y, Liu S-L, Adams KL. Concerted Divergence after Gene Duplication in Polycomb Repressive Complexes1[OPEN]. *Plant Physiol*. 2017;174(2):1192-1204. doi:10.1104/pp.16.01983

Ragazzini R, Pérez-Palacios R, Baymaz IH, et al. EZHIP constrains Polycomb Repressive Complex 2 activity in germ cells. *Nat Commun*. 2019;10(1):3858. doi:10.1038/s41467-019-11800-x

Rahni R, Birnbaum KD. Week-long imaging of cell divisions in the Arabidopsis root meristem. *Plant Methods*. 2019;15(1):30. doi:10.1186/s13007-019-0417-9

Rahni R, Efroni I, Birnbaum KD. A Case for Distributed Control of Local Stem Cell Behavior in Plants. *Developmental Cell*. 2016;38(6):635-642. doi:10.1016/j.devcel.2016.08.015

Ramírez F, Ryan DP, Grüning B, et al. deepTools2: a next generation web server for deep-sequencing data analysis. *Nucleic Acids Res*. 2016;44(Web Server issue):W160-W165. doi:10.1093/nar/gkw257

Rensing SA, Goffinet B, Meyberg R, Wu S-Z, Bezanilla M. The Moss Physcomitrium (Physcomitrella) patens: A Model Organism for Non-Seed Plants[OPEN]. *Plant Cell*. 2020;32(5):1361-1376. doi:10.1105/tpc.19.00828

Roh T-Y, Cuddapah S, Cui K, Zhao K. The genomic landscape of histone modifications in human T cells. *Proc Natl Acad Sci U S A*. 2006;103(43):15782-15787. doi:10.1073/pnas.0607617103

Roudier F, Ahmed I, Bérard C, et al. Integrative epigenomic mapping defines four main chromatin states in Arabidopsis. *The EMBO journal*. 2011;30(10):1928-1938. doi:10.1038/emboj.2011.103

Rymen B, Kawamura A, Lambolez A, et al. Histone acetylation orchestrates wound-induced transcriptional activation and cellular reprogramming in Arabidopsis. *Commun Biol*. 2019;2:404. doi:10.1038/s42003-019-0646-5

Ryu KH, Huang L, Kang HM, Schiefelbein J. Single-Cell RNA Sequencing Resolves Molecular Relationships Among Individual Plant Cells. *Plant Physiology*. 2019;179(4):1444-1456. doi:10.1104/pp.18.01482

Sabatini S, Beis D, Wolkenfelt H, et al. An auxin-dependent distal organizer of pattern and polarity in the Arabidopsis root. *Cell*. 1999;99(5):463-472. doi:10.1016/s0092-8674(00)81535-4

Salvi E, Rutten JP, Di Mambro R, et al. A Self-Organized PLT/Auxin/ARR-B Network Controls the Dynamics of Root Zonation Development in Arabidopsis thaliana. *Developmental Cell*. 2020;53(4):431-443.e23. doi:10.1016/j.devcel.2020.04.004

Sanchez A, Choubey S, Kondev J. Regulation of noise in gene expression. *Annu Rev Biophys*. 2013;42:469-491. doi:10.1146/annurev-biophys-083012-130401

Schubert D, Primavesi L, Bishopp A, et al. Silencing by plant Polycomb-group genes requires dispersed trimethylation of histone H3 at lysine 27. *EMBO J*. 2006;25(19):4638-4649. doi:10.1038/sj.emboj.7601311

Schuettengruber B, Bourbon H-M, Croce LD, Cavalli G. Genome Regulation by Polycomb and Trithorax: 70 Years and Counting. *Cell*. 2017;171(1):34-57. doi:10.1016/j.cell.2017.08.002

Sequeira-Mendes J, Aragüez I, Peiró R, et al. The Functional Topography of the Arabidopsis Genome Is Organized in a Reduced Number of Linear Motifs of Chromatin States[C][W]. *Plant Cell*. 2014;26(6):2351-2366. doi:10.1105/tpc.114.124578

Shu J, Chen C, Thapa RK, et al. Genome-wide occupancy of histone H3K27 methyltransferases CURLY LEAF and SWINGER in Arabidopsis seedlings. *Plant Direct*. 2019;3(1):e00100. doi:10.1002/pld3.100

Shulse CN, Cole BJ, Ciobanu D, et al. High-Throughput Single-Cell Transcriptome Profiling of Plant Cell Types. *Cell Reports*. 2019;27(7):2241-2247.e4. doi:10.1016/j.celrep.2019.04.054

Spillane C, Schmid KJ, Laoueillé-Duprat S, et al. Positive darwinian selection at the imprinted MEDEA locus in plants. *Nature*. 2007;448(7151):349-352. doi:10.1038/nature05984

Strahl BD, Allis CD. The language of covalent histone modifications. *Nature*. 2000;403(6765):41-45. doi:10.1038/47412

Ulmasov T, Murfett J, Hagen G, Guilfoyle TJ. Aux/IAA proteins repress expression of reporter genes containing natural and highly active synthetic auxin response elements. *The Plant Cell*. 1997;9(11):1963-1971. doi:10.1105/tpc.9.11.1963

Velanis CN, Perera P, Thomson B, et al. The domesticated transposase ALP2 mediates formation of a novel Polycomb protein complex by direct interaction with MSI1, a core subunit of Polycomb Repressive Complex 2 (PRC2). Mittelsten Scheid O, ed. *PLoS Genet*. 2020;16(5):e1008681. doi:10.1371/journal.pgen.1008681

Vernoux T, Brunoud G, Farcot E, et al. The auxin signalling network translates dynamic input into robust patterning at the shoot apex. *Mol Syst Biol*. 2011;7:508. doi:10.1038/msb.2011.39

Wang D, Tyson MD, Jackson SS, Yadegari R. Partially redundant functions of two SET-domain polycomb-group proteins in controlling initiation of seed development in Arabidopsis. *Proceedings of the National Academy of Sciences*. 2006;103(35):13244-13249. doi:10.1073/pnas.0605551103

Wang H, Liu C, Cheng J, et al. Arabidopsis Flower and Embryo Developmental Genes are Repressed in Seedlings by Different Combinations of Polycomb Group Proteins in Association with Distinct Sets of Cis-regulatory Elements. *PLoS Genet*. 2016;12(1):e1005771. doi:10.1371/journal.pgen.1005771

Wang X, Long Y, Paucek RD, et al. Regulation of histone methylation by automethylation of PRC2. *Genes Dev*. 2019;33(19-20):1416-1427. doi:10.1101/gad.328849.119

Wei C, Xiao R, Chen L, et al. RBFox2 Binds Nascent RNA to Globally Regulate Polycomb Complex 2 Targeting in Mammalian Genomes. *Mol Cell*. 2016;62(6):875-889. doi:10.1016/j.molcel.2016.04.013

Xiao J, Jin R, Yu X, et al. Cis and trans determinants of epigenetic silencing by Polycomb repressive complex 2 in Arabidopsis. *Nature Genetics*. 2017;49(10):1546-1552. doi:10.1038/ng.3937

Xu M, Hu T, Smith MR, Poethig RS. Epigenetic Regulation of Vegetative Phase Change in Arabidopsis. *Plant Cell*. 2016;28(1):28-41. doi:10.1105/tpc.15.00854

Yamada M, Han X, Benfey PN. RGF1 controls root meristem size through ROS signalling. *Nature*. 2020;577(7788):85-88. doi:10.1038/s41586-019-1819-6

Yan W, Chen D, Schumacher J, et al. Dynamic control of enhancer activity drives stage-specific gene expression during flower morphogenesis. *Nature Communications*. 2019;10(1):1705. doi:10.1038/s41467-019-09513-2

Yang H, Berry S, Olsson TSG, Hartley M, Howard M, Dean C. Distinct phases of Polycomb silencing to hold epigenetic memory of cold in Arabidopsis. *Science*. 2017;357(6356):1142-1145. doi:10.1126/science.aan1121

Ye Z, Sarkar CA. Towards a Quantitative Understanding of Cell Identity. *Trends in Cell Biology*. 2018;28(12):1030-1048. doi:10.1016/j.tcb.2018.09.002

You Y, Sawikowska A, Neumann M, et al. Temporal dynamics of gene expression and histone marks at the Arabidopsis shoot meristem during flowering. *Nat Commun*. 2017;8:15120. doi:10.1038/ncomms15120

Young MD, Willson TA, Wakefield MJ, et al. ChIP-seq analysis reveals distinct H3K27me3 profiles that correlate with transcriptional activity. *Nucleic Acids Res*. 2011;39(17):7415-7427. doi:10.1093/nar/gkr416

Zhang T-Q, Xu Z-G, Shang G-D, Wang J-W. A Single-Cell RNA Sequencing Profiles the Developmental Landscape of Arabidopsis Root. *Molecular Plant*. 2019;12(5):648-660. doi:10.1016/j.molp.2019.04.004

Zhang Y, Liu T, Meyer CA, et al. Model-based Analysis of ChIP-Seq (MACS). *Genome Biology*. 2008;9(9):R137. doi:10.1186/gb-2008-9-9-r137

Zhao J, Ohsumi TK, Kung JT, et al. Genome-wide identification of Polycomb-associated RNAs by RIP-seq. *Mol Cell*. 2010;40(6):939-953. doi:10.1016/j.molcel.2010.12.011

Zhou Y, Tergemina E, Cui H, et al. Ctf4-related protein recruits LHP1-PRC2 to maintain H3K27me3 levels in dividing cells in Arabidopsis thaliana. *Proc Natl Acad Sci USA*. 2017;114(18):4833-4838. doi:10.1073/pnas.1620955114

Zhou Y, Wang Y, Krause K, et al. Telobox motifs recruit CLF/SWN–PRC2 for H3K27me3 deposition via TRB factors in Arabidopsis. *Nature Genetics*. 2018;50(5):638. doi:10.1038/s41588-018-0109-9

7. Annexe

Table 1: Primers used for RT-qPCR

CLF	Sense primer: 5'-CTGAAATTCGCCAACCATTCTC-3' Antisense primer: 5'-TCCAGCCAGTATCCTCTCTT-3'
SWN	Sense primer: 5'-AGCTCTTCGCTAGCTTCTATTC-3' Antisense primer: 5'-TTTGCCAATCACTCAGCTAAAC-3'
PP2AA3	Sense primer: 5'-GACCAAGTGAACCAGGTTATTGG-3' Antisense primer: 5'-TACTCTCCAGTGCCTGTCTTCA-3'
ACT2	Sense primer: 5'-GCCATCCAAGCTGTTCTCTC-3' Antisense primer: 5'-CCCTCGTAGATTGGCACAGT-3'
GAPDH	Sense primer: 5'-TTGGTGACAACAGGTCAAGCA-3' Antisense primer: 5'-AAACTTGTCGCTCAATGCAATC-3'

Table 2: Primers used for ChIP validation by qPCR

AT3G11260	Sense primer: 5'- TACATGTGTGTGGCGAACCT -3' Antisense primer: 5'- TGACACTTGAGGAACGTTGG -3'
AT1G28300	Sense primer: 5'- CCTGTTGATCCTTGCCATCT -3' Antisense primer: 5'- TGAATCCTCAGCCGGTTTAC -3'
AT5G12330	Sense primer: 5'- GTAGGCCGTAACGGACAGAA -3' Antisense primer: 5'- GGCTACAACGAGGAGGCATA-3'
AT5G49520	Sense primer: 5'- TCAGATCATCATCCGTTGGA -3' Antisense primer: 5'- GGAAAGGCATCGAATGAAAA -3'
AT5G10140	Sense primer: 5'- CGAGCACGCATCAGATCG -3' Antisense primer: 5'- GGCGGATCTCTTGTTGTTTCTC-3'
AT5G13440	Sense primer: 5'- GATCATTGGAGCAGGGAAGA -3' Antisense primer: 5'- TCTGTTGTGCCCTTGTCCTGA -3'
AT3G18780	Sense primer: 5'- GCCATCCAAGCTGTTCTCTC -3' Antisense primer: 5'- CCCTCGTAGATTGGCACAGT -3'

Table 3: Primers used for cloning

CLF_5'	Sense primer: 5'- AATTGAAGACATGGAGCTGAATTACAAAGCTAATAATCATATCCCAG -3' Antisense primer: 5'- AATTGAAGACAACATTTGTCAAGAAACCAGATCGGAAC -3'
CLF_3'	Sense primer: 5'- TTGAAGACATGCTTGCTTAGCAACAAAAGAAACAACC -3' Antisense primer: 5'- TTGAAGACAAAGCGCTTGTGGTATCTCAAATATTGAAGAAAC -3'
SWN_5'	Sense primer: 5'- TTGAAGACATGGAGAACCATCAGATATACAAATAGAATTTGAATATAC -3' Antisense primer: 5'- TTGAAGACAACATTTGATGACTCCTCGAGCTTTCC -3'
SWN_3'	Sense primer: 5'- TTGAAGACATGCTTCTCATTGATGATTACTGGCTAAGAGAA -3' Antisense primer: 5'- TTGAAGACAAAGCGGAAAAAGCAAGAAGAAACTGGATCC -3'
WOX5_promoter	Sense primer: 5'- TTGAAGACATGGAGTGACTAATTGGGTGCTGGGTGCATGC -3' Antisense primer: 5'- AATTGAAGACAACATTGTTCAGATGTAAAGTCCTCAAC -3'

Table 4: Primers used for genotyping

clf-28 *(SALK_139371)*	LP: 5'- TTCGGTTGGCACTAAACTCAC -3' RP: 5'- TGTAGAAGATGGACCTGCCAG -3'
clf-29 *(SALK_021003)*	LP: 5'- TCGACCCACTACAGACTGGTC -3' RP: 5'- TTTTGGGTTCGTTTAGGAACC -3'
swn-7 *(SALK_109121)*	LP: 5'- TGATTATTGCTCCGTTTCCAC -3' RP: 5'- CGAGGAATTTTCTAATTCCGG -3'
LBb1.3	5'- ATTTTGCCGATTTCGGAAC -3'